MATERIALs of Conference

XI-th International Conference

Topical Problems of Semiconductor Physics

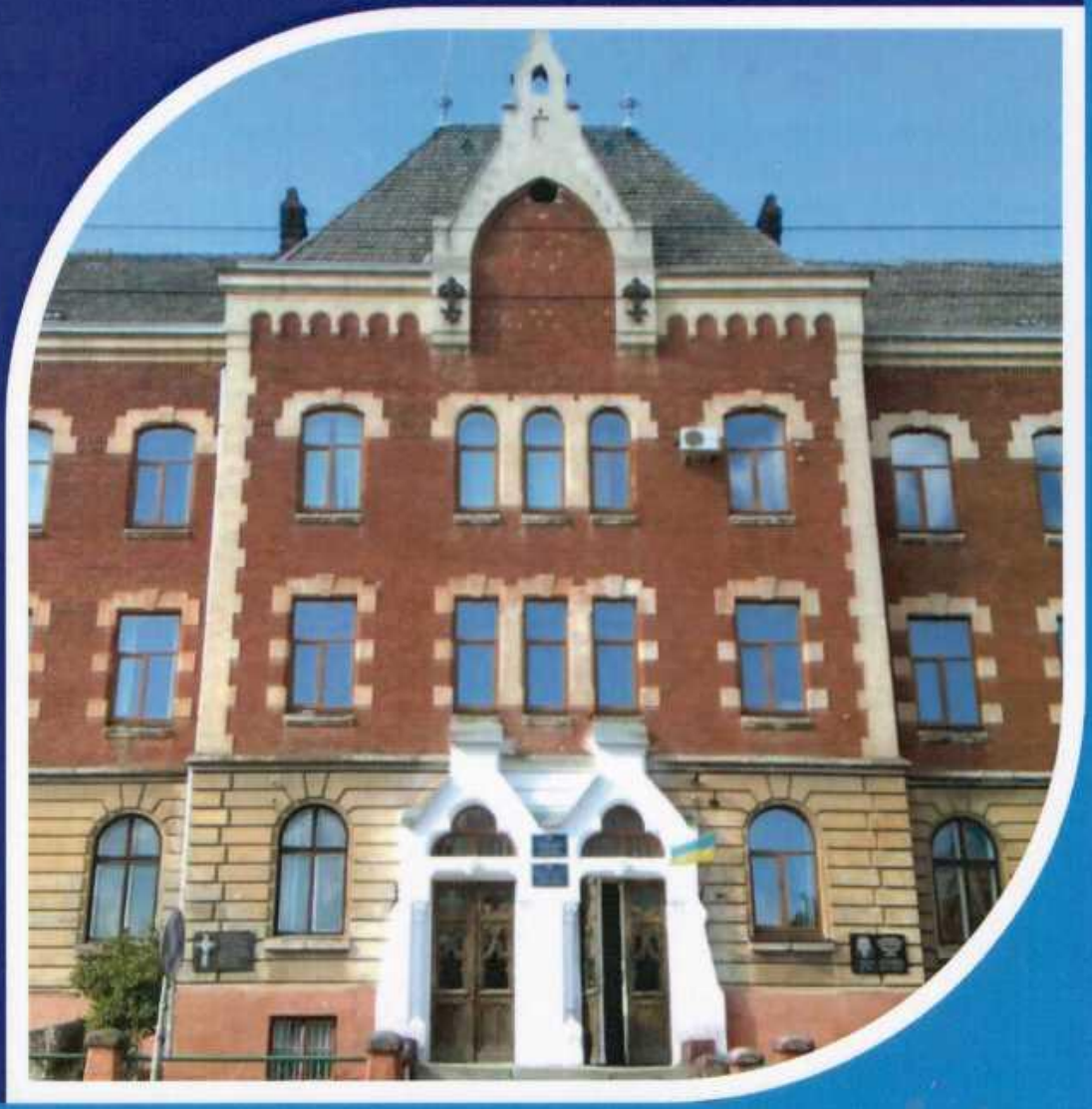

Drohobych, UKRAINE

May 27-31, 2024

Ministry of Education and Science of Ukraine

Institute of Physics of NASU

V.E. Lashkaryov Institute of Semiconductor Physics NAS of Ukraine

**Scientific Council "Semiconductor and Dielectric Physics"
at Physics and Astronomy Department of NASU**

Drohobych Ivan Franko State Pedagogical University

XI-th International Conference

TOPICAL PROBLEMS OF SEMICONDUCTOR PHYSICS

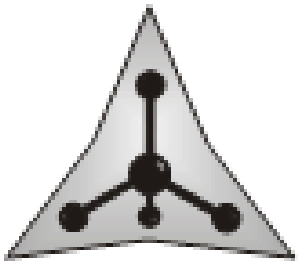

Prykarpattya,

Drohobych, UKRAINE

MAY 27-31, 2024

Proceedings of the XI-th International Conference “Topical Problems of Semiconductors Physics” / Edited by Ihor Stolyarchuk. – Drohobych : Publishing Department of Ivan Franko DSPU, 2024. – 86 p.

Actual problems and important achievements of modern semiconductors physics are presented in the Proceedings of the XI-th International Conference “Topical Problems of Semiconductors Physics”. The abstracts are grouped into 7 sections, according to the Conference Thematic: “Section A. New frontiers in semiconductors and their based structures for electronics, optoelectronics, spintronic and sensing”, “Section B. Semiconductor low-dimensional structures: advances in synthesis, characterization, theoretical modeling and applications”, “Section C. The semiconductors for LEDs, solar and related energy technologies and sensor materials”, “Section D. Synthesis, processing and characterization of multifunctional oxide materials”, “Section E. Advanced strategies for smart functional and multifunctional bionanomaterials and biointerfaces”, “Section F. Laser material processing: from fundamental interactions to innovative applications”, “Section G. Modern computational methods and their applications in materials science: Synergy of theory and experiment”. The Proceedings were prepared for publication by the Conference Program Committee and presented in the author’s edition.

Recommended for publication by the Academic Council of Drohobych Ivan Franko State Pedagogical University.

INTERNATIONAL PROGRAM COMMITTEE

M. Brodyn (Kyiv, Ukraine)
I. Blonskyi (Kyiv, Ukraine)
O. Belyaev (Kyiv, Ukraine)
I. Bolesta (Lviv, Ukraine)
P. Dluzewcki (Warsaw, Poland)
V. Fediv (Chernivtsi, Ukraine)
Yu. Hnatenko (Kyiv, Ukraine)
V. Kadan (Kyiv, Ukraine)
A. Kiv (Be'er Sheva, Israel)
V. Kochelap (Kyiv, Ukraine)
I. Kogoutiouk (Minessota, USA)
O. Kovalenko (Dnipro, Ukraine)
M. Kuzma (Rzeszów, Poland)
Ya. Lepikh (Odessa, Ukraine)
V. Manzhara (Kyiv, Ukraine)
A. Medvid' (Riga, Latvia)
L. Nykyruy (Ivano-Frankivsk, Ukraine)
L. Poperenko (Kyiv, Ukraine)
V. Poroshyn (Kyiv, Ukraine)
S. Ryabchenko (Kyiv, Ukraine)
V. Shenderovskyi (Kyiv, Ukraine)
M. Shiojiri (Kyoto, Japan)
O. Shpotyuk (Lviv, Ukraine)
F. Sizov (Kyiv, Ukraine)
I. Stolyarchuk (Drohobych, Ukraine)
O. Stronskyi (Kyiv, Ukraine)
H. Terletska (Murfreesboro, USA)
M. Tkach (Chernivtsi, Ukraine)
M. Vakiv (Lviv, Ukraine)
R. Zdyb (Lublin, Poland)

ORGANIZING COMMITTEE

Co-chairman: Ivan Blonskyi, Corresponding member of NAS of Ukraine, Professor
Co-chairman: **Olexander Stronskyi**, Professor
Co-chairman: **Ihor Stolyarchuk**, Professor

M. Brodyn (Kyiv, Ukraine)
V. Boichuk (Ivano-Frankivsk, Ukraine)
I. Bilynskyi, (Kryvyi Rih, Ukraine)
I. Dmytruk (Kyiv, Ukraine)
A. Dmytruk (Kyiv, Ukraine)
I. Hadzaman (Drohobych, Ukraine)
D. Korbutyak (Kyiv, Ukraine)
M. Krupa (Kyiv, Ukraine)
Ya. Lepikh (Odessa, Ukraine)
O. Makhanets (Chernivtsi, Ukraine)
A. Medvid' (Riga, Latvia)
S. Melnychuk (Chernivtsi, Ukraine)
V. Mitsa (Uzhhorod, Ukraine)
L. Nykyruy (Ivano-Frankivsk, Ukraine)
B. Pavlyk (Lviv, Ukraine)
R. Peleshchak (Lviv, Ukraine)
L. Poperenko (Kyiv, Ukraine)
V. Popovych (Drohobych, Ukraine)
V. Poroshyn (Kyiv, Ukraine)
A. Rovenchak (Lviv, Ukraine)
S. Ryabchenko (Kyiv, Ukraine)
V. Stadnyk (Lviv, Ukraine)
O. Stronskyi (Kyiv, Ukraine)
H. Terletska (Murfreesboro, USA)
Z. Tsibriy (Kyiv, Ukraine)
M. Vakiv (Kyiv, Ukraine)
Yu. Vaksman (Odessa, Ukraine)
I. Virt (Drohobych, Ukraine)
V.Yuhymchuk (Kyiv, Ukraine)
D. Zayachuk (Lviv, Ukraine)

LOCAL ORGANIZING COMMITEE

Chairman: Ihor Stolyarchuk
Vice-chairmen: O. Kuzyk, V. Holskyi, V. Popovych
Coordinator: V. Holskyi

G. Bandura
V. Brytan
O. Dan'kiv
D. Karpyn
A. Kripak
R. Leshko
Yu. Maturin
H. Metsan
L. Pan'kiv
Yu. Pavlovskyi
R. Pazyuk
A. Popovych
I. Shakleina
Yu. Uhryn

TABLE OF CONTENTS

SECTION A: NEW FRONTIERS IN SEMICONDUCTORS AND THEIR BASED STRUCTURES FOR ELECTRONICS, OPTOELECTRONICS, SPINTRONIC AND SENSING 10

Chalcogenide glasses: properties and applications in optoelectronics and photonics 11
Stronski A.

Optical studies of exciton-plasmon interactions in semiconductor-metal multilayer films and nanostructures 13
Stolyarchuk I.D., Dan'kiv O.O., Stolyarchuk A.I., Kuzyk O.V.

Half-metallicity and ferromagnetism in two-dimensional Cr_3Te_4 nanosheets ... 14
Kuzma M.

Infrared damping, visible and microwave transparent polymeric films with thin AlN coatings 15
Tsybrii Z.F., Sizov F.F.

Stimulated incoherent radiation of ZnO nanocrystals 16
Fedorenko L.L., Korbutyak D.V., Evtukh A.A., Naumov V.V., Yukhymchuk V.O.

Raman spectroscopy and X-ray diffraction studies of Ga-Ge-Te alloys 17
Popovych M., Kochubei H., Shportko K., Lotnyk A., Venger E., Stronski A.

Features of structural transformations during thermal annealing of InSb implanted with beryllium ions 18
Sapon S., Kulbachynskyi O., Gudymenko O.Yo., Dubikovskyi O., Maziar D.

Ultrafast inertia-free switching of double magnetic tunnel junctions 19
Dzhezherya Yu., Polynchuk P., Kravets A. and Korenivski V.

Doping-induced extrinsic magnetism in CdTe:Cr crystals 20
Popovych V.D., Dluzewski P., Morawiec K., Zajkowska W., Popovych A.V., Stolyarchuk I.D., Żywczak A., Kuzma M., Shiojiri Makoto

Structural studies of As_2S_3:Mn glasses 21
Kochubei H., Stronski A., Paiuk O., Gudymenko A.

Some peculiarities of structural changes in chalcogenide glasses $(GeS_3)_{100-x}Ag_x$, $(GeS_2)_{100-x}Ag_x$ and $(Ge_{42}S_{58})_{100-x}Ag_x$ 22
Lishchynskyy I.M., Kaban I.G., Voitkiv H.V., Poplavskyy O.P., Stronski A.V.

Doping-induced second phases in vapour-grown CdTe crystals 23
Popovych A.V., Rehei M.A., Shakleina I.O., Popovych V.D.

Advanced organic-inorganic ureasil-based and photocross-linked polymers for controlled biosensing 24
Kavetskyy T.S., Kukhazh Y.Y., Hoivanovych N.K., Dyachok D.O., Demkiv O.M., Ostrauskaite J., Zgardzińska B., Šauša O., Kiv A.E.

About decisive role of minority current carriers in the emergence of superconductivity 25
Uhryn Yu.O.

SECTION B: SEMICONDUCTOR LOW-DIMENSIONAL STRUCTURES: ADVANCES IN SYNTHESIS, CHARACTERIZATION, THEORETICAL MODELING AND APPLICATIONS 26

Strain stresses in ZnO:Mn nanocrystals 27
Kovalenko O.V., Vorovsky V.Yu., Slavnyi V.V.

Antimonene: from a large scale growth of new structural phase to ferromagnetic heterostructures 28
Zdyb R.

Quantum Cluster Embedding Description of Electron Localization in Disordered and Strongly Correlated Systems 29
Terletska H.

Quantum Cone – Nano Source of Light with Dispersive Spectrum, Separated in Time and Space 30
Medvids A., Ščajev P., Kazuhiko H.

Напівпровідникові властивості комплексних сполук германію 31
Ленік Я.І.

Perspectives, problems and tasks in the theory of multi-level quasiparticles interacting with phonons in nanostructures 32
Tkach M.V., Seti Ju.O., Voitsekhivska O.M.

Ultra-small quantum dots: effect of crystal structure disorder 33
Kupchak I.M., Korbutyak D.V.

Features of surface morphology and defect formation of $Pb_{1-x}Cd_xTe$ thin films prepared by PVD..... 34
Mazur T.M., Naidych B.P., Holovata O.B., Parashchuk T.O., Zamurujeva O.V., Yavorskyi Y.S., Mazur M.P., Nykyruy L.I., Yavorskyi R.S.

Application of artificial intelligence methods in solving ab initio problems..... 35
Tuzhykov A.V., Kavetskyy T.S., Kiv A.E., Soloviev V.N.

Synthesis Technology and Optical Characteristics of Ultrasmall CdTe Quantum Dots..... 36
Dremliuzhenko K.S., Kulchytskyi B.N., Korbutyak D.V., Isaieva O.F., Trischuk L.I.

Modelling the electric field effect on the optical characteristics of lens-shaped quantum dots 37
Holovatsky V.A., Holovatsky I.V., Makhanets O.M.

IV-VI semiconductor low-dimensional structures formed by ion sputtering 38
Zayachuk D.M.

Electric field effect on the absorption coefficient of elliptical quantum wires.. 39
Holovatsky V.A., Yarema V.V.

The effect of dynamic deformation on the nanowires conductivity of AlGaN/GaN..... 40
Kaliuzhnyi V.V., Tymochko M.D., Olikh O.Ya., Belyaev A.E.

The energy spectrum of nanopod-shaped structures in the form of tetrapods.... 41
Bilynskyi I.V., Melnyk Ya.Yu., Bobyliev D.Ye., Popov M.Yu.

Control of the structural perfection of functional materials of electronic equipment by the modulation electroreflection spectroscopy method 42
Demchyna L.A., Mynaylo M.A., Pekur D.V., Vuichyk M.V., Kyiak J.P., Gentsar P.O., Vlasenko O.I.

Energy spectrum of heterogeneous tunnel-coupled quantum dots 43
Bilynskyi I.V., Melnyk Ya.Yu., Slusarenko M.A., Popov M.Yu.

The influence of impurities and electric fields on light absorption by spherical non-concentric core-shell quantum dots 44
Leshko R.Ya., Leshko O.V., Bilynskyi I.V.

Photophysical behavior of MeLPPP/SBA-15 nanocomposite 45
Mykytyuk T.V., Shcherban N.D., Dmytruk A.M., Dmytruk M., Ostapenko Yu.V., Ostapenko N.I.

Multifunctional sensor structures based on porous silicon and reduced graphene oxide 46
Olenych I.B., Horbenko Y.Y., Pavlyk M.R.

Optical spectroscopy of high-resistence CdTe single crystals 47
Gentsar P.O., Mynaylo M.A., Pekur D.V., Demchyna L.A., Vuichyk M.V., Kyiak J.P., Zayats M.S., Vlasenko O.I.

The influence of hydrostatic pressure on the synthesis of colloidal core-shell quantum dots 48
Dan'kiv O.O., Kuzyk O.V., Peleshchak R.M., Stolyarchuk I.D., Satcyk V.V., Guba S.K.

Energy Spectrum Analysis of GaAs/AlAs Quantum Dots of Complex Shapes Using Plane Wave Method 49
Bilynskyi I.V., Maturin Yu.P.

Spectral parameters of an electron in double quantum rings in magnetic and electric fields 50
Hnidko I.S., Gutsul V.I., Koziarskyi I.P., Makhanets O.M., Kuchak A.I.

Optical properties of germanium doped n-CdTe single crystals in the fundamental optical transition E_0 51
Gentsar P.O., Mynaylo M.A., Pekur D.V., Vuichyk M.V., Strilchyk O.M., Kyiak J.P., Demchyna L.A., Zayats M.S., Trischuk L.I.

Raman spectroscopy study of the structure of Cu_2ZnSnS_4 and Cu_2NiSnS_4 nanocrystals synthesized by hydrothermal route 52
Ivakhno-Tsehelnyk O., Karnaukhov A., Kotsyubynsky V.O., Selyshchev O., Boychuk V.M., Dzhagan V.M., Mazur N., Zahn D.R.T.

The mechanism of the influence of ultrasonic cavitation on the growth of A^2B^6 colloidal nanoparticles 53
Kuzyk O.V., Dan'kiv O.O., Stolyarchuk I.D., Peleshchak R.M., Kuhivchak V.A., Krisa Ya.P.

The Energy Spectrum of an Electron in a Linear Quantum Molecule Formed from Four Quantum Dots Nanoparticles 54
Holskiy V.B., Leshko R.Ya., Holska S.V., Karpiy V.R.

Optical reflection of silicon nanowires 57
Demchyna L.A., Mynaylo M.A., Pekur D.V., Vuichyk M.V., Kyiak J.P., Gentsar P.O., Vlasenko O.I.

An ordered array with two different quantum dots in a unit cell 58
Bilynskyi I.V., Leshko R.Ya., Bandura H.Ya.

SECTION C: THE SEMICONDUCTORS FOR LEDS, SOLAR AND RELATED ENERGY TECHNOLOGIES AND SENSOR MATERIALS 59

Structural Studies of Semiconductor and Dielectric Materials 60
Shiojiri Makoto, Chen Miin-Jang

Ultraviolet photodetectors based on polymer/zinc oxide nanoparticles hybrid materials 62
Stolyarchuk A.I., Dan'kiv O.O., Bachynsky O.I., Stolyarchuk I.D.

Technological aspects of deposition cadmium sulphide thin films as buffer layer 63
Katanova L.O., Nykyruy L.I., Yavorskyi R.S., Kashuba A.I., Semkiv I.V.

The effect of growth conditions of PbTe layers on their IR properties 64
Vuichyk M.V., Svezhentsova K.V., Tsybrii Z.F.

Thermal conductivity of GeBiTe solid solutions 65
Matkivskyi O.M., Balan V.R., Dadiak I.B., Horichok I.V.

Effect of structure defects on the microhardness of CdTe-ZnTe single crystals grown by sublimation 66
Brytan V.B., Tymkiv A.V., Kovalko M.C., Pavlovsky Y.V., Kovalchuk Yu.V., Uhryn Yu.O.

SECTION D: SYNTHESIS, PROCESSING AND CHARACTERIZATION OF MULTIFUNCTIONAL OXIDE MATERIALS 67

Refractive parameters of rubidium sulfate crystals at low temperatures 68
Pryshko I.A., Stadnyk V.Yo., Shtuka O.V., Novosad I.S.

Optical characteristics of ZnMnO nanoparticles prepared by ball milling technique 69
Stolyarchuk A.I., Popovych A.V., Hadzaman I.V., Kuzyk O.V.

Influence of the structure of $Fe_xSi_yO_z$ films obtained by the ion-plasma sputtering method on their electrophysical properties 70
Kykot A.M., Bratus O.L., Gudymenko O.Yo., Evtukh A.A.

Transparent conducting In_2O_3:Sn films made by reactive magnetron sputtering from the alloy target oxide 71
Zayats M.S., Boiko V.G., Pekur D.V., Romanyuk B.M., Gentsar P.O.

Noise properties of n-ZnO/p-Si heterojunctions 72
Virt I.S., Padalka I.V.

Obtaining modified $La_{0.7}Sr_{0.3}MnO_3$ for cathodes of fuel cells 73
Kolkovska H.M., Kolkovskyi P.I., Kotsyubynsky V.O., Yaremiy I.P., Rachiy B.I., Ivanichok N.Ya.

Manganese Dioxide (MnO_2) for Supercapacitor Applications 74
Misiuk O.I., Kolkovskyi P.I., Kotsyubynsky V.O., Rachiy B.I., Yaremiy I.P., Tymofii T.M.

SECTION E: ADVANCED STRATEGIES FOR SMART FUNCTIONAL AND MULTIFUNCTIONAL BIONANOMATERIALS AND BIOINTERFACES 75

Study of trophic activity of Daphnia magna through analysis of optical density of Chlorella vulgaris 76
Leshko O.V., Leshko R.Ya., Atamanyuk A.M.

SECTION F: LASER MATERIAL PROCESSING: FROM FUNDAMENTAL INTERACTIONS TO INNOVATIVE APPLICATIONS 77

Time-resolved kinetics of laser destruction of materials for optoelectronic applications 78
Blonskyi I.V., Dmytruk A.M., Dmitruk I.M., Kadan V.M.

Photon drag effect and diffusion of atoms in multilayer films 79
Krupa M.M.

Features of the origin and propagation of a shock wave in semiconductors during nanosecond laser irradiation 80
Cao Z., Levytskyi S., Stronski A.

Calculation of phonon scattering cross sections on impurity atoms (In) in CdTe for thermal diffusion during pulse laser irradiation 81
Levytskyi S., Stronski A.

SECTION G: MODERN COMPUTATIONAL METHODS AND THEIR APPLICATIONS IN MATERIALS SCIENCE: SYNERGY OF THEORY AND EXPERIMENT 82

Machine Learning-Based Characterization of Recombination Active Defects in Photovoltaic Cells 83
Zavhorodnii O.V., Olikh O.Ya.

LIST OF AUTHORS 84

SECTION A:

New frontiers in semiconductors and their based structures for electronics, optoelectronics, spintronic and sensing

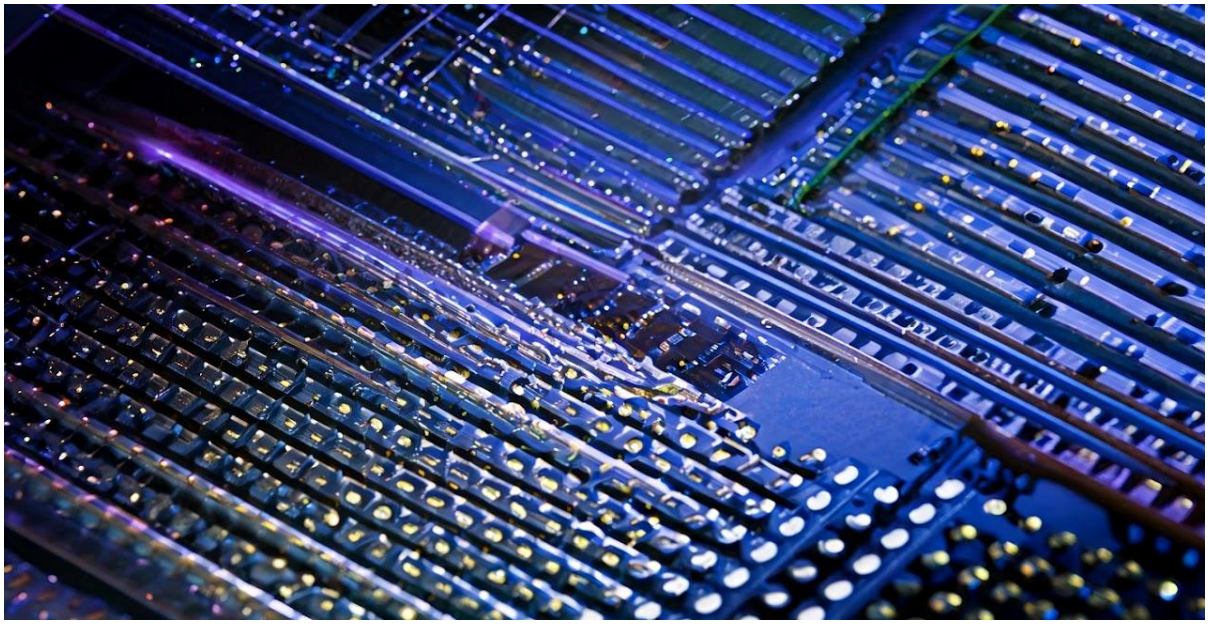

Chalcogenide glasses: properties and applications in optoelectronics and photonics

Stronski A.

V. Lashkaryov Institute of Semiconductor Physics NAS Ukraine, Kyiv, Ukraine
stronski@isp.kiev.ua

Due to their unique properties such as high IR transparency, numerous photoinduced effects, high non-linear optical properties, etc., chalcogenide glasses (CG) are perspective materials for various applications in the modern photonics and nanotechnology. CG are widely used in versatile technological applications for fabrication of optical elements and devices for optoelectronics, holography and information storage media.

In present report the investigation results of chalcogenides glasses (CG) structural properties and their applications are reviewed. CG structural properties of are discussed in [1-6]. XRD, EXAFS, AFM, SEM techniques and Raman spectroscopy were used as tools in studying the structural properties of CG's. As_2S_3-As_2Se_3, As_2S_3-Sb_2S_3, Ge-As-Se, Ge-As-S, Ge-Sb-Te, Ga-Ge-Te and Ge-S-Ag, Ag–As–S, As_2S_3:Mn chalcogenide glasses.

The experimental X-ray diffraction profiles confirmed amorphous nature of studied glasses. Pair distribution functions and RDF were obtained for samples of As-Ge-Se, As-Ge-S, As-Sb-S glasses and Ga-Ge-Te glasses As-S glasses doped with Ag, Mn. The addition of silver and germanium does not significantly affect the position of first coordination sphere r_1. Radius of first coordination sphere for As-S-Ag glasses correspond to 2.29A value, for As-Ge-S glasses – 2.25 A and for second coordination sphere – 3.48 A for both glass compositions. Changes of short range order parameters (r_1) of As_2S_3:Mn glasses with Mn concentration were within calculation errors. In the case of As-Sb-S glasses with the increase of Sb content position of first coordination sphere radius is shifted towards the longer distances (from 2.29A to 2.42 A), positions of the second peaks – 3.45-3.54 Å for studied glasses.

Systematic compositional changes in As_2S_3-Sb_2S_3 alloys have been observed in the evolution of Raman bands. Raman data show that pseudo-binary As_2S_3–Sb_2S_3 glasses contain different nanophases: $AsS_{3/2}$ and $SbS_{3/2}$ pyramidal units, As_4S_4 units and S rings or S_8 rings fragments, whose concentration changes along the chosen compositional cross-section. Raman spectra of Ge-As-S samples showed that the backbones of the studied samples consist of $AsS_{3/2}$ pyramidal units, edge- and corner-shared $Ge(S_{1/2})_4$ tetrahedral units. Compositional changes in studied glasses result in the evolution of the observed Raman bands. Such dependences of characteristic constituent Raman bands' intensities showed that Ge-As-S samples contain different nanophases whose concentration is changing along chosen compositional cross-section. For Ag–

As–S chalcogenide glasses the main effect that is observed at introduction of silver into nanostructured As_2S_3 glass is the change of the relative concentration of the main and non-stoichiometric molecular structural units..

Gaussians were used to fit the obtained Raman spectra of Ge-As-Se, Ge-As-S As-Sb-S and Ga-Ge-Te glasses and were attributed mainly to the vibrations of the structural units in respective binary glasses. Systematic compositional dependencies of the intensities of the characteristic Raman bands correlate with evolution of concentration of the different structural units in Ge-As-Se, Ge-As-S and Ga-Ge-Te alloys along the studied compositional lines. Obtained compositional trends in the intensities of Raman bands may enable one to predict vibrational properties of other glasses compositions. For $(GeS_3)_{100-x}Ag_x$, $(GeS_2)_{100-x}Ag_x$, $(Ge_{42}S_{58})_{100-x}Ag_x$ glasses area of phase separation were revealed. Observed bands in the Raman spectra of studied glasses show that such glasses contain different nanophases and can be explained in the terms of vibrational modes of the respective binary glasses and films.

CG glasses and different structures on their base are promising for application in photonics and optical data storage. Direct surface patterning using composite nanomultilayer structures on the base of CG by a laser or electron beam without chemical etching, attracts high interest. Surface relief holographic diffraction gratings were directly recorded using composite As_2S_3:Ag/Se nano-multilayered structures. Diffraction efficiency values of the recorded gratings in transmission were ~22%. AFM measurements have shown high quality of the recorded gratings relief's. Process of surface relief formation depended on the polarization of recording light beams. Such media are also perspective for the recording of digital holograms. Reviewed investigation results concerning chalcogenide glasses show that chalcogenide glasses are perspective for various applications in photonics.

1. A.V. Stronski, L.O. Revutska, K.V. Shportko, Y. Polishchuk, O.P. Paiuk, V.Yu. Goroneskul. Journal of Optoelectronics and Advanced Materials, V. 25, No. 1-2, 2023, pp. 49-55.
2. M.V. Popovych, A.V. Stronski, K.V. Shportko. Structural properties of $Ga_{11.7}Ge_{14.1}Te_{74.2}$ alloys. Physics and Chemistry of Solid State, V. 23, No. 4, 2022, pp. 830-835.
3. A. Stronski, T. Kavetskyy, L. Revutska, K. Shportko, M. Popovych, I. Kaban, P. Jóvári. Journal of Non-Crystalline Solids, V. 572, 2021, p. 121075.
4. A.Stronski, L.Revutska, A.Meshalkin, O.Paiuk, E.Achimova, A.Korchovyi, K.Shportko, O.Gudymenko, A.Prisacar, A.Gubanova, G.Triduh. Optical Materials, V. 94, 2019, pp. 393-397.
5. A.Stronski, T.Kavetskyy, L.Revutska, I.Kaban, K.Shportko, J.Baran, M.Trzebiatowska. Journal of Non-Crystalline Solids, V. 521, 2019, p. 119533.
6. K.Shportko, L.Revutska, O.Paiuk, J.Baran, A.Stronski, A.Gubanova, E.Venger. Optical Materials, V. 73, 2017, pp. 4890-4896.

Optical studies of exciton-plasmon interactions in semiconductor-metal multilayer films and nanostructures

Stolyarchuk I.D., Dan'kiv O.O., Stolyarchuk A.I., Kuzyk O.V.

Drohobych Ivan Franko State Pedagogical University, Drohobych, Ukraine,
i.stolyarchuk@dspu.edu.ua

The developed in recent years new nanofabrication processes have led to a wealth of novel, engineered nanostructures with tunable size and shape parameters, providing researchers with unprecendented control over their electronic, optical and mechanical properties. The advantages of nanomaterials are not limited to controllable optical properties of single components but extend to the unique possibilities to combine different nanomaterials into composite structures. Such hybrid materials feature properties of two or more components and potentially synergistic properties caused by interactions between the nanoscale constituents. The number of possible hybrid materials that can be built from existing nanostructures is enormous. Hence, the potential for creating highly functional hybrid materials that enable, modify, and control energy processes and pathways is very promising. Especially, great perspectives are promised from deep optical studies of interactions of optical excitations in semiconductor-metal nanostructures. In particular, for semiconductor nanostructures optical excitations are defined by the electronic levels in the conduction and valence bands. Due to quantum confinement, the electronic levels in low-dimensional semiconductor structures are transformed in discrete energy sub-levels and this discrettance can be tuned by shape and size of nanoobjects. The fundamental optical excitations are transitions between these discrete sub-levels in both bands that lead to the formation of bound electron-hole pairs or excitons. In metal nanostructures the equivalents of excitons are so-called plasmons that are collective oscillations of conduction band electrons. The surface plasmons arise from dielectric contrast between the metal nanostructures and the nonconductive environment, and related surface plasmon resonance frequency can be tuned by their shape and size [1].

In this work, as examples of semiconductor-metal structures ZnO/Ag/ZnO multilayer films and CdS/Au colloidal nanocomposites have been chosen. ZnO thin films with thickness about 80 nm have been deposited by magnetron sputtering and pulsed laser deposition techniques. Thin layers of Ag with thicknesses from 0.5 nm to 10 nm have been deposited by thermal vacuum deposition method. The optical transmission spectra of the separate semiconductor, metal components and composite multilayer structures were measured for comparison. It was observed the enhancement of transmission coefficient in ZnO/Ag/ZnO multilayer films. This enhancement significantly depends on thickness of the Ag layer and crystal quality of the ZnO layers. In case of another structure type of CdS/Au colloidal nanocomposites it was found that mixing of conduction states at the interface of metal and semiconductor leads to the onset of unique optoelectronic properties. It was demonstrated suppression of surface plasmon oscillations in Au domains, which is attributed to the delocalization of plasma electrons into CdS part of the structure.

1. M. Achermannn, Exciton-Plasmon Interactions in Metal−Semiconductor Nanostructures. *J. Phys. Chem. Lett.* 2010. V. 1, P. 2837.

Half-metallicity and ferromagnetism in two-dimensional Cr_3Te_4 nanosheets

Kuzma M.

Institute of Materials Engineering, College of Natural Science, University of Rzeszow, Pigonia Str.1, 35-959 Rzeszow, Poland
mkuzma@ur.edu.pl

Two-dimensional ferromagnets with total spin polarization have recently been intensively studied due to their prospective application in spintronics. In two-dimensional systems, there is no long-range order according to Mermin-Wagner's theory [1]. In recent years, it has been possible to synthesize monolayers of the compounds $Cr_2Ge_2Te_6$ [2] ,CrI_3[3], Fe_3Te_2 [4], in which long-range order was observed. However, the Curie temperatures in these materials are far below room temperature. There is much hope for the non-stoichiometric chromium tellurides $Cr_{1-x}Te$. In the form of volume crystals, these compounds have been known for a long time [5]. Two-dimensional properties have been studied in monolayers of these compounds obtained by MCVD or MBE [6]. Some bulk crystals of chromium tellurides (*e.g.* Cr_2Te_3, Cr_3Te_4 , Cr_5Te_6) have layered crystal structure and they show quasi-two-dimensional magnetic properties [7].

In this work, we compare the structure and magnetic properties of monolayer Cr_3Te_4 with those of Cr_3Te_4 thick films. We also illustrate the quasi-two-dimensional magnetism of this material with the results of electron paramagnetic resonance measurements.

1. Mermin N.D., Wagner H. Absence of Ferromagnetism or Antiferromagnetism in One- or Two-Dimensional Isotropic Heisenberg Models. *Phys.Rev.Lett.* 1966. V. 17. P.1133-1136.
2. Gong C., Li L., Li Z., Ji H., Stern A., Xia Y., Cao T., Bao W., Wang C., Wang Y., Qiu Z.Q., Cava R.J., Louie S.G., Xia J., Zhang X. Discovery of intrinsic ferromagnetism in two-dimensional van der Waals crystals. *Nature.* 2017. V. 546. P. 265-269.
3. Huang B., Clark G., Navarro-Moratalla E., Klein D.R., Cheng R., Seyler K.L., Zhong D., Schmidgall E., McGuire M.A., Cobden D.H., Yao W., Xiao D., Jarillo-Herrero P., Xu X. Layer-dependent ferromagnetism in a van der Waals crystal down to the monolayer limit. *Nature.* 2017. V.546. P. 270-273.
4. Fei Z., Huang B., Malinowski P, Wang W., Song T., Sanchez J., Yao W., Xiao D., X. Zhu, May A.F., Wu W., Cobden D.H., Chu J.-H., X. Xu. Two-dimensional itinerant ferromagnetism in atomically thin Fe_3GeTe_2. *Nat. Mater.* 2018. V. 17. P.778-782.
5. Ipser H., Komarek K.L., Klepp K.O., Transition Metal-Chalcogen Systems: The Cr-Te Phase Diagram. *J. Less Common Met.* 1983. V. 92. P. 265-282.
6. Yang J., Zhu C., Deng Y., Tang B., Liu Z. Magnetism of two-dimensional chromium tellurides. *iScience.* V. 26. 2023. P. 106567.
7. Bester M., Stefaniuk I., Kuzma M. Quasi-Two-Dimensional Ferromagnetism in Cr_2Te_3 and Cr_5Te_8Crystals. *Acta Physica Polonica A.* V. 127. 2015. P. 433-435.

Infrared damping, visible and microwave transparent polymeric films with thin AlN coatings

Tsybrii Z.F., Sizov F.F.

V. Lashkaryov Institute of Semiconductor Physics, NAS of Ukraine,
41, pr. Nauky, 03028 Kyiv, Ukraine,
tsybrii@isp.kiev.ua

One of the important tasks for camouflage implementation is the development of flexible thin film coatings, which totally block IR radiation especially, e.g., in the range of wavelengths $\lambda \approx 7.5$ to 14 μm – that is a spectral range of operation of contemporary thermal IR cameras. In this spectral range up to 47% of the black body (b. b.) radiation of the whole EM spectral range, is radiated at temperatures t ~ 270 – 470 K (~ 0 – 200 ºC). In the spectral range of $\lambda \approx 7.5$ to 25 μm at these temperatures, up to 75% of the b. b. radiation is concentrated compared to the whole EM spectral region by the b. b. object. Therefore, it is an important task to reduce the IR visibility of objects heated to these temperatures at the specified spectral regions. It is also important to get such flexible coating layers shielding the IR radiation, which are at the same time being transparent in the visible, microwave and the THz spectral ranges (the latter two to be used, e.g., for 3G to 6G communications).

Flexible substrates based on Mylar, Polyethylene Terephthalate/$BaSO_4$ filling and Teflon polymeric films were applied to grow the AlN layers having the Reststrahlen Band at λ ~ 11–17 μm for filters, damping the IR radiation at this spectral region. The transparency and reflectivity properties of a number of the flexible polymeric thin films with the amorphous AlN coatings were investigated, together with the structural and morphological data, to prove the decrease of thermal visibility at the extended spectral range $\lambda \approx 7.5$ to 25 μm. The classical dielectric function model, using large damping factors Γ ~ 0.3, was applied to describe the reflection and absorption coefficients in polymeric films/AlN structures.

The best combination of polymers was determined, namely Polyvinyl chloride polymeric films without coatings and the Mylar/AlN structures to make composed damping filters for spectral range λ ~ 7.5 – 25 μm. The transparency of such composed filters in the spectral range λ ~ 7.5 to 25 μm can suppress about 96-98% of radiation from the objects being at t ~ 310 K. Polyvinyl chloride
(300 μm)/Mylar (20 μm)/AlN (3 μm) structures are transparent in the visible spectral range. The transparency of all polymeric/AlN structures in the microwave frequency range (ν = 60 – 270 GHz) gains T ≥ 80-90%.

Stimulated incoherent radiation of ZnO nanocrystals

Fedorenko L.L., Korbutyak D.V., Evtukh A.A., Naumov V.V., Yukhymchuk V.O.

V.E. Lashkaryov Institute of Semiconductor Physics,
National Academy of Sciences of Ukraine, 41 Prospect Nauky, Kyiv, Ukraine;
leonfdrn@gmail.com

In this work, scientific problems related to the fundamental possibility of developing new effective sources of incoherent stimulated radiation of a disordered medium based on nanostructured semiconductor layers of nano- and micro-sized ZnO crystals are solved. Such sources are able to prevent the speckles, as optical noise [1]. The structures of the disordered medium were produced on the basis of polydisperse nano- and microcrystalline (PNMC) ZnO powder, produced by the classic chemical-metallurgical method according to French technology in the high-temperature Velts furnace at the "UkrZink" enterprise. The technology for the formation and construction of the stimulated radiation source in the form of layers of compressed PNMC ZnO powder was developed and worked out. A comparative analysis of the optical, X-ray, spectral and structural properties of various types of disordered media based on ZnO crystallites led to the following conclusions:

• among the ZnO crystalline systems considered, PNMC ZnO showed random UV stimulated radiation (UV) (λ = 387 nm) with incoherent feedback, prevented the speckles in all excitation intensity ranges used.

• the average value of optical gain k at λ = 387 nm in PNMC ZnO powder as a random laser is estimated as ~ 150 cm^{-1}.

• increasing the light amplification efficiency of a disordered environment based on ZnO is considered promising in the case of using powders with 2D ZnO nanocrystallites.

• the dominant mechanism of UV emission at λ = 387 nm in ZnO PNMC powder at room temperature is radiative transitions caused by exciton-exciton scattering.

1. Cao H., Chriki R., Bittner S., Friesem A.A., Davidson N. Complex lasers with controllable coherence. *Nat. Rev. Phys*. 2019, 1, 156-168, https://doi.org/10.1038/s42254-018-0010-6.

Raman spectroscopy and X-ray diffraction studies of Ga-Ge-Te alloys

Popovych M.[1], Kochubei H.[1], Shportko K.[1], Lotnyk A.[2], Venger E.[1], Stronski A.[1]

[1]V.Lashkaryov Institute of Semiconductor Physics NAS Ukraine, Kyiv, Ukraine,
[2]Leibniz Institute of Surface Engineering, Leipzig, Germany
kochubei.hanna@gmail.com

Family of Ga-Ge-Te alloys is interesting due to versatile far-IR optics, phase change-type memory and sensor applications [1]. The structural features of chalcogenide glasses and films are important for various characteristics and processes, including photoinduced ones. The addition of Ga to GeTe alloys can influence crystallization timings and room [1] temperature stability. Accordingly, better understanding of the structural properties can help in the optimization of the sensitivity and relief formation processes of composite nanomultilayer structures based on chalcogenide glasses, which are promising for the direct recording of optical elements.

In the present report the amorphous Ga-Ge-Te alloys have been studied by X-ray diffraction and Raman spectroscopy. Studied bulk Ga-Ge-Te alloys were prepared by the conventional melt quenching technique. Composition was controlled using EDX. X-ray diffraction patterns of samples were recorded with use of the X-ray diffractometer with Bragg–Brentano geometry, using Cu Kα radiation 1.54178 Å and mounted graphite monochromator for a diffracted beam. The diffraction data were collected in the range of scattering vector magnitudes Q between 0.4 and 8 Å, $Q = 4\pi \sin\theta/\lambda$. All samples were examined in transmission geometry. Raman spectra of Ga-Ge-Te samples were measured in the spectral range from 50 to 400 cm^{-1} with the resolution set to 1 cm^{-1} with 256 scans collected in each experiment. All X-ray and Raman experiments were performed at ambient temperature.

The experimental X-ray diffraction patterns were used for calculations of radial distribution functions which have given the positions of the nearest-neighbour bond length r_1 and second-neighbour bond length r_2. Obtained r_1 values (2,65A for $Ga_{0.01}Ge_{0.19}Te_{0.8}$ and $Ga_{0.079}Ge_{0.114}Te_{0.806}$ glasses) were similar to observed for Ga-Ge-Te glasses of other compositions known from reference literature. The values of the r_2 / r_1 ratio are 1.63 and 1.68, respectively, which is close to typical 1.63 value for a regular tetrahedron structure. The calculated bond angle φ values are also in good agreement with other published data on GaGeTe alloys. Observed bands in the Raman spectra of Ga-Ge-Te alloys show that such glasses contain different nanophases and can be explained in the terms of vibrational modes of Ga-Te and Ge-Te glasses and films.

1. Popovych M.V., Stronski A.V., Shportko K.V. Structural properties of $Ga_{11.7}Ge_{14.1}Te_{74.2}$ alloys. *Physics and Chemistry of Solid State*. 2022. V. 23, No. 4, pp. 830-835.

Features of structural transformations during thermal annealing of InSb implanted with beryllium ions

Sapon S., Kulbachynskyi O., Gudymenko O.Yo., Dubikovskyi O., Maziar D.

V. Ye. Lashkaryov Institute of Semiconductor Physics, Kyiv, Ukraine
s.kulbachynskyi@gmail.com

Narrow-band indium antimonide semiconductor crystals are widely used to create highly sensitive IR sensors in the 3-5 μm spectral range. Almost the only method of forming p-n junctions in InSb is the ion implantation. Since implantation leads to the generation of defects, an important step in the formation of p-n junctions is the annealing of implanted structures.

In this work, n-type Te-doped InSb wafers with <111> orientation and current carrier concentration of $3\cdot10^{14}$cm^{-3} were implanted with Be^+ ions in two steps: 1) E=40 keV, D=$1\cdot10^{14}$ cm^{-2}; 2) E=110 keV, D=$1\cdot10^{13}$ cm^{-2} (Fig. 1a). The annealing of the structures was carried out in vacuum in the temperature range 280-380˚C for 50-300 sec. A 2-stage annealing at low and high temperatures was also performed. The map of the X-ray reflex (111) (Fig. 1b) shows additional diffuse scattering in the 2Theta-omega direction, which indicates the formation of a strain field in the near-surface region of the crystal. The shift of scattering in the omega direction, which forms peculiar bends, indicates the appearance of locally misoriented regions in the implanted area. Annealing to temperatures of 280^0 C does not lead to a significant change in the structure, and only an increase in temperature to 360^0 C allows to obtain a perfect structure in the implanted region (Fig. 1c), in which no deformations are observed and no additional mosaic blocks are formed.

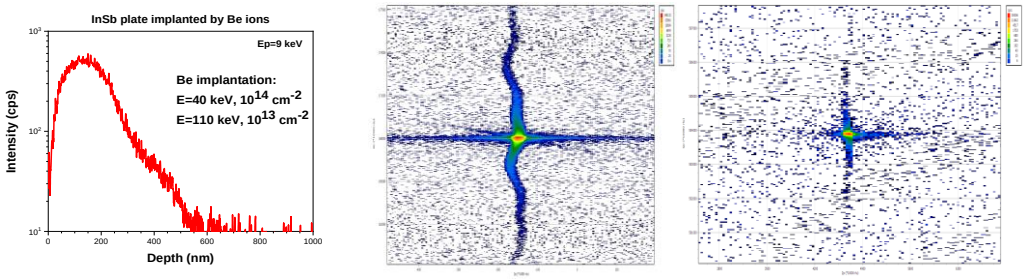

a b c

Fig. 1 SIMS distribution profile of the implanted Be^+9(a), map of the X-ray reflex (111) of the implanted sample (b) and after annealing (c)

A further increase in temperature leads to sublimation of Sb and its accumulation on the surface, which was confirmed by studies of Raman spectra. Electron microscopic studies of the structure were carried out. It was shown that the use of encapsulating coatings and the rate of increase in the annealing temperature are important factors for the annealing of defects. A model of the dynamics of annealing of point defects was constructed and their activation energy was determined.

Ultrafast inertia-free switching of double magnetic tunnel junctions

Dzhezherya Yu.[1], *Polynchuk P.*[1], *Kravets A.*[2,1] *and Korenivski V.*[2]

[1] *Institute of Magnetism of the NAS of Ukraine and MES of Ukraine, 03142 Kyiv, Ukraine*
[2] *Nanostructure Physics, Royal Institute of Technology, 10691 Stockholm, Sweden*
vk@kth.se

The development and improvement of non-volatile magnetic memory (MRAM) remains an important issue in the field of nanomagnetism. For such applications, it is extremely important to achieve reliable and fast magnetization switching [1], which exceeds the conventional slow precession switching, which can take up to nanoseconds to reorient the magnetization vector of a device.

We investigate the switching of a magnetic nanoparticle comprising the middle free layer of a memory cell based on a double magnetic tunnel junction under the combined effect of spin-polarized current and weak on-chip magnetic field. We obtain the timing and amplitude parameters for the current and field pulses needed to achieve 100 ps range inertia-free switching under least-power dissipation.

Based on the results of work [2], in our case for a double MRAM contact, under the condition P_1^2 , P_2^2 , $P^2 \ll 1$, we have $\kappa = \frac{\hbar \cdot (P_1 + P_2) \cdot J}{e \cdot 8\pi \cdot M_S^2 \cdot d}$, where P_1 and P_2 are the degree of polarization of conduction electrons in the upper and lower magnetic particles, P is the degree of polarization in the functional element. According to estimates, at $P \simeq 0.5$ the value of the current density will give the result $J = 1.7 \times 10^8$ A cm^{-2} $\sim 5 \times 10^{17}$ CGS unit I cm^{-2}. At first glance, this is a large current value. However, given the speed of the process, it will not lead to critical changes in the system.

We have determined the methods of controlling the magnetization states of a memory cell in a high-speed inertial-free mode. The optimal forms, sequences, and amplitudes of field pulses are defined.

1. Q.F. Xiao, B.C. Choi, J. Rudge, Y.K. Hong, G. Donohoe, J. Appl. Phys. 101 (2007) 024306.
2. D.C. Worledge, Theory of spin torque switching current for the double magnetic tunnel junction, IEEE Magnetics Letters 8, 4306505 (2017).

Doping-induced extrinsic magnetism in CdTe:Cr crystals

Popovych V.D.[1], *Dluzewski P.*[2], *Morawiec K.*[2], *Zajkowska W.*[2], *Popovych A.V.*[1], *Stolyarchuk I.D.*[1], *Żywczak A.*[3], *Kuzma M.*[4], *Shiojiri Makoto*[5]

[1]*Drohobych Ivan Franko State Pedagogical University, Drohobych, Ukraine,* vpopovych@dspu.edu.ua
[2]*Institute of Physics, Polish Academy of Science, Warsaw, Poland*
[3]*AGH University of Science and Technology, Krakow, Poland*
[4]*University of Rzeszow, Rzeszow, Poland*
[5]*Kyoto Institute of Technology, Kyoto, Japan*

Poor solubility of transition metals, except for Mn, in II-VI compounds hinders the formation of the homogeneous solid solution with FM of intrinsic type and leads to dopant separation. The above effect had been considered detrimental, however, controllable precipitation of magnetic elements was recently proposed to use as a tool to realize novel hybrid spintronic systems consisting of the semiconductor matrix with embedded TM-rich ferromagnetic nanocrystals [1].

We investigated crystallographic phase separation and its effect on the magnetism of CdTe single crystals doped with Cr to exceedance the solubility limit of this element. The doping was performed both directly during the crystals' growth by the physical vapor transport method [2] and by their implantation with a high fluence of Cr^+ ions [3]. XRD, SIMS and different analytical electron microscopy techniques revealed monoclinic Cr_3Te_4 precipitates in the form of a crystallographically oriented network of quasi-two-dimensional lamellas for the as-grown crystals, and nano-sized particles for the implanted ones. The crystals were found to be ferromagnetic from liquid nitrogen to above room temperatures by magnetization measurements. Off-axis electron holography experiments proved that their magnetic behavior was mainly governed by the Cr_3Te_4 particles, although a weak contribution of the $Cd_{1-x}Cr_xTe$ matrix can be also supposed. Lorentz holography and EMR investigations revealed the magnetocrystalline and shape anisotropies of the precipitates with their easy magnetic axis perpendicular to the [101] crystallographic direction of the zinc-blende structure.

1. Dietl T., Sato K., Fukushima T., Bonanni A., Jamet M., Barski A., Kuroda S., Tanaka M., Hai P.N. Spinodal nanodecomposition in semiconductors doped with transition metals. *Rev. Mod. Phys.* 2015. V. 87. P. 1311-1377.
2. Morawiec K., Popovych V.D., Zajkowska W., Dluzewski P., Zywczak A., Sagan P., Skvarok Yu.Yu., Kuzma M., Shiojiri M. Microstructure and magnetic properties of vapor-grown CdTe:Cr crystals with doping-induced precipitates. *J. Mater. Sci*. 2023. V. 58. P. 5705-5717.
3. Popovych V.D., Böttger R., Heller R., Zhou S., Bester M., Cieniek B., Mroczka R., Lopucki R., Sagan P., Kuzma M. Heavy doping of CdTe single crystals by Cr ion implantation. *Nucl. Instr, Meth. Pnys. Res. B.* 2018. V. 419. P. 26-31.

Structural studies of As_2S_3:Mn glasses

Kochubei H., Stronski A., Paiuk O., Gudymenko A.

V. Lashkaryov Institute of Semiconductor Physics NAS Ukraine, Kyiv, Ukraine
kochubei.hanna@gmail.com

Chalcogenide glasses can be used in various photonics applications: IR optics, sensorics, optoelectronics, holography, integrated and fiber optics both for passive and active applications. Optical, luminescent, electrical, thermophysical, mechanical, magnetic properties of chalcogenide glasses can be changed by doping with different elements (optically active rare-earth and transition metal ions, etc.) [1], and this area is of special interest and numerous studies. The present work was devoted to studies of the influence of Mn doping on structural properties of As_2S_3 chalcogenide glasses by X-ray diffraction.

Glasses were prepared by the conventional melt quenching technique. The prepared bulk glasses As_2S_3:Mn ($Mn0{,}1\%$; $Mn0{,}5\%$; $Mn1\%$; $Mn2\%$; $Mn2{,}5\%$) were cut into plates of 1 mm in thickness and polished to yield samples with high quality flat surfaces. X-ray diffraction measurements (XRD) were carried out using ARL X'tra (Thermo scientific) installation. Cu Kα radiation (λ=0.154 nm) was used. Measurements were carried out at room temperature. X-ray diffraction patterns (diffraction spectra were recorded by Θ-Θ -scanning in 2–140° range) confirm the amorphous nature of the bulk samples of studied chalcogenide glasses. Obtained diffraction data were used for calculation (program RAD GTK+ was used) of radial distribution functions and short range order parameters (shown in table 1).

Table 1. Radial distribution functions and short range order parameters

Composition	r_1	r_2	r_2/r_1	φ
As_2S_3	2,31	3,35	1,45	92,96
$As_2S_3:Mn0{,}1\%$	2,31	3,36	1,46	93,32
$As_2S_3:Mn0{,}5\%$	2,32	3,37	1,45	93,15
$As_2S_3:Mn1\%$	2,32	3,37	1,45	93,15
$As_2S_3:Mn2\%$	2,32	3,36	1,45	92,79
$As_2S_3:Mn2{,}5\%$	2,33	3,37	1,45	92,64

Bond angle φ values were calculated using obtained positions of the nearest-neighbor bond length r_1 and second-neighbor bond length r_2 in relation: $\varphi = 2\cdot\arcsin(r_2/2r_1)$. Changes of short range order parameters with Mn concentration of As_2S_3:Mn glasses were within calculation errors of RAD GTK+ program: ± 0.02 Å.

1. A. Stronski, O. Paiuk, A. Gudymenko, et.al. Ceramics International, V. 41, I. 6, 2015, pp. 7543-7548.

Some peculiarities of structural changes in chalcogenide glasses $(GeS_3)_{100-x}Ag_x$, $(GeS_2)_{100-x}Ag_x$ and $(Ge_{42}S_{58})_{100-x}Ag_x$

Lishchynskyy I.M.[1], *Kaban I.G.*[2], *Voitkiv H.V.*[1], *Poplavskyy O.P.*[1], *Stronski A.V.*[3]

[1]*Vasyl Stefanyk Precarpathian National University, Ivano-Frankivsk, Ukraine,*
igor.lishchynskyy@pnu.edu.ua
[2]*Leibniz Institute for Solid State and Materials Research, Dresden, Germany*
[3]*V.Lashkaryov Institute of semiconductor physics NAS Ukraine, Kyiv, Ukraine*

In our time, the amount of digital information is increasing, and the demand for memory devices capable of storing, transmitting, and processing this information is also growing. Currently, flash memory based on charge storage is widely used in mobile phones and music players, steadily replacing hard drives in PCs and even in data processing centers. However, flash memory faces a scaling-down problem due to charge leakage from the storage layer. From this point of view, alternative memory technologies have been proposed, such as phase-change memory (PCM) and conductive bridging memory (CBM).

PCM operates based on energy-independent reversible switching of the active material, e.g., Ge-Sb-Te chalcogenide, from amorphous to crystalline state, characterized by a significant difference in specific electrical resistance. The transformation from amorphous to crystalline state is thermally controlled by the current passing through the material.

It has long been known that chalcogenide glasses, which are primarily semiconductors, become superionic conductors when doped with metals. Ge-S-Ag glasses are very attractive, primarily due to significantly higher glass transition temperature and, as a result, better thermal stability compared to glasses based on other materials. Additionally, Ge-S-Ag glasses do not contain toxic elements.

In this work, we investigate the microstructure of chalcogenide glasses $(GeS_3)_{100-x}Ag_x$, $(GeS_2)_{100-x}Ag_x$ and $(Ge_{42}S_{58})_{100-x}Ag_x$, expanding the available composition range. Studies along the system of „chalcogenide glass-silver“ lines are also of interest for CBM applications, where the chalcogenide glass acts as a matrix and Ag atoms diffuse into the matrix from the silver electrode.

The intensities of the main three XRD and ND peaks were analyzed and compared with corresponding SEM images. The intensity of the first sharp diffraction peak (FSDP) of XRD of GeS_3 and $Ge_{42}S_{58}$ glasses decreases, while its position at approximately 1.06 $Å^{-1}$ remains constant.

The second maximum shifts towards smaller values of the diffraction vector Q, and its intensity increases. Subsequent maxima also shift towards smaller values of Q, but the intensity of oscillations decreases with increasing Ag concentration.

A more detailed analysis shows that for homogeneous glasses $Ge_{42}S_{58}$, the position of Q_{FSDP} increases almost linearly, while for segregated phases GeS_3 and GeS_2, it deviates from linearity.

Doping-induced second phases in vapour-grown CdTe crystals

Popovych A.V.[1], *Rehei M.A.*[1], *Shakleina I.O.*[1,2], *Popovych V.D.*[1]

[1]*Drohobych Ivan Franko State Pedagogical University, Drohobych, Ukraine,*
andriy.popovich@dspu.edu.ua
[2]*Lviv Polytechnic National University, Lviv, Ukraine*

Cadmium telluride crystals are now used on the industrial scale for the fabrication of a great variety of optoelectronic components [1], which is largely due to the possibility of a considerable tuning of their physical properties by the appropriate doping. In particular, compensating doping with chlorine is a typical approach to obtain semi-insulating material for the production of uncooled high-energy radiation detectors, whereas alloying with chromium should induce high-temperature ferromagnetism into this compound making it very perspective for the spintronic application. However, since the solubility of the above impurities in CdTe is rather low, a high doping level may result in their separation.

The work presents a comparative analysis of the impurity segregation effect in the heavily doped CdTe:Cl and CdTe:Cr single crystals grown by the modified physical vapour transport method [2]. Dopant-enriched particles were revealed by optical and electron microscopy and energy-dispersive X-ray analysis on the chemically treated surfaces of both types of crystals. They are developed when the solubility limits of Cl and Cr in the CdTe matrix are exceeded, estimated to be about 10^{19} cm^{-3} and 0.1 at.%, respectively, from the secondary ion mass-spectroscopy experiments. The morphology, crystallography and mechanism of formation of the above second phases were found to be quite different. The predominant size of the particles in CdTe:Cl are from several to several tens of μm. The particles are considered as inclusions since their formation can be explained by the transition from two- (vapour-solid) to three-phase (vapor-liquid-solid) crystallization mechanism due to the appearance of hypoeutectic solutions of the pseudobinary system CdTe–$CdCl_2$ in the morphologically unstable sites of the crystallization front. The dopant separation in CdTe:Cr brings out a regular network of quasi-two-dimensional lamellas, which were crystallographically oriented with respect to the host lattice. They were identified by high-resolution transmission electron microscopy as the precipitates of monoclinic Cr_3Te_4 compound developed upon the post-grown cooling of the crystals.

1. Triboulet R., Siffert P. CdTe and Related Compounds: Physics, Defects, Hetero- and Nano-Structures, Crystal Growth, Surface and Applications, Elsevier Ltd., Amsterdam, 2010.
2. Popovych V.D., Virt I.S., Sizov F.F., Tetyorkin V.V., Tsybrii (Ivasiv) Z.F., Darchuk L.O., Parfenjuk O.A., Ilashchuk M.I. The effect of chlorine doping concentration on the quality of CdTe single crystals grown by the modified physical vapor transport method, J. Cryst. Growth, 2007, V. 308, P. 63-70.

Advanced organic-inorganic ureasil-based and photocross-linked polymers for controlled biosensing

Kavetskyy T.S.[1,2], *Kukhazh Y.Y.*[1], *Hoivanovych N.K.*[1], *Dyachok D.O.*[3], *Demkiv O.M.*[4,5], *Ostrauskaite J.*[6], *Zgardzińska B.*[7], *Šauša O.*[2,8], *Kiv A.E.*[3,9]

[1]*Drohobych Ivan Franko State Pedagogical University, Drohobych, Ukraine,*
[2]*Institute of Physics, Slovak Academy of Sciences, Bratislava, Slovakia,*
kavetskyy@yahoo.com,
[3]*South Ukrainian National Pedagogical University named after K.D. Ushynsky, Odesa, Ukraine, kiv.arnold20@gmail.com,*
[4]*Institute of Cell Biology, NAS of Ukraine, Lviv, Ukraine,*
[5]*Institute of Physical Chemistry, Polish Academy of Sciences, Warsaw, Poland,*
[6]*Kaunas University of Technology, Kaunas, Lithuania,*
[7]*Institute of Physics, Maria Curie-Sklodowska University, Lublin, Poland,*
[8]*Department of Nuclear Chemistry, Comenius University, Bratislava, Slovakia,*
[9]*Ben-Gurion University of the Negev, Beer-Sheva, Israel*

Usage of polymer materials as holding matrixes of immobilized enzyme is an innovative approach in a construction of the amperometric biosensors. The constructed laccase-biosensor based on the ureasil-polymer composite was characterized by a very high sensitivity, but a weak point of the biosensor was very strong unexpected electrochemical noise at chronoamperometric test [1]. New perspectives of the ureasil-based and photocross-linked polymers for construction of amperometric enzyme biosensors were further found. On the basis of comprehensive analysis of the results obtained on the nanostructure and detection properties of ureasil and photocross-linked polymers of different prehistory and composition, a correlation of network properties of polymer matrixes with parameters of electrochemical biosensors is verified and it seems to be fundamental in origin for controlled biosensing. The development of the predicted laccase-biosensor can be used for assay of phenolic compounds in the wastewater and drinking water according to the required needs of analysis.

This work was supported in part by the MESU (projects Nos. 0122U000850, 0122U000874, and 0123U103572), NRFU (projects Nos. 2020.02/0100 and 2021.01/0010), VEGA (project No. 2/0134/21), and APVV (project No. APVV-21-0335). K.T.S. and K.Y.Y. also acknowledge the SAIA for NSP scholarships. This work has also received funding through the MSCA4Ukraine project (grant No. 1128327), which is funded by the European Union, and the EURIZON project (grant EU-3022), which is funded by the European Union (EURIZON H2020 project) under grant agreement No. 871072.

1. Kavetskyy T., Smutok O., Gonchar M., et al. Laccase-containing ureasil-polymer composite as the sensing layer of an amperometric biosensor. *J. Appl. Polym. Sci.* 2017. V. 134. P. 45278.

About decisive role of minority current carriers in the emergence of superconductivity

Uhryn Yu.O.

Drohobych Ivan Franko State Pedagogical University, Drohobych, Ukraine,
yuriyuhryn@yahoo.com.ua

It is known that minority current carriers in solids influence on their galvanomagnetic effects only when their mobility is much more then mobility of majority ones. The essence of new method of minority current carriers parameters determination in solids [1] consist in that we should measure magnetofield dependence of resistivity $\rho_{xx,}$ find there flex point B_f, resistivity in this point ρ_f and zero field resistivity ρ_0. Then minority current carriers mobility one can calculate by equation:

$$\mu = \frac{\sqrt{3}}{B_f}\left(\frac{4\rho_f}{3\rho_0} - 1\right). \quad (1)$$

The applying this method to conventional as well as high-temperature superconductors shows that by cooling them in a small temperature range ($\approx$1K) near the critical temperature, the mobility of minority current carriers increases by an orders. For example, in $YBa_2Cu_3O_7$ with T_c=92K this mobility increases from 8 to 60 m^2/ (Vs) when the temperature decreases from 92.7 to 92.1 K. In the same time, majority current carriers mobility remains to be constant as it follows by another equation from [1]:

$$\frac{\sigma_{min}}{\sigma_{maj}} = 4\left(\frac{\rho_f}{\rho_0} - 1\right), \quad (2)$$

where σ_{min} and σ_{maj} are minority and majority current carriers conductivity correspondingly.

Hall-effect experiments in superconductors [2] with our two-band model analysis shows the same outcome. The magnetofield dependence of the Hall resistivity with the the superconducting transition onset indicates the participation in the phenomenon of another type of current carriers that did not manifest themselves in the normal state. The calculation by the two-band model shows a large mobility of these carriers.

Consequently, quantitative analysis of galvanomagnetic effects near critical temperature in superconductors prompts us to make conclusion that exactly minority charge carriers are responsible for superconductivity.

1. Y.O. Uhryn, R.M. Peleshchak, V.B. Brytan, A.A. Velchenko, Magnetoresistance based determination of basic parameters of minority charge carriers in solid matter. Condensed Matter Physics, 2017, V. 20, No 4, P. 43702: 1-7.
2. N.P. Breznay, A. Kapitulnik, Observation of the ghost critical field for superconducting fluctuations in a disordered TaN thin film. Phys. Rev. B. 2013, V. 88, P. 10451.

SECTION B:

Semiconductor low-dimensional structures: advances in synthesis, characterization, theoretical modeling and applications

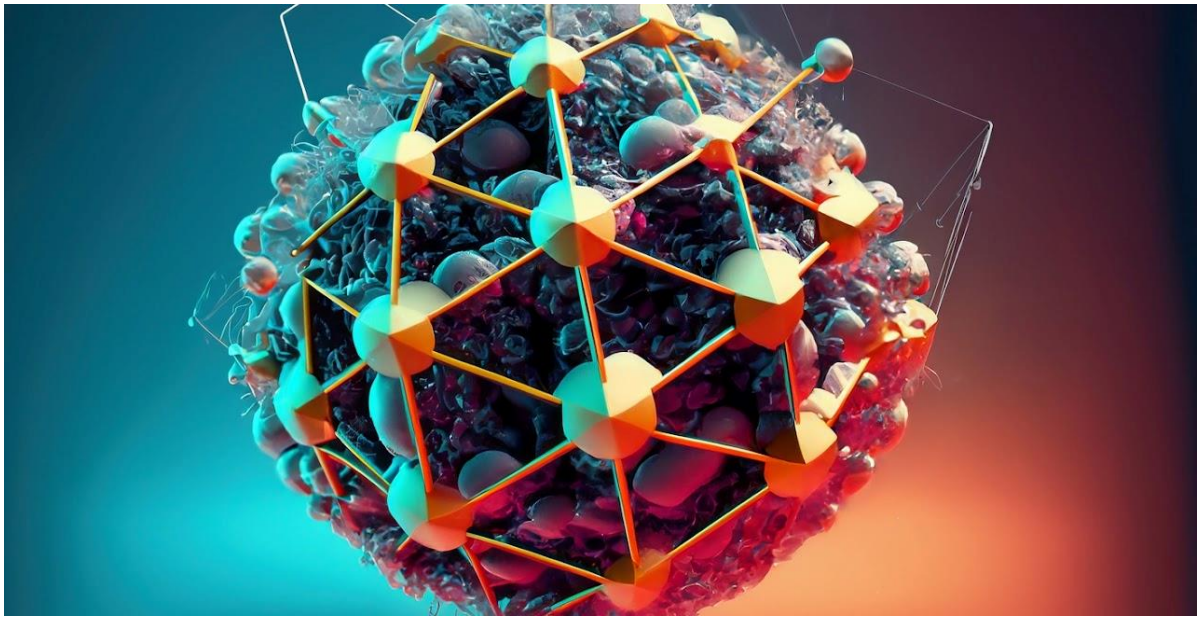

Strain stresses in ZnO:Mn nanocrystals

Kovalenko O.V., Vorovsky V.Yu., Slavnyi V.V.

Oles Honchar Dnipro National University, Dnipro, Ukraine
e-mail: kovalenko.dnu@gmail.com

The paper presents the results of studies of the strain stresses (ε) that occur in the crystal lattice of ZnO:Mn nanocrystals (NCs) during their synthesis by the method of ultrasonic spray pyrolysis (USP). Samples of ZnO and ZnO:Mn NCs with a concentration of Mn impurity of 2 at.% and 4 at.% were synthesized using a zinc nitrate solution with a concentration of 5%. By analyzing the reflexes of the X-ray diffraction patterns of the samples using the Williamson-Hall method [1], it was shown that with an increase in the concentration of Mn impurity, the value of ε varies from $3.27 \cdot 10^{-4}$ to $22.4 \cdot 10^{-4}$ (Fig. 1.a). These values of ε are much lower than those obtained for samples of ZnO:Mn NCs synthesized from a solution of zinc nitrate with a concentration of 10%. This decrease in the value of ε is explained by an increase in the time interval during which the NCs were in a state of thermal annealing. This, in turn, affects the process of doping ZnO NCs with an Mn impurity.

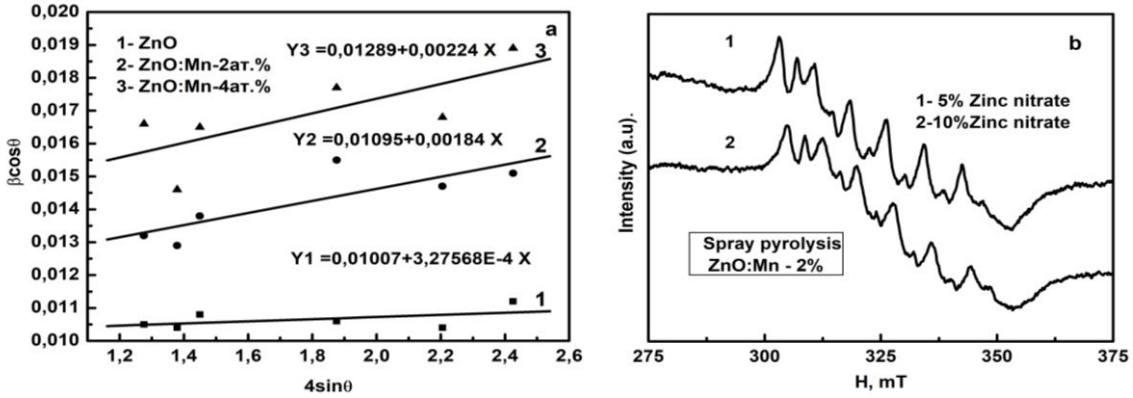

Fig. 1. Results of stress calculations in NC by the Williamson-Hall method (a): 1 - ZnO, 2 - ZnO:Mn - 2at.%, 3 - ZnO:Mn - 4at.%. EPR spectra of ZnO:Mn - 2at.% NC samples (b) obtained from a zinc nitrate solution of 5% -1, 10% -2.

EPR studies of the samples confirm this assumption. In Fig. 1b shows the EPR spectra of ZnO:Mn NCs with a concentration of Mn 2at.%, which were obtained from solutions of different concentrations of zinc nitrate. The greater intensity of the lines of the ultrafine structure of Mn^{2+} ions in the EPR spectrum of the ZnO:Mn - 2at.% NC sample obtained from a 5% zinc nitrate solution indicates a more intense process of NC doping with Mn admixture.

1. Williamson G.K., Hall W.H. X-ray line broadening from filed aluminum and wolfram // Acta Metall. – 1953. – V.1. – P. 22-31.

Antimonene: from a large scale growth of new structural phase to ferromagnetic heterostructures

Zdyb R.

Institute of Physics, Maria Curie-Sklodowska University, Lublin, Poland,
ryszard.zdyb@umcs.pl

Like many other two-dimensional (2D) materials those built of elements of the 15th group of the periodic table are believed to be good candidates for future electronic, optoelectronic and spintronic devices. Phosphorene, arsenene, antimonene and bizmuthene are expected to possess high mobility of charge carriers and direct band gap. Moreover, it appears that basic properties of the band gap (direct or indirect and its value) can be easily tuned by functionalization of 2D materials. Among its neighbours antimonene has many additional advantages e.g. it is resistant to oxidation, it does not degrade in contact with water and may possess ferromagnetic order at room temperature. Theory predicts numerous phases of antimonene [1], however, only two of them have been synthesized: the α phase with a puckered structure with two atomic sublayers [2] and the β phase with a buckled honeycomb structure [3].

This contribution presents results of experimental and theoretical studies of various phases and heterostructures consisting of antimonene. It starts from a new structural phase of single layer of antimony atoms [4] with its unique electronic structure. Then, the temperature dependent growth of antimonene is presented. It results either in a step flow growth of a large scale homogenous single layer of the α phase or a mixture of the alpha and beta phases forming self-twisted bilayers. In the final part an example of ferromagnetic heterostructure consisting of antimonene will be presented.

Acknowledgments: This research was in part funded by the National Science Centre (Poland) under Grant No 2020/37/B/ST5/03540.

1. Zhang S., Xie M., Li F., Yan Z., Li Y., Kan E., Liu W., Chen Z., Zeng H. Semiconducting Group 15 Monolayers: A Broad Range of Band Gaps and High Carrier Mobilities. *Angew. Chem.* 2016. V. 128, P. 1698.
2. Märkl T., Kowalczyk P.J., Le Ster M., Mahajan I.V., Pirie H., Ahmed Z., Bian G., Wang X., Chiang T.-C., Brown S.A. Engineering multiple topological phases in nanoscale Van der Waals heterostructures: realisation of α-antimonene. *2D Mater.* 2018. V. 5, P. 011002.
3. Ji J., Song X., Liu J., Yan Z., Huo C., Zhang S., Su M., Liao L., Wang W., Ni Z., Hao Y., Zeng H. Two-dimensional antimonene single crystals grown by van der Waals epitaxy. *Nat. Commun.* 2016. V. 7, P. 13352.

Quantum Cluster Embedding Description of Electron Localization in Disordered and Strongly Correlated Systems

Terletska H.

Department of Physics and Astronomy, Middle Tennessee State University, Murfreesboro, TN 37132, USA, Hanna.Terletska@mtsu.edu

Many-body quantum cluster embedding schemes—DCA (Dynamical Cluster Approximation), CDMFT (Cluster DMFT), and TMDCA (Typical Medium DCA)—serve as robust computational tools to address the critical non-local spatial correlations relevant for understanding the interaction and disorder-induced phase transitions.

In this talk, I will present our recent study using cluster embedding methods applied to both two and three-dimensional Anderson and Hubbard models.

Our findings underscore pronounced non-local, long-range correlation effects around localizations, emphasizing the important role of non-local descriptions in capturing metal-insulator transitions in such systems.

Furthermore, we conduct a comparative benchmark between various quantum cluster embedding DMFT techniques, accentuating their precision in delineating metal-to-insulator phase transitions within the Hubbard and Anderson model frameworks.

This work is supported by NSF DMR grant # 1944974 and DOE DE-SC0024196 grant.

Quantum Cone – Nano Source of Light with Dispersive Spectrum, Separated in Time and Space

Medvids A.[1], *Ščajev P.*[2], *Kazuhiko H.*[3]

[1]*Riga Technical University, LV 1048, Latvia, medvids@latnet.lv*
[2]*Vilnius University, Vilnius 10257, Saulėtekio Av. 3, Lithuania*
[3]*Shizuoka University, 3-5-1 Johoku, Naka-ku, Hamamatsu, Japan*

Nanostructures (NSs) are the most investigated object in solid-state physics, especially the Quantum confinement effect in quantum dots – 0D, quantum wires – 1D, and quantum wells – 2D systems. Because at these conditions constructing new electronic and optical devices is possible. Twenty years ago, have found a new quantum system, so-called Quantum cone in Ge single crystal [1, 2] possesses unique optical properties: huge "blue shift" of photoluminescence (PL) spectrum on 1.1 eV with increased intensity more than a million times, with period 1 μ of pattern C_{6i} point group symmetry and "redshift" of LO phonon line frequency on 6 cm^{-1} in Raman spectrum. The symmetry of PL band and sharp LO phonon line in Raman spectrum is evidence present of OD quantum cone. The appearance of a new band in the PL spectrum of CdZnTe slid solution is explained by the exciton quantum confinement effect in quantum cones [3]. Irradiation of SiO_2/Si structure by Nd:YAG laser as led to the formation of nanocones which possesses unique PL spectrum: "blue shift" on 1.1 eV, an asymmetric wide band from 1.1 eV till 2.2 eV with gradually decreases intensity in the red part of the spectrum, rainbow-like spectrum, and maximum of PL intensity increase more than million times [4]. These properties of the system of PL spectrum are typical for graded bandgap semiconductors. It means that the quantum cone with the solid angle at top of the cone less than 60° is a 1D system with a gradually decreasing diameter from the base to the top of the cone. Therefore, where the cone diameter is equal to or less than Bohr's radius of an electron or exciton quantum confinement effect takes place [5]. Colossal increase intensity of PL and shift of maximum in the blue part of the spectrum takes place due to transformation of Si and Ge crystal from indirect to quasi direct and confinement of electron-hole pair in the quantum cone. These facts speak in forward to the possibility of a gradual decrease of the lifetime of electron-hole pairs or excitons from base to top of a cone. The aim of this study is to determine the change of electron-hole pairs lifetime depending on height in a cone using the kinetics of the PL method. PL kinetic of diamond-like carbon sample with nanocones diameters on the base 100 nm and top 2 nm and hight 60 nm is investigated. The kinetic is described by stretched exponent $I_{PL} = I_0 \exp(-(t/\tau_0)\beta)$, where $\tau_0 = 5 \cdot 10^2$ ps, $\beta = 0.5$. It means, τ decreases from base to top of cone monotonously from 1 ns to 50 ps.

1. A. Medvid', Y. Fukuda, A. Michko, P. Onufrievs, Y. Anma. *Applied Surface Science*, 2005, 244. P.120-125.
2. A. Medvid', I. Dmytruk, P. Onufrijevs, I. Pundyk. *Physica status solidi (c)*, 2007, 4. P.3066.
3. A. Medvid', A. Mychko, V. Gnatyuk, S. Levytskyi, Y. Naseka. *Optical Materials*, 2010, 32. P.836-840.
4. A. Medvid', I. Dmitruk, P. Onufrijevs, I. Pundyk. *Solid State Phenomena*, 2008, 131. P.559.
5. A. Medvids, P. Onufrijevs, A. Mychko. *Nanoscale research letters*, 2011, 6. P.582-586.

Напівпровідникові властивості комплексних сполук германію

Лепіх Я.І.

Міжвідомчий науково-навчальний фізико-технічний центр МОН і НАН України при ОНУ імені І.І. Мечникова, Одеса, Україна, ndl_lepikh@onu.edu.ua

Комплексні сполуки германію Ge(IV) з органічними молекулами являються новим і перспективним класом функціональних матеріалів з достатньо вдалим поєднанням фізико-хімічних і електрофізичних властивостей корисних в багатьох аспектах їх використання від медицини до мікроелектроніки.

Проведені нами раніше дослідження стосувалися головним чином структури комплексонів, їх оптичних, електрофізичних і адсорбційних властивостей і можливостей їх практичного застосування [1-2].

Особливістю таких комплексонатів є їх супрамолекулярна структура, в якій Ge поєднуються з органічними молекулами у вигляді певного координаційного з'єднання, а також те, що фізико-хімічні і електрофізичні властивості можуть бути відносно легко модифіковані шляхом введення до їх складу відповідних домішок.

В даній роботі наведені результати досліджень напівпровідникових властивостей Ge (IV) з оксиетилендифосфонова оксиетилендифосфоновою кислотою, за відомим скороченням ОЕДФ, яка випускається промисловістю різних країн. Відмінною рисою молекули ОЕДФ як ліганда являється її висока гнучкість і можливість широкого варіювання міжатомними відстанями в комплексах різних металів.

Дослідження напівпровідникових властивостей комплексонату Ge - ОЕДФ проводилось на зразках плівок товщиною 1 мкм, отриманих з водних розчинів на поверхні скляних підкладок. Для зміцнення поверхні плівок у розчин КГ додавався полівініловий спирт. Срібні контакти наносились методом трафаретного друку. Визначалась питома провідність плівки, ВАХ, залежність σ(T) від температури для комплексонату Ge – ОЕДФ – винна кислота, Ge – ОЕДФ – лимонна кислота.

Дослідження залежності електричного опору плівок ОЕДФ – Ge від температури показали наявність суттєвого пониження ρ з ростом температури, що характерно для напівпровідникових матеріалів. Залежність σ(T) мала експоненціальний характер, з яких були визначені енергії активації носіїв заряду для всіх зразків. Залежність lnσ(T) мала лінійних характер для всіх зразків, а енергія активації Ea≈1,26 еВ для температур менших 333К, а для Т більших за 333К Ea≈1,279 еВ.

Таким чином, дослідження показали, що комплексні сполуки Ge з супрамолекулярною структурою органічних молекул володіють напівпровідниковими властивостями, що може бути корисним для практичних застосувань.

1. Lepikh Ya.I., Pronichkin V.D., Martsynko E.E. // Ukr.J.Phys. – 2005. – V.50 – N 4. – P. 380-384.
2. Lepikh Ya.I. // Abstract Book of the International research and practice conference "Nanotechnology and nanomaterials" (August 16-19, 2023, Bukovel). – Kyiv : LLC APFPOLYGRAPH SERVICE, 2023. – P. 363.

Perspectives, problems and tasks in the theory of multi-level quasiparticles interacting with phonons in nanostructures

Tkach M.V.[1], *Seti Ju.O.*[1, 2], *Voitsekhivska O.M.*[1]

[1]*Yuriy Fedkovych Chernivtsi National University, Chernivtsi, Ukraine,*
m.tkach@chnu.edu.ua, j.seti@chnu.edu.ua, o.voitsekhivska@chnu.edu.ua
[2]*Lviv Polytechnic National University, Lviv, Ukraine, yuliia.o.seti@lpnu.ua*

Multi-level (multi-band) systems of electrons interacting with polarization phonons in nanostructures are the main elements ensuring the successful functioning of modern nano devices – quantum cascade detectors and quantum cascade lasers operating in actual infrared range [1, 2]. However, despite their practical implementation, a consistent theory of physical processes in such structures is still absent due to the mathematical problems of quantum field theory. In particular, in general case of multi-band systems there are difficulties when calculating the renormalized mass operator of quasiparticles because of well-known problem of sign.

In our previous papers based at the Feynman-Pines diagram technique, the models of localized quasiparticles (at $\vec{k} = 0$) interacting with polarization phonons were studied within the approach in which in the process of summing of infinite ranges of mass operator diagrams, part of diagrams degenerate. As a result, the complete mass operator is essentially simplified. I made possible to present consistently the mass operator by arranging in blocks of series of diagrams with respect to the maximal number of phonons in each.

For the examples of two- and three-level systems in the abovementioned (schematic) approach [3, 4], the renormalized energy spectra of quasiparticle are calculated and analyzed. It turned out that these spectra contain both the main and satellite states. Their properties are similar to that obtained in the presented paper. Here the one- and two- phonon processes are accurately taken into account for the first time. Such approach will be obviously be valid in the case of a bigger number of phonons. That will open the perspective to expand the developed theory for the localized quasiparticle for the case of multi-level quasiparticles in nanostructures.

1. Faist J. Quantum cascade lasers. Oxford University Press, 2013, 328 p.
2. Delga A. Quantum cascade detectors: A review. Woodhead Publishing Series in Electronic and Optical Materials, 2020, P. 337-377.
3. Tkach M.V., Seti Ju.O., Voitsekhivska O.M Diagram technique in the method of Green's functions for the quasiparticles interacting with phonons. Chernivtsi, 2019, 164 p.
4. Tkach M., Seti Ju., Pytiuk O., Voitsekhivska O., Gutiv V. Spectrum of localized three-level quasiparticle resonantly interacting with polarization phonons at cryogenic temperature. Applied Nanoscience, 2020, V. 10, P. 2581-2591.

Ultra-small quantum dots: effect of crystal structure disorder

Kupchak I.M., Korbutyak D.V.

V. Lashkaryov Institute of Semiconductor Physics, NAS Ukraine, Kyiv, Ukraine
kupchak@isp.kiev.ua

Semiconductor Quantum dots (QDs) are an important material for use in medical purposes for "contrasting" in magnetic resonance imaging, as a material for targeted delivery of drugs to diseased cells, etc. [1]. However, the most straightforward is their application in light-emitting devices due to the spatial confinement effect, which provides a unique opportunity to change the band gap and, accordingly, obtain a wide range of exciton luminescence spectra with a high quantum yield. With further reduction the size of QDs, the surface/volume ratio increases rapidly, leading to practically jump-like changes in the optical spectra due to the activation of additional luminescence channels. This effect is most prominent in ultra-small (less than 2 nm) quantum dots containing a certain, well-defined number of atoms (magic numbers), and characterized by sharp absorption of light and almost completely surface luminescence [2].

In this paper we investigate the effect of crystal structure disordering on the electronic and optical characteristics of ultrasmall A_2B_6 quantum dots. The characteristics of quasiparticles (electron, hole, and phonon) were calculated in the approximation of effective masses based on the local atomic structure of the QD, which, in turn, was calculated by the density functional method. The calculations were performed on the model atomic cluster $(CdX)_n$, n=9..98, X=Te, S, passivated by effective fragments of the thiol-glycolic acid molecule. It is shown that for clusters of large sizes, the atomic structure is practically homogeneous, but the near-surface layer demonstrates significant reorganisation of chemical bonds and, therefore, can strongly influence the characteristics of quasiparticles. Such effect is partially eliminated by the surface passivation for the CdS clusters due to more natural Cd-S bonds with S atoms from thiol-glycolic acid molecule, but remains significant for CdTe clusters. For smaller clusters, the entair crystal structure is strongly disordered even for passivated surfaces, what significantly affects their optical characteristics, although this affect is somewhat weeker in the case of CdS clusters.

1. Korbutyak D.V., Kovalenko O.V, Budzulyak S.I, Melnychuk O.V. Nanostructures of A_2B_6 semiconductors : *Monograph* (Nizhyn Mykola Gogol State University) 2020, 183 p. [ISBN: 978-617-527-223-7].
2. Valakh M., Dzhagan V., Raevskaya O., Kuchmiy C. Optical investigations of ultra-small colloidal nanoparticles and heteronanoparticles based on II−VI semiconductors // Ukr. J. Phys. – 2011. – V. 56. – № 10. – P. 1080-1090.

Features of surface morphology and defect formation of $Pb_{1-x}Cd_xTe$ thin films prepared by PVD

Mazur T.M.[1], Naidych B.P.[2], Holovata O.B.[2], Parashchuk T.O.[3], Zamurujeva O.V.[4], Yavorskyi Y.S.[2], Mazur M.P.[1], Nykyruy L.I.[2], Yavorskyi R.S.[2]

[1]Ivano-Frankivsk National Technical University of Oil and Gas, Ivano-Frankivsk, Ukraine, tetiana.mazur@nung.edu.ua
[2]Vasyl Stefanyk Precarpathian National University, Ivano-Frankivsk, Ukraine, lyubomyr.nykyruy@pnu.edu.ua
[3]AGH University of Krakow, Krakow, Poland, parashchuk@agh.edu.pl
[4]Lesya Ukrainka Volyn National University, Lutsk, Ukraine, zamurueva.o@gmail.com

Semiconductor materials such as the PbCdTe system are interesting for practical applications in thermoelectricity or as sensors in the IR range [1]. The substitution impurity in the metal sublattice allows correct the system of defects, which is important for reducing of thermal conductivity and, accordingly, improving thermoelectric properties. On the other hand, the deposition of thin films by vacuum methods allows to smoothly adjust the spectrum of structural characteristics, while changing the technological parameters, such as a deposition and evaporation temperatures, deposition time, and material of substrate. PbTe-CdTe solid solutions are characterized by rather low solubility due to the large difference between the crystal structures. An increase in the cadmium content leads to an increase in the band gap. The formation of such a solid solution is interesting because of the significant difference in the band gap widths of the components of the solid solution (about 1 eV). The starting solid solution in this case has a much higher value of thermoelectric factor than each compound separately.

The ternary system $Pb_{0.9}Cd_{0.1}Te$: Pb (3 at.%.) investigated at room temperatures, and the surface morphology and crystallographic parameters were key points of view. Size, shape, architecture and symmetry of the grains for different size and thickness films lead to certain conclusions about growth mechanism. The lattice evolution simulation corresponds to transition: the initial PbTe compound – replacement of the lead atom with a cadmium atom – formation of the cadmium atom-tellurium vacancy complex. The Vollmer-Weber growth mechanism confirmed as the influence of defects of the "cadmium nodal atom - tellurium vacancy" type.

1. Naidych B., Parashchuk T., Yaremiy I., Moyseyenk M., Kostyuk O., Voznyak O., Nykyruy L. Structural and thermodynamic properties of Pb-Cd-Te thin films: Experimental study and DFT analysis. Journal of Electronic Materials, 2021, 50, P. 580-591.

Application of artificial intelligence methods in solving ab initio problems

Tuzhykov A.V.[1], *Kavetskyy T.S.*[2,3], *Kiv A.E.*[1,4], *Soloviev V.N.*[1,5]

[1]*South Ukrainian National Pedagogical University named after K.D. Ushynsky, Odesa, Ukraine, andrewtuzhykov@gmail.com, kiv.arnold20@gmail.com;*
[2]*Drohobych Ivan Franko State Pedagogical University, Drohobych, Ukraine, kavetskyy@yahoo.com;*
[3]*Institute of Physics, Slovak Academy of Sciences, Bratislava, Slovakia;*
[4]*Ben-Gurion University of the Negev, Beer-Sheva, Israel;*
[5]*Kryvyi Rih State Pedagogical University, Kryvyi Rih, Ukraine, vnsoloviev2016@gmail.com*

Recent advancements in Artificial Intelligence (AI) methodologies have significantly influenced computational physics and chemistry, particularly in the domain of ab initio molecular simulations.

Graph Neural Networks (GNNs) have reshaped the landscape of structural prediction in materials science. By representing atomic structures as graphs with atoms as nodes and bonds as edges, GNNs can capture the three-dimensional structure of materials. Models such as Crystal Hamiltonian Graph neural Network (CHGNet) and Machine Learning Force Fields (MACE) have demonstrated the capability to learn the underlying physics of interatomic interactions from quantum mechanical data, thereby predicting properties like potential energy surfaces without explicit electronic density calculations. This results in a drastic reduction in computational time and resources while maintaining the accuracy needed for semiconductor (materials science) applications. For instance, AI algorithms can iteratively adjust molecular structures *in silico* to achieve desired properties, such as bandgap optimization in semiconductors.

Ab initio approaches, like Density Functional Theory, are powerful for materials science but become increasingly expensive as systems grow larger. Machine learning interatomic potentials, like MACE, offer a promising solution by utilizing graph neural networks to represent interatomic interactions. CHGNet addresses this limitation by incorporating magnetic moments as a proxy for atomic charge. The development of Graph Networks for Materials Exploration [1] has enabled the prediction of stability for over a million new semiconductors, polymers and composites.

This work was supported in part by the Ministry of Education and Science of Ukraine (projects Nos. 0122U000850, 0122U000874, and 0122U001694). This work has also received funding through the MSCA4Ukraine project (grant No. 1128327), which is funded by the European Union.

1. Merchant A., Batzner S., Schoenholz S.S., et al. Scaling deep learning for materials discovery. *Nature*. 2023. V. 624, P. 80-85.

Synthesis Technology and Optical Characteristics of Ultrasmall CdTe Quantum Dots

Dremliuzhenko K.S., Kulchytskyi B.N., Korbutyak D.V., Isaieva O.F., Trischuk L.I.

V.E. Lashkaryov Institute of Semiconductor Physics NAS of Ukraine
xeniyadr@gmail.com

In the last decade, interest in ultra-small quantum dots (USQDs) of semiconductor compounds A_2B_6 with dimensions on the order of 2 nm has increased. Due to the dominant role of the surface, USQDs are promising for the development of white light emitters and are an important material for use in medicine, solar energy, etc. [1].

CdTe nanocrystals (NCs) were prepared by colloidal synthesis. The source of Cd^{2+} ions was the salt CdI_2, and Te^{2-} ions was the gas H_2Te. After the precursors are introduced into the reaction chamber, they decompose and form new reactive units that cause nucleation and growth of NCs. The H_2Te required for the synthesis of nanoparticles was obtained electrochemically in a galvanostatic cell. Thioglycolic acid (TGA) was used as a stabilizer to prevent the aggregation of particles in the dispersed phase. It was found that an increase in the pH of the reaction medium leads to a decrease in the average size of CdTe NCs. A colloidal solution of CdTe NCs was separated by centrifugation into fractions of USQDs with sizes ≤ 2 nm [2].

For these centrifuged nanoparticles, a quantitative study was performed using the Zetasizer Nano ZS, which confirmed the presence of USQDs.

In this work, optical absorption and photoluminescence excitation spectroscopy was used to determine the electronic energy levels of the USQDs.

1. Korbutyak D.V., Kosynov O.H., Kulchytskyi B.N. Ultrasmall quantum dots: features of synthesis, optical properties and prospects for practical use (review). Optoelectron. Semicond. Tech., 2023, 58, P. 21-45.
2. Kapush O.A., Trischuk L.I., Tomashyk V.M., Tomashyk Z.F., Boruk S.D. The influence of the nature of stabilizers and the pH of the environment on the patterns of CdTe nanocrystal formation in colloidal solutions. Physics and Chemistry of Solids, 2012, 13(4), P. 1022-1026.

Modelling the electric field effect on the optical characteristics of lens-shaped quantum dots

Holovatsky V.A., Holovatsky I.V., Makhanets O.M.

Yuriy Fedkovych Chernivtsi National University, Chernivtsi, Ukraine,
v.holovatsky@chnu.edu.ua

Molecular beam epitaxy and colloidal chemistry are the main methods for quantum dots creating. Each of these methods does not exclude the other, but only complements the variety of nanostructures that are used in modern nanoelectronics. Epitaxial quantum dots are a large class of a wide range of semiconductor nanostructures grown on a crystal surface by various technological methods [1]. Depending on the semiconductor materials and growing methods, quantum dots of various sizes and shapes are obtained, which affects their optical characteristics, and therefore significantly complicates theoretical research. For modelling, the finite element method is most often used within the integrated platform for numerical simulation COMSOL Multiphysics. In this work, the energy spectrum and wave functions of an electron in a lens-shaped quantum dot were calculated, based on which the influence of the electric field on the oscillator strength of quantum transitions was investigated.

Two models of a lens-shaped quantum dot are considered: a spherical segment and half of an oblate ellipsoid Fig1. For the second model, there are exact solutions of the Schrödinger equation in the form of spheroidal functions of the first kind that make up the orthonormal basis [1-2], which allows to study the effect of the electric field on the energies and wave functions of the electron in the nanostructure by the matrix method. In this study, calculations absorption coefficient for both models were performed using the finite element method in COMSOL Multiphysics. Research results obtained by various methods coincide with high accuracy.

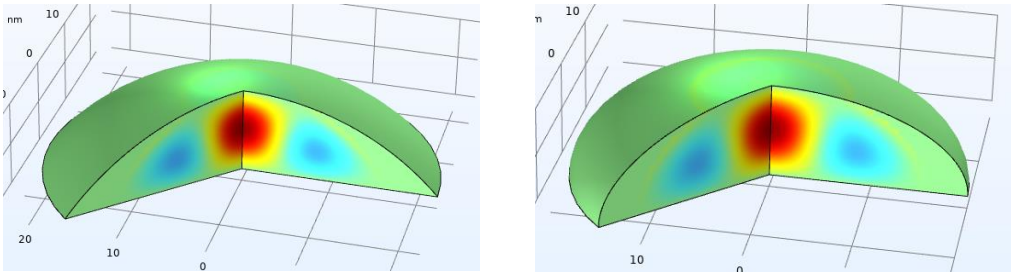

Fig. 1. Models a lens shaped QD: a) spherical segment, b) oblate hemispheroid.

1. Wu S. Anisotropic exciton Stark shift in hemispherical quantum dots. *Chinese Phys B.* 2021. V.30, No 5. P.053201.
2. Baghdasaryan D.A., Hayrapetyan D.B., Kazaryan E.M. Oblate spheroidal quantum dot: electronic states, direct interband light absorption and pressure dependence. *Eur Phys J B.* 2015, V.88, No 9. P. 1-6.

IV-VI semiconductor low-dimensional structures formed by ion sputtering

Zayachuk D.M.

Lviv Polytechnic National University, Lviv, Ukraine,
zayachuk@polynet.lviv.ua

The report is devoted to the generalization of the results of research on the formation of low-dimensional structures on the single-crystal surfaces of IV-VI semiconductors of cubic symmetry PbTe and SnTe under the impact of sputtering with low-energy beams of Ar^+ ions [1-3], that widely used for structuring the surface of solids, which is of great practical importance for various technical and technological applications. The surfaces of PbTe and SnTe crystals irradiated with Ar+ ions are covered with various surface structures and pits of the surface relief. The most important low-dimensional structures forming under the impact of Ar^+ ion beams are both sharped conical structures, as well as surface structures combining a conical base and a pyramidal apex, the ratio between the contributions of which depends on the duration of the sputtering process. The conical structures are formed when SnTe surfaces are sputtered. In the case of sputtering of PbTe surfaces, the conical structures formed at the initial stage of sputtering turn into pyramidal shapes during prolonged sputtering. The shape of the pyramidal top depends on the crystallographic orientation of the sputtering surface. When the (100) crystallographic surfaces were sputtered, the initial conical structures were transformed into small tetrahedral pyramids with ordered ripples on their faces. When the (111) crystallographic surfaces were sputtered, the original conical structures were transformed into pseudohexagonal pyramidal structures, which, in turn, were further transformed into trihedral pyramidal structures. The edges of the pseudo-hexagonal pyramids are indistinct, and the lateral facets are rough, while the edges of the trihedral pyramids, into which the hexagonal pyramids are transformed in the process of long-term sputtering, are sharp, and the facets are mirror smooth.

The possible causes and mechanisms of the formation of various types of low-dimensional structures on the surfaces of the studied semiconductors during their sputtering by low-energy ions, the influence of the reticular density of different crystallographic planes, the processes of easy chipping and the related self-organization processes are analyzed.

1. D.M. Zayachuk, Y.D. Zayachuk, Cs. Buga, V.E. Slynko, and A. Csík, Vacuum, 186 (2021) 110058, doi.org/10.1016/j.vacuum.2021.110058
2. D.M. Zayachuk, Y.D. Zayachuk, M. Hunyadi, V.E. Slynko, and A. Csík, J. All. Comp. 883 (2021) 160978, doi.org/10.1016/j.jallcom.2021.160978
3. D.M. Zayachuk, Y.D. Zayachuk, V.E. Slynko, T. Fodor, and A. Csík, J. All. Comp. 924 (2022) 166628, doi.org/10.1016/j.jallcom.2022.166628

Electric field effect on the absorption coefficient of elliptical quantum wires

Holovatsky V.A., Yarema V.V.

Yuriy Fedkovych Chernivtsi National University, Chernivtsi, Ukraine,
v.holovatsky@chnu.edu.ua

Within the framework of the effective mass approximation the electric field effect on the optical properties of the elliptical quantum wire (EQW) was investigated. Exact solutions of the Schrödinger equation for an electron in a GaAs wire with hard walls were obtained in an elliptic coordinate system. The energy spectrum of a quasiparticle consists of energies of both even and odd states, with their respective wave functions expressed using even and odd Mathieu functions of the first kind. Using these solutions, an orthonormal basis was constructed [1]. The effect of the electric field perpendicular to the quantum wire on the energies and oscillator strengths of electron quantum transitions was assessed using both the matrix method and the finite element method implemented in COMSOL Multiphysics.

It is shown that the ellipticity of the quantum wire leads to the removal of the degeneracy of the energy spectrum of quasiparticles, since the energies of even and odd electronic states depend differently on the ratio of the EQW semi-axes. The ground state of the electron is the even state, which remains nondegenerate due to the absence of a corresponding odd state. The electric field has a greater effect on energy states with a lower value of the magnetic quantum number. As the electric field strength increases, the energies of even and odd states shift to the region of lower energies. The electron density distribution of the ground state shifts more than other states in the direction opposite to the direction of the electric field. This leads to a decrease in the oscillator strengths of allowed quantum transitions with an increase in the intensity of the electric field.

The selection rules for quantum transitions in an elliptical quantum wire are similar to the corresponding rules for cylindrical wires. The paper investigates the peculiarities of the polarization of an electromagnetic wave emitted or absorbed by an elliptical quantum wire. It is shown that during quantum transitions of an electron from the ground state to the even states, an electromagnetic wave is linearly polarized along the major axis of the ellipse. In the case of transitions to odd states – along the minor axis of the ellipse.

The results obtained by the matrix method completely coincide with the results of modelling in COMSOL Multiphysics, but allow obtaining additional information about the states formed under the influence of an electric field.

1. Holovatsky V.A., Gutsul V.I. Electron energy spectrum and wave functions in complicated elliptic quantum wires. *J Optoelectron Adv Mater*., 2007, V.9, No 5, P. 1437-1441.

The effect of dynamic deformation on the nanowires conductivity of AlGaN/GaN

Kaliuzhnyi V.V.[1], *Tymochko M.D.*[1], *Olikh O.Ya.*[2], *Belyaev A.E.*[1]

[1] *V.E. Lashkaryov Institute of Semiconductor Physics National Academy of Sciences of Ukraine, Kyiv, Ukraine, tymochko@ukr.net*

[2] *Physics Faculty, Taras Shevchenko National University, Kyiv, Ukraine*

AlGaN/GaN-based devices are being used for both electronic and optoelectronic applications. Lately, they are also studied as biosensors based on nanowires (NWs). Their interfaces are extremely sensitive to surrounding substances and environmental conditions. In our case, AlGaN/GaN NWs contain one-dimensional electron gas (1 DEG). In previous works [1-2], we studied a dependence of NWs current-voltage characteristics (CVCs) on wavelength and intensity of ultraviolet excitation for the depletion widths and space charge-limited transport control in NWs. Also we have investigated the effect of ultrasound vibrations for the adjustment of AlGaN/GaN transport properties. Nanowires with near critical width (185 nm) appear to be especially sensitive to the UV excitation due to space-charge-limited current. All nanowires demonstrated persistent photoconductivity. Ultrasound loading leads to similar effects as UV excitation, such as persistent conductivity.

The purpose of the study was the influence of acoustic loading on the current-voltage characteristics of nanowires based on GaN/AlGaN heterostructure with different wire thickness of 280, 470, 720, 930 and 1100 nm. Temperature dependence of CVCs under the ultrasound loading was obtained in the range of 200 – 300 K in the dark conditions. The ultrasound amplitude on piezotransducer was 22 V, the frequency was 4 MHz. Measurements were done for both heating and cooling cycle, and the dependence of current on temperature at fixed bias was plotted. The time dependences of the current change when the ultrasound is turned on and off were studied. It was found that there is a decrease in the current due to the acoustic loading. The magnitude of the effect depends on both the temperature and the width of the nanowires.

1. Naumov A.V., Kaliuzhnyi V.V., Vitusevich S.A., Hardtdegen H., Belyaev A.E. Electron transport in AlGaN/GaN HEMT-like nanowires: Effect of depletion and UV excitation. *SPQEO*. 2021. V. 24, No 4. P. 407-412.
2. Kaliuzhnyi V.V., Liubchenko O.I., Tymochko M.D., Olikh Y.M., Kladko V.P., Belyaev A.E. Investigation of traps in AlGaN/GaN heterostructures by ultrasonic vibrations. *Ukr. J. Phys.* 2021. V. 66. No 12. P. 1058-1062.

The energy spectrum of nanopod-shaped structures in the form of tetrapods

Bilynskyi I.V., Melnyk Ya.Yu., Bobyliev D.Ye., Popov M.Yu.

Physics Department, Kryvyi Rih State Pedagogical University,
54 Gagarin Avenue, 50086 Kryvyi Rih, Ukraine,
iv.bilynskyi@gmail.com

Semiconductor quantum nanostructures, including quantum wires and quantum dots (QDs), exhibit intriguing electronic and optical properties, making them subjects of extensive theoretical and experimental investigation by numerous scientists. Advancements in nanotechnology are crucial for scientific development across various fields, from electronics to medicine.

Nanopod-like structures, including tetrapods, are intriguing subjects of study due to their unique properties and potential impact on emerging technologies. Specifically, nanopods based on spherical quantum dots could find applications in photonics, quantum computing, and electronics. Their exceptional optical properties could be harnessed for creating novel sensor types, efficient energy sources, and highly sensitive photodetectors.

Theoretical calculations can help establish a relationship between the geometric parameters of tetrapods and their optical characteristics. This, in turn, can open up new opportunities for creating more efficient and functional materials. We are not aware of any theoretical works at present that extensively explore tetrapods based on spherical quantum dots.

To calculate the electron energy spectrum and wave functions, the Schrödinger equation should be solved. In the non-spherical-symmetry case this equation cannot be solved exactly. That is why, we use the plane wave method.

Control of the structural perfection of functional materials of electronic equipment by the modulation electroreflection spectroscopy method

Demchyna L.A., Mynaylo M.A., Pekur D.V., Vuichyk M.V., Kyiak J.P., Gentsar P.O., Vlasenko O.I.

V. Lashkaryov Institute of Semiconductor Physics, National Academy of Sciences of Ukraine, Kyiv, Ukraine, rastneg@isp.kiev.ua

When analyzing experimental data, it is necessary to take into account the presence of charge carrier scattering processes due to their interaction with crystal lattice fluctuations, impurities and defects, including those of a surface nature. Relaxation effects in the phenomenon of absorption of light (electromagnetic) waves by a crystal are described by the phenomenological broadening parameter Γ, which is related to the energy relaxation time τ of photogenerated free charge carriers by the ratio $\Gamma = \frac{\hbar}{\tau}$. This work is devoted to establishing the relationship between the mobilities μ_e of free charge carriers and the concentration of free charge carriers N_e in single-crystal semiconductors *n-Si*, *n-Ge*, *n-GaAs* at concentrations of charged impurities from 10^{20} m^{-3} to 10^{25} m^{-3} with the phenomenological broadening parameter Γ optical spectrum and energy relaxation time τ of photogenerated free charge carriers. In semiconductors at these concentrations, an important mechanism of optical spectra broadening is the broadening mechanism due to the scattering of electrons on charged impurities. Based on the Heisenberg uncertainty principle for energy E and time t ($\Delta E \cdot \Delta t \geq \hbar$) in the assumption of independence of scattering processes of photogenerated electron and hole (this assumption must be fulfilled for weakly bound pairs (electron and hole)), when the exciton binding energy E_{exc} satisfies the inequality $E_{exc} \ll \Gamma$. In this case, the broadening parameter Γ can be written in the form: $\Gamma = e\hbar\left[\left(m_e\mu_e\right)^{-1} + \left(m_p\mu_p\right)^{-1}\right]$, where m_e, m_p - effective masses of the electron and hole, respectively; μ_e, μ_p - electron and hole mobilities, respectively ($\mu_e = \frac{e<\tau>}{m_e}$; $\mu_p = \frac{e<\tau>}{m_p}$). Thus, we performed numerical calculations of the dependence of the phenomenological broadening parameter Γ and the energy relaxation time of free charge carriers τ_e on the electron mobility μ_e, electron concentration N_e for semiconductor materials *n-Si*, *n-Ge*, *n- GaAs* when the electron concentration of N_e changes in the range of 10^{20} m^{-3}- 10^{25} m^{-3}. The obtained data indicate the possibility of non-destructive control of mobility (electrons) of functional materials of electronic equipment.

Energy spectrum of heterogeneous tunnel-coupled quantum dots

Bilynskyi I.V., Melnyk Ya.Yu., Slusarenko M.A., Popov M.Yu.

Physics Department, Kryvyi Rih State Pedagogical University,
54 Gagarin Avenue, 50086 Kryvyi Rih, Ukraine,
iv.bilynskyi@gmail.com

Studying structures with pairwise coupled quantum nanostructures is essential due to their potential application in developing quantum switches necessary for quantum processors implementation. Research on the spectra of excitonic luminescence in double GaAs quantum wells under electric and magnetic fields revealed the induced magnetic field shift of the indirect exciton to low-energy regions and the emergence of periodic fluctuations in the intensity of indirect exciton lines over time. At specific values of external electric field and temperature, a significant increase in the intensity of luminescence for a portion of the spectral contour of indirect exciton lines in double GaAs/AlGaAs quantum wells was observed.

Experimental investigations of a pair of vertically coupled InAs/GaAs quantum dots (analogous to a diatomic molecule) have demonstrated the possibility of controlling carrier tunneling in such structures. Moreover, it has been shown that depending on the intensity of the magnetic field, the energy levels shift in one of the quantum dots relative to the other, enabling electrons to resonantly tunnel between the quantum dots. Currently, there is no theory that explains the obtained results. The work is dedicated to studying the energy spectrum of charge in a system of two tunnel-coupled quantum dots of different types with spherical shapes.

We investigated pairs of tunnel-coupled GaAs/AlAs quantum dots of various sizes and types. Layers with self-assembled gallium quantum dots were separated by AlAs barriers of different widths. Each dot had a spherical shape with a radius of approximately 3-5 nm. The fine structure of the exciton ground state was investigated using photoluminescence spectra. For samples without a magnetic field, a splitting of the exciton ground state into two states was observed at a distance of 1 nm between the quantum dots, which qualitatively agrees with the results of experimental studies. For a quantitative comparison of theory and experiment, quantum dots with radii larger than 3 nm should be considered. In quantum dots with radii of 15-20 nm, at least 8-10 energy states should be taken into account, which significantly complicates the calculations.

The influence of impurities and electric fields on light absorption by spherical non-concentric core-shell quantum dots

Leshko R.Ya.[1], *Leshko O.V.*[1], *Bilynskyi I.V.*[2]

[1]*Drohobych Ivan Franko State Pedagogical University, Drohobych, Ukraine,*
[2]*Kryvyi Rih State Pedagogical University, Kryvyi Rih, Ukraine,*
leshkoroman@dspu.edu.ua

Today, there are various methods for obtaining nanosystems, including quantum dots (QDs). The cheapest and relatively simple methods are colloidal technologies for synthesizing quantum dots. Thanks to the utilization of these techniques, quantum dots in most cases have a shape close to spherical.

Experimental studies show that many QDs exhibit blinking when emitting electromagnetic waves in the visible spectrum. This is explained by several reasons, including non-radiative electron or hole trapping by surface defects and volume defects. One way to reduce blinking is the use of core-shell QDs.

When growing spherical core-shell QDs in colloidal solutions, there is always a possibility that the core and shell do not have a common geometric center. That is, the core will be displaced relative to the shell or vice versa. Therefore, most core-shell QDs are non-concentric.

In this work, we apply the plane wave method to calculate the electronic and hole spectra in spherical non-concentric core-shell QDs. The obtained results showed a significant influence of the non-concentricity parameter on the energy spectra. Additionally, in the study, we investigate the influence of impurities and electric field on the energy spectra of electrons and holes in spherical non-concentric core-shell QDs. It has been shown that the electric field and displaced impurity can both enhance the splitting of excited electronic and hole levels and induce the restoration of their degeneracy. Such behavior depends on the impurity location, non-concentricity parameter, and magnitude and direction of the electric field.

The obtained spectra and wave functions allowed us to determine the light absorption coefficient caused by interband transitions. The distribution of QDs by core/shell displacement from the common center to half the absorption band width is also considered. The obtained results are consistent with the results of other experimental and theoretical works by other authors.

Photophysical behavior of MeLPPP/SBA-15 nanocomposite

Mykytyuk T.V.[1], Shcherban N.D.[2], Dmytruk A.M.[1], Dmytruk M.[3], Ostapenko Yu.V.[1], Ostapenko N.I.[1]

[1] Institute of Physics, National Academy of Sciences of Ukraine, Kyiv, Ukraine,

[2] L.V. Pisarzhevsky Institute of Physical Chemistry, NASU, Kyiv, Ukraine,

[3] Faculty of Physics, Taras Shevchenko National University of Kyiv, Kyiv, Ukraine,

nina.ostapenko@gmail.com

Photoluminescence spectra of the MeLPPP/SBA-15 nanocomposite in the temperature range from 5 to 220 K, as well as its photoluminescence decay kinetics at room temperature were studied. For the sake of comparison, similar dependencies were taken for the film and the polymer solution.

It was shown that the optical spectrum of the MeLPPP/SBA-15 nanocomposite differs from the spectrum of the bulk film and is close to the spectrum of the solution. A hypsochromic shift for the photoluminescence spectra of the polymer film, solutions, and nanocomposite at an increase in temperature from 5 to 220 K was found. The results confirm the diffusion of excited singlet states in an inhomogeneously broadened density of states during their energy relaxation. The value of this shift for nanocomposites is 3-fold lower compared to the film. A significant decrease in this shift, as well as a twofold increase in the photoluminescence lifetime of the nanocomposite and three times weaker temperature dependence of the photoluminescence intensity in comparison with the film, is associated with a decrease in the number of polymer chains in a low-dimensional structure and a reduced role of exciton diffusion.

Long photoluminescence lifetime of nanocomposite indicates the increased efficiency of its photoluminescence, opens up promising perspectives for the application of nanocomposite materials in light emitting diodes.

Multifunctional sensor structures based on porous silicon and reduced graphene oxide

Olenych I.B., Horbenko Y.Y., Pavlyk M.R.

Ivan Franko Lviv National University, Lviv, Ukraine, iolenych@gmail.com

The development of high-speed sensors compatible with real-time microprocessor signal processing meets the challenges of the IoT paradigm. In particular, the creation of an effective system of environmental monitoring requires low-cost sensors with miniature sizes of sensitive elements and low power consumption that operate at room temperatures. These criteria are satisfied by sensors based on nanostructures and composite nanomaterials with an ultra-high surface area. Special attention is focused on the sensory properties of graphene and porous silicon (PS) nanostructures. On the one hand, graphene field-effect transistors (FETs) are used in gas sensors due to the high mobility of charge carriers and the ability to change the conductivity of graphene by the electric field of adsorbed molecules [1]. On the other hand, the extensive network of the PS pores contributes to the efficient adsorption of molecules of various gases. Besides, the PS is an ideal matrix to deposit graphene that enables the formation of hybrid structures with improved functional properties [2].

In this work, the sensor structures were created by depositing a film of reduced graphene oxide (RGO) on the surface of the PS layer. The obtained structures were used as FETs sensitive to the local electric field of adsorbed gas molecules. The RGO film and the silicon substrate were used as the conducting channel and gate of the FET, respectively. It was established that an increase in the relative humidity of the air or the concentration of ammonia, ethanol, and acetone molecules in the air leads to a decrease in the RGO film resistance. In addition, the Dirac point position and the ratio between the electron and hole components of the conductivity profile of the FET based on the RGO–PS structure depended on both the nature and concentration of adsorbed molecules. The sensitivity of the RGO film conductivity to local changes in the electric field also makes it possible to detect light photons and various types of ionizing radiation due to radiation-induced charge carriers in the silicon substrate and the PS layer. The obtained results can be used to create multifunctional sensor systems based on the RGO–PS structures.

1. Hayasaka T. et al. An electronic nose using a single graphene FET and machine learning for water, methanol, and ethanol. *Microsystems & Nanoengineering*, 2020, V. 6, P. 50.
2. Olenych I.B. et al. Humidity sensor element based on porous silicon–reduced graphene oxide sandwich-like structures. *Molecular Crystals and Liquid Crystals*, 2023, V. 767, P. 9-15.

Optical spectroscopy of high-resistence CdTe single crystals

Gentsar P.O., Mynaylo M.A., Pekur D.V., Demchyna L.A., Vuichyk M.V., Kyiak J.P., Zayats M.S., Vlasenko O.I.

V. Lashkaryov Institute of Semiconductor Physics, National Academy of Sciences of Ukraine, Kyiv, Ukraine, rastneg@isp.kiev.ua

Recently, more and more attention has been paid to the technology of growing high-resistance CdTe crystals. The development of the technology is based on the control of the synthesis processes, the determination of the defective structure and its effect on the physical properties of the material. The conditions for obtaining the material determine the composition and distribution of point defects, which significantly affect the electronic processes in the material. Cadmium telluride is used to make uncooled gamma radiation detectors. CdTe doped with chlorine turned out to be especially promising in this regard. One of the main problems when using the A_2B_6 semiconductor compounds as the basic material of optoelectronics is obtaining a homogeneous material.

This work presents the experimental results of the study of optical reflection and transmission spectra in the spectral range 800 nm - 1100 nm, optical reflection and transmission spectra in the spectral range $(1.4 – 25)\cdot10^{-6}$ m of high-resistance CdTe single crystals of (111) orientation with with specific resistance $\rho = 2\cdot10^9$ Om·cm -$5\cdot10^9$ Om·cm, doped with chlorine. Optical spectra of reflection and transmission in the region of the fundamental optical transition E_0 of CdTe (111) single crystals (spectral range 800 nm - 1100 nm) were measured using a diffraction grating monochromator MDR-23. The resolution of the MDR-23 diffraction grating monochromator is $2\cdot10^{-4}$ eV. Registration of optical spectra of reflection and transmission in the spectral range $(1.4 – 25)\cdot10^{-6}$ m was carried out on a PerkinElmer SpectrumBXII infrared Fourier spectrometer. The measurement error of the optical spectra is equal to 2 cm^{-1}. The measurements were carried out at room temperature.

It was determined that the energy of the fundamental optical transition E_0 of CdTe single crystals doped with chlorine of the (111) orientation with a resistivity $\rho = 2\cdot10^9$ Om·cm - $5\cdot10^9$ Om·cm at T = 300 K is equal to 1.44 eV. The energy relaxation time of free charge carriers τ and the effective optical mobility of free charge carriers for high-resistance single crystals of CdTe (111) were estimated. It is shown that the studied crystals have a high (detector) quality, which is decisive for the manufacture of highly sensitive and high resolution sensors of ionizing radiation.

The influence of hydrostatic pressure on the synthesis of colloidal core-shell quantum dots

Dan'kiv O.O.[1], *Kuzyk O.V.*[1], *Peleshchak R.M.*[1,2], *Stolyarchuk I.D.*[1], *Satcyk V.V.*[1], *Guba S.K.*[2]

[1]*Drohobych Ivan Franko State Pedagogical University, Drohobych, Ukraine,* dankivolesya@dspu.edu.ua

[2]*Lviv Polytechnic National University, Lviv, Ukraine*

Despite significant successes in the synthesis of colloidal quantum dots of the core-shell type, their quality has not yet reached the quality of nanocrystals with a simple core. Foremost, it concerns the uniformly of the structure, controllability of size and concentration. In [1], two main critical problems for preserving the size distribution of nanocrystals during shell growth are singled out, which have not been fully resolved to date. This is the elimination of homogeneous nucleation of shell materials with subsequent coalescence of homogeneous nanoparticles and ensuring layer-by-layer growth of shells on all cores in solution with the formation of layers of the shell of the same thickness around each core. To fulfill these conditions, the reactivity of the precursors must be weak enough to prevent independent nucleation, but strong enough to promote epitaxial growth around existing core nanocrystals.

In this work, we have considered the process of heteroepitaxial growth of the ZnS shell on the surface of the CdSe core and the homogeneous nucleation of ZnS nanoparticles in the colloidal solution which are subject to external comprehensive compression. It is assumed that such hydrostatic pressure should complicate the independent formation of nanoparticles of the shell material and, conversely, practically not change the conditions of heteroepitaxial growth of the shell on the core.

Within the framework of the developed model, the regularities of change in the homogeneous nucleation of colloidal ZnS NPs, which is the material of the shell, and the heteroepitaxial growth of the ZnS shell on the CdSe core under the action of external pressure have been established. The obtained results allow us to propose a method of eliminating the homogeneous nucleation of shell materials regardless of the core, which is a negative phenomenon in the formation of the core-shell heterostructure. The creation of additional hydrostatic pressure in the colloidal solution practically makes homogeneous nucleation and growth of NPs of the shell material impossible due to an increase in the energy barrier and an increase in the critical radius, at exceeding which this growth is possible.

1. Li J.J., Wang Y.A, Guo W., Keay J.C., Mishima T.D. Large-Scale Synthesis of Nearly Monodisperse CdSe/CdS Core/Shell Nanocrystals Using Air-Stable Reagents via Successive Ion Layer Adsorption and Reaction. *J. Am. Chem. Soc*., 2003, V. 125, No 41, pp. 12567-12575.

Energy Spectrum Analysis of GaAs/AlAs Quantum Dots of Complex Shapes Using Plane Wave Method

Bilynskyi I.V.[1], *Maturin Yu.P.*[2]

[1]*Kryvyi Rih State Pedagogical University, Kryvyi Rih, Ukraine,*
iv.bilynskyi@gmail.com;
[2]*Drohobych Ivan Franko State Pedagogical University, Drohobych, Ukraine,*
yuriy.maturin@gmail.com

Nanostructures are currently extremely relevant in modern scientific research and technologies. One important example of nanostructures is quantum dots. Recently, quantum dots of complex shapes have been studied quite thoroughly. Their synthesis is particularly important as they enhance properties such as optical absorption, luminescence efficiency, and charge carrier mobility. These enhancements are crucial for applications in photovoltaics, LED technology, and biomedical imaging.

Today, the mathematical models for theoretically describing quantum dots of complex shapes remain little studied. Our main task was to construct a mathematical model that allows for the calculation of the energy spectrum in the case of GaAs/AlAs type nanostructures.

Calculations were conducted using the plane wave method. For this, the corresponding Hamiltonian was written down, and the wave function was expanded in a series of plane waves. Solving the Schrödinger equation was reduced to solving a homogeneous system of linear equations with respect to the coefficients of the series. Then, by setting the determinant of the corresponding system to zero, we obtain the dispersion equation for determining the energy spectrum.

Calculations were conducted for the GaAs/AlAs nanopods in the form of stacked spheres.

As a result, it was shown that the loss of spherical symmetry leads to the splitting of energy levels by the modulus of the quantum number |m|.

It was also shown that there is a shift in energy levels due to changes in the dimensions of both the core of the quantum dot and its arms.

1. Xing, W., Zhang, S., An, R., Bi, W., Geng, C., & Xu, S. Low-temperature synthesis of tetrapod CdSe/CdS quantum dots through a microfluidic reactor. *Nanoscale*. 2021. V.13, Is. 46. 19474-19483.

Spectral parameters of an electron in double quantum rings in magnetic and electric fields

Hnidko I.S., Gutsul V.I., Koziarskyi I.P., Makhanets O.M., Kuchak A.I.

Yuriy Fedkovych Chernivtsi National University, Chernivtsi, Ukraine,
hnidko.ihor@chnu.edu.ua

Multilayer semiconductor nanostructures have been studied both theoretically and experimentally for quite a long time. The unique properties of quasiparticles in such systems allow them to be used as basic elements in modern nanoelectronic devices: tunnel nanodiodes, nanolasers, nanodetectors [1, 2].

The work investigated the influence of magnetic and electric fields on the energy spectrum of the electron and the oscillator strengths of quantum intraband transitions in double semiconductor quantum nanorings. To find the energy spectrum and wave functions of the electron, the stationary Schrödinger equation is solved in a cylindrical coordinate system. Such an equation cannot be solved exactly. Therefore, the spectrum of the electron interacting with the electric and magnetic fields in the nanorings was found by the method of decomposing the unknown wave function of the electron by the full orthonormal set of wave functions of the quasiparticle in the nanostructure in the absence of fields and solving the resulting secular equation.

It is shown that in a magnetic field the degeneracy of the electron energy spectrum in terms of the quantum magnetic number, which occurs in an arbitrary cylindrical nanosystem in the absence of a field, is removed. Depending on the magnitude of the magnetic field induction, states with negative quantum numbers periodically become the ground state of the electron in double nanorings. This feature is a peculiar manifestation of the Aharonov-Bohm effect.

It is shown that the electric field significantly changes the density distribution of the probability of finding a quasiparticle in a nanosystem. Thus, if without a field in the ground state the electron is in the inner ring, then with an increase in the electric field strength, the quasiparticle tunnels into the outer nanoring.

The electron energies and oscillator strengths of quantum intraband transitions depend non-monotonically on the strength of the electric field and induction of the magnetic field.

1. Young Joon Hong, Rajendra K. Saroj, Won Park, Gyu-Chul Yi // APL Mater. – 2021. – V. 9. – P. 060907.
2. M. Zervos // Nanoscale Research Letters. – 2014. – V. 9. – P. 509.

Optical properties of germanium doped n-CdTe single crystals in the fundamental optical transition E_0

Gentsar P.O., Mynaylo M.A., Pekur D.V., Vuichyk M.V., Strilchyk O.M., Kyiak J.P., Demchyna L.A., Zayats M.S., Trischuk L.I.

V. Lashkaryov Institute of Semiconductor Physics, National Academy of Sciences of Ukraine, Kyiv, Ukraine, rastneg@isp.kiev.ua

To improve the obtaining chalcogenide semiconductor materials in technological processes, it is necessary to perform a number of electrical and optical studies. One of the ways to stabilize the physical parameters of functional materials of electronic equipment is doping with various impurities of chemical elements. Doping cadmium telluride single crystals with germanium atoms leads to stability and reproducibility of the electrophysical properties of electronic devices based on cadmium telluride. In connection with the above, the study of the physical properties of doped semiconductors is relevant.

In this work, optical (reflection spectra, transmission spectra) studies of n-CdTe single crystals doped with germanium with a concentration of $N_{Ge} = (2\text{-}10)\cdot10^{24}$ м$^{-3}$ with a resistivity $\rho = 10^4$ Ω·cm – $5\cdot10^6$ Ω·cm in the spectral range were carried out $(0.8\text{-}25)\cdot10^{-6}$ m. Optical reflection and transmission spectra of in the spectral range of 800 nm - 1100 nm was measured using an MDR-23 diffraction grating monochromator with a resolution of $2\cdot10^{-4}$ eV. Photoluminescence spectra of germanium doped n-CdTe single crystals were measured at a temperature of 77 K upon 660 nm laser excitation in the 1.3 eV - 1.65 eV energy range.

The band gap temperature coefficient of n-CdTe single crystals doped with germanium ($N = (2\text{-}10)\cdot10^{24}$ m^{-3}) is equal to – $5.426\cdot10^{-4}$ eV/K.·The dependence the fundamental optical transition E_0 energy from the temperature T in the temperature range $77 \leq T \leq 300$ K was obtained: E_0(CdTe:Ge)=1.580 eV – $5.426\cdot10^{-4}$ eV/K (T – 77 *K*).

The energy relaxation time τ and the effective optical mobility of free charge carriers for germanium-doped n-CdTe single crystals were estimated.

The practical value of the obtained results consist in the determination of the electronic and physical parameters of the technically important semiconductor CdTe, doped with germanium, in the manufacture of highly sensitive and high resolution sensors of ionizing radiation.

Raman spectroscopy study of the structure of Cu_2ZnSnS_4 and Cu_2NiSnS_4 nanocrystals synthesized by hydrothermal route

Ivakhno-Tsehelnyk O.[1,2], *Karnaukhov A.*[3], *Kotsyubynsky V.O.*[4], *Selyshchev O.*[1,2], *Boychuk V.M.*[4], *Dzhagan V.M.*[3], *Mazur N.*[3], *Zahn D.R.T.*[1,2]

[1] *Semiconductor Physics, Chemnitz University of Technology, Chemnitz, Germany*
[2] *Center for Materials, Architectures and Integration of Nanomembranes (MAIN), Technical University of Chemnitz, Chemnitz, Germany*
[3] *V. Lashkaryov Institute of Semiconductors Physics, National Academy of Sciences of Ukraine, Kyiv, Ukraine, an.karnauhov@gmail.com*
[4] *Vasyl Stefanyk Precarpathian University, Ivano-Frankivsk, Ukraine*

Cu_2ZnSnS_4 (CZTS) and alike compounds are intensively studied for various potential energy applications [1]. Their advantages are the high absorption coefficient, appropriate bandgaps, nontoxic and affordable elements. Colloidal nanocrystals (NCs) are promising for large-area thin-film solar cells, compatible with printing technologies [2]. However, there is a high probability of defects and impurity phases (Cu_xS, ZnS, *etc*) in CZTS [3]. One of the approaches to avoid their formation is a partial or complete replacement of (one or two) cations. Until now, most works have focused on the substitution of Cu (for Ag) and Sn (for Ge) [1], while the substitution of the group II element was less studied [1].

In this work, we compare the NCs of Cu_2ZnSnS_4 and Cu_2NiSnS_4 synthesized in aqueous solutions by means of hydrothermal chemical route (at 200 °C and 10-12 atm in an autoclave) and synthesis at ambient pressure and low temperature (<100°C). We compare results of X-ray diffraction (XRD), which is indicative of overall crystallinity of the NCs, with vibrational Raman spectroscopy at different excitation wavelengths. Raman spectroscopy could reveal the presence Cu_3SnS_4, Cu_2SnS_3, Cu_xS as secondary impurity phases, which was not detected by XRD because their reflexes are not discernible from those of Cu_2ZnSnS_4 and Cu_2NiSnS_4. Based on these data, the synthesis conditions of the CZTS and CNTS NCs were optimized.

The work was supported by the DFG project ZA 146/59-1 (517869265).

1. Kush P. and Deka S. Multifunctional Copper-Based Quaternary Chalcogenide Semiconductors Toward State-of-the-Art Energy Applications. *ChemNanoMat* 2019, V. 5, pp. 373-402.
2. Stroyuk, O. et al. Solar Light Harvesting with Multinary Metal Chalcogenide Nanocrystals. *Chem. Soc. Rev.* 2018, V. 7, pp. 5354-5422.
3. Selyshchev O. et al. Raman and X-ray photoemission identification of colloidal metal sulfides as potential secondary phases in nanocrystalline Cu_2ZnSnS_4 photovoltaic absorbers. *ACS Appl. Nano Mater.* 2020, V. 3 (6), P. 5706.

The mechanism of the influence of ultrasonic cavitation on the growth of A^2B^6 colloidal nanoparticles

Kuzyk O.V.[1], *Dan'kiv O.O.*[1], *Stolyarchuk I.D.*[1], *Peleshchak R.M.*[1,2], *Kuhivchak V.A.*[1], *Krisa Ya.P.*[1]

[1]*Drohobych Ivan Franko State Pedagogical University, Drohobych, Ukraine,* olehkuzyk@dspu.edu.ua

[2]*Lviv Polytechnic National University, Lviv, Ukraine*

An important prerequisite for the use of quantum dots (QDs) in optoelectronics or biomedical researches is the improvement of synthesis technologies, which will ensure obtaining QDs with low dispersion of their sizes, high stability and the ability to predictably control the change in their composition. Despite significant progress in the technology of synthesis of colloidal A^2B^6 QDs and obtaining nanocomposites based on them, to date there are still problems of obtaining them with predicted physicochemical properties.

Recently, experimental researches have shown that the use of ultrasonic treatment of a colloidal solution in the process of QD synthesis can significantly improve their properties (reduce size dispersion, increase stability) [1]. This especially applies to colloidal A^2B^6 QDs.

Thus, there is a great need to develop a theory of the synthesis of colloidal QDs, which could predict the influence of an ultrasonic wave on the process of obtaining QDs at all its stages. At present, there are no models in the literature that would adequately describe the synthesis of QDs using ultrasound both at the nucleation stage and at the nanocrystal growth stage.

In this work, the theory of synthesis of CdSe semiconductor colloidal QDs using ultrasonic treatment is developed.

The proposed theory is based on an increase in the temperature of the colloidal solution and the diffusion coefficient of the monomer under the influence of ultrasonic cavitation. The regularities of the influence of ultrasound on the conditions for the nucleation of nanoparticles in a colloidal solution have been established. It is shown that an increase in the intensity of ultrasonic oscillations leads to a decrease in the energy barrier for the formation of nanoparticles. It was established that ultrasound leads to a decrease in the critical radius of colloidal nanoparticles. And when the radius of nanoparticles exceeds this critical value, their growth is observed. It is shown that at the beginning of nanocrystal growth, an increase in intensity of ultrasound leads to an increase in the growth rate, followed by a sharp decrease.

1. Entezar M.H., Ghows N. Micro-emulsion under ultrasound facilitates the fast synthesis of quantum dots of CdS at low temperature. *Ultrasonics Sonochemistry*, 2023, V. 18, No 1, pp. 127-134.

The Energy Spectrum of an Electron in a Linear Quantum Molecule Formed From Four Quantum Dots Nanoparticles

Holskiy V.B., Leshko R.Ya., Holska S.V., Karpiy V.R.

Department of Physics and Information Systems, Drohobych Ivan Franko State Pedagogical University, Drohobych, Ukraine, hol.wit@dspu.edu.ua

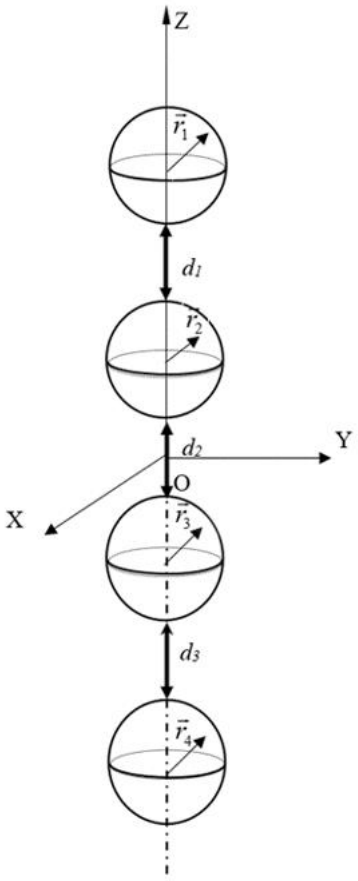

Fig. 1. LQM scheme.

Semiconductor quantum dots (QDs) are a promising platform for processing quantum information in solid-state devices [1]. The QD system has advantages in realizing quantum bits (qubits), including a relatively long electron spin coherence time, potential scalability due to well-established fabrication technologies, and small physical size per qubit. To date, QDs with given parameters have been formed into double [2], triple [3], four [4] and five QD [5] quantum molecules (QMs) to increase the number of qubits. Recently, half-filled QDs in a nine-QD array have been demonstrated. Multiple QDs can also be used to study the physics of electron interactions, such as quantum cellular automata, the Fermi-Hubbard model, and negative exchange couplings.

Modeling of a linear quantum molecule (LQM) from four spherical QDs will be carried out using a system of four spherical potential quantum wells (QWs) located along a straight line. The problem will be solved in the Cartesian coordinate system. Let the centers of the quantum wells be on the OZ axis, and let the origin of the coordinates be between the second and third QW. We will choose the coordinate system so that the QD centers lie on the OZ axis, and point O is located in the center of the middle QD (Fig. 1).

To find the energy of the electron, you need to solve the stationary Schrödinger equation

$$\hat{H}\Psi(x,y,z)=E\Psi(x,y,z) \tag{1}$$

with the Hamiltonian in the approximate effective mass. For this heterostructure, it has the form:

$$\hat{H}=-\frac{\hbar^2}{2}\nabla\frac{1}{m}\nabla+U(x,y,z). \tag{2}$$

Here, m is the effective mass of the electron for the corresponding region, $U_0 < 0$.

To solve the Schrödinger equation, we will use the approximation of a linear combination of quantum well orbitals. According to this method, the wave function of an electron must be represented as a linear combination of the wave functions of individual quantum wells:

$$\Psi(x,y,z) = C_1\Psi_{1s}(x,y,z) + C_2\Psi_{2s}(x,y,z) + C_3\Psi_{3s}(x,y,z) + C_4\Psi_{4s}(x,y,z), \quad (3)$$

where $\Psi_{is}(x,y,z) \equiv \Psi_{is}$ is the wave function of the ground state i-th QW (i = 1, 2, 3, 4).

A study of the stationary states of the electron in the LQM formed from four spherical QDs of the system was carried out $GaAs / AlAs$. The following values were used for the calculation: the effective mass of the electron in the QD $m_{GaAs} = 0,063m_0$ and in the matrix $m_{AlAs} = 0,15m_0$, gap of zones in this heterosystem, which determines the depth of the potential well – 560 меВ. The range of radii of the considered QDs is 2.5-4.5 constant grids *GaAs* (a_{GaAs}=5,65 $Å$), or approximately from 14,1 $Å$ to 25,4 $Å$.

In Fig. 2 the dependence of the energy spectrum of the electron on the distance between the nanocrystals in the symmetric case is given.

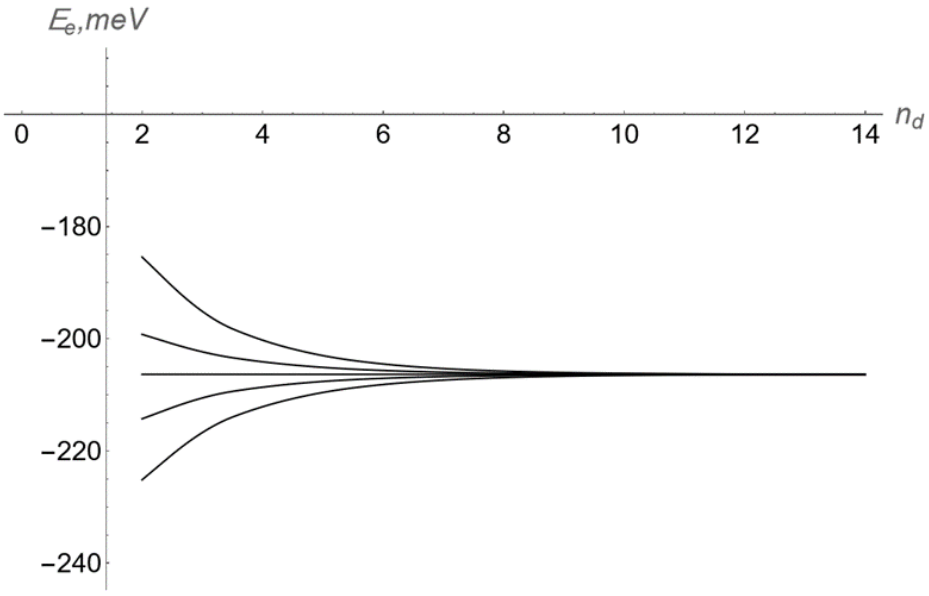

Fig. 2. Dependence of electron energy in a quantum molecule formed from four spherical quantum dots of the same radius ($R_1 = R_2 = R_3 = R_4 = 4a_{GaAs}$) from the distance between them (symmetric case $d_1 = d_2 = d_3$)

The sizes of all QDs are equal to 4 solid lattices *GaAs* ($R_1 = R_2 = R_3 = R_4 = 22{,}61\ Å$), and the distance n_d (the number of stable grids AlAs) between the boundaries of the division changed.

For LQM (Fig. 2, when $d_1 = d_2 = d_3$, from 2 to 14 steel grids AlAs (a_{AlAs} =5,66 $Å$). In this case, LQM is characterized by four rins (E_1, E_2, E_3 and E_4), which are obtained by splitting the level of isolated QDs. With increasing distance (approx $n_d = 8a_{AlAs}$) these levels merge into one corresponding to the electron energy in an isolated QD.

So, the dispersion equation for studying the energy spectrum of an electron in a linear QM of four spherical QDs was obtained in the work. The influence of the distance between CTs and the size of QDs on the energy case in a symmetric QD is analyzed. In this case, the system is characterized by four states that merge into one as the distance increases.

It should also be noted that an increase in volume leads to a decrease in the splitting of electron energy levels.

1. Koppens F. H. L., and other // Nature 442, 766 (2006).
2. Blick R. H., and other // Phys. Rev. B 53, 7899 (1996).
3. Gaudreau L., and other //Nature Physics 8, pp. 54-58 (2012)
4. Takakura T., and other //Appl. Phys. Lett. 104, 113109 (2014)
5. Zajac D. M., and other // Phys. Rev. Appl. 6, 054013 (2016).

Optical reflection of silicon nanowires

Demchyna L.A., Mynaylo M.A., Pekur D.V., Vuichyk M.V., Kyiak J.P., Gentsar P.O., Vlasenko O.I.

V. Lashkaryov Institute of Semiconductor Physics, National Academy of Sciences of Ukraine, Kyiv, Ukraine, rastneg@isp.kiev.ua

A promising material for modern micro- and nanoelectronics are silicon nanowires (NWs) [1]. The aim of this work is to study the reflection optical spectra in the spectral range (0.2÷25) 10^{-6} m of silicon NWs of different heights to obtain data on the energy band structure and other properties. Silicon NWs are grown on the surface of a single crystal silicon plate (100) - p+-type oriented silicon (thickness 510 ± 20 μm and resistivity 0.01 Ω·cm). The produced samples of silicon NWs had a porosity of 60%. The length of silicon NWs l_{NW} was 5.5 μm; 20 μm; 50 microns [2].Based on the Heisenberg uncertainty principle for energy E and time t ($\Delta E \cdot \Delta t \geq \hbar$), the relaxation effects in the absorption of electromagnetic waves by a crystal are described by the broadening parameter $\Gamma = \hbar/\tau$ (broadening of the electronic transition E_0 is related to the lifetime of free charge carriers due to the interaction them with fluctuations of the crystal lattice, impurities, defects, including those of a surface nature), where τ is the energy relaxation time of photogenerated charge carriers. In the optical reflection spectra of silicon NWsin the spectral range of wavelengths 200 nm ÷ 1700 nm, two energy peaks are observed at energies of 0.862 eV and 1.046 eV. From the optical reflection spectra for silicon NWswith these lengths, the energy broadening of the optical spectra of the materials equal to 0.184 eV and the energy relaxation time of photogenerated charge carriers τ equal to 3.577·10-15 s were determined.

Experimental data and calculations indicate a change in the energy band structure of silicon nanowires in comparison with a single crystal p-Si (100), that can be explained by the quantum-dimensional effect that occurs in the studied objects.

1. Ming Hu, Hua Bao, Yaping Dan, Si nanowires for evolutionary nanotechnology in: Silicon Nanomaterials Sourcebook, ed. K.D. Sattler, CRC Press, 2017.
2. Gentsar P.O., Vuichyk M.V., Isaev M.V., Lischuk P.O. Optical Properties of Porous Silicon p-Si(100). *Physics and Chemistry of Solid State*. 2019. V. 20, No 3. P. 264-268.

An ordered array with two different quantum dots in a unit cell

Bilynskyi I.V.[1], *Leshko R.Ya.*[2], *Bandura H.Ya.*[2]

[1]*Kryvyi Rih State Pedagogical University, Kryvyi Rih, Ukraine,*
[2]*Drohobych Ivan Franko State Pedagogical University, Drohobych, Ukraine,*
galinka.bandura@gmail.com

An important task of modern science and technology is to create artificial materials with desired physical properties that are not found in nature. Modern nanomaterial technologies enable the fabrication of artificial materials composed of hundreds or even thousands of nanoscale components with diverse structures. One promising element is the semiconductor quantum dot, and their large quantity can lead to a superstructure.

Up to now, most of the theoretical models used have investigated arrays of quantum dots with identical quantum properties. The review paper [1] describes superstructures of quantum dots and their characteristics. The authors of the experimental study demonstrated models and proved that different layers could have different quantum dots. This work encourages the development of a model that takes into account the variety of quantum dots within the structure.

Our work presents a theory that describes a one-dimensional periodically ordered array with two different quantum dots in the elementary cell. By applying this theory, we performed calculations of dispersion dependencies and bandwidths. Due to the presence of different quantum dots, a division into upper and lower minibands of the ground state occurred. Each of them has been analyzed.

The theory allows for the study of various structures. Examples include superstructure elements that differ in the type or size of quantum dots. It is possible to adjust or alter the distances between the quantum dots. Distances between surfaces may also vary. Therefore, we have the capability to investigate energy spectra, band widths, and other properties of the superstructure.

1. Hongbo Lan, Y.H. Ding, Ordering, positioning and uniformity of quantum dot arrays, 2012, *Nano Today*, 7(2), pp. 94-123. DOI:10.1016/j.nantod.2012.02.006

SECTION C:

The semiconductors for LEDs,

solar and related energy technologies and sensor materials

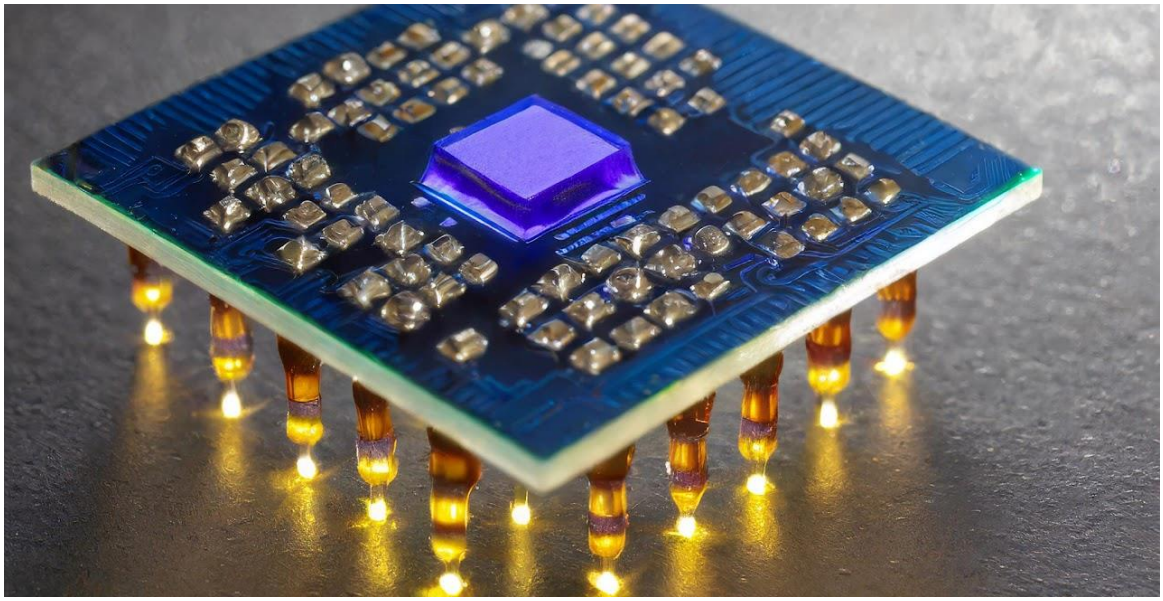

Structural Studies of Semiconductor and Dielectric Materials

Shiojiri Makoto[1], *Chen Miin-Jang*[2]

[1]*Kyoto Institute of Technology, Kyoto, Japan,*
shiojiri@pc4.so-net.ne.jp
[2]*Department of Materials Science & Engineering and Graduate Institute of Electronics Engineering, National Taiwan University, Taipei, Taiwan, ROC*

We review some of our investigations on (1) high crystallinity nitride layers and (2) dielectric ZrO_2 thin films, prepared by new atomic layer deposition (ALD) techniques, following touching on our early investigations of semiconductors.

In 1961, MS published his first paper on alkali antimonides which was to use in image orthicon for TV camera tubes [1]. The specimens were prepared in specially designed ultra-high vacuum tubes for X-ray study and electrical measurement. In 1997, we first equipped a commercial FE-TEM/STEM microscope with a high-angle annular dark field detector and performed quantitative elementary analysis of Sr(Bi)TiO_3 and Si(As) in *Z*-contrast images, with the aid of an image simulation program developed by us. We evaluated the concentration of As atoms in every Si atomic column in a Si crystal ion-implanted with As [2].

(1): GaN-based materials used in conventional LED are grown by MOCVD. They have a high misfit threading dislocations (TD) density of 10^7-10^{10} cm^{-2}. A V-defect generally nucleates at the intersection of a TD with the first of the InGaN multiple quantum well (MQW) layers in InGaN/GaN LED, having small MQWs on its side walls [3, 4]. The V-defect prevents the carriers from entering to recombine nonradiatively at the TD by enclosing it. This is a reason why InGaN/GaN can be used as LED despite the presence of numerous TDs. However, some of the carriers recombine radiatively at the small MQWs enclosing the V-defect [5, 6]. The V-defects also reduce the effective volume of the main MQW. Therefore, the efficiency of the LED increases if the TD density is reduced. We fabricated an ultrahigh crystallinity GaN film on the sapphire substrate by ALD (500^{o}C) and post-deposition annealing (PDL) (1130^{o}C) [7]. A LED using this GaN film as a buffer layer (BL) yielded a higher EL efficiency. The TD density of the GaN epilayer on the BL was as low as $2.2\times10^5/cm^2$. TEM observation elucidated why the BL grew with such high crystallinity. We also fabricated AlN films as thin as ~30 nm with good crystallinity on the sapphire substrates by low-temperature (300^{o}C) ALD with layer-by-layer, *in-situ* atomic layer annealing (ALA), accomplishing 2D-electron gas characteristics of the AlN/GaN hetero-junction [8].

(2): We prepared ferroelectric (FE) ZrO_2/HfO_2, paraelectric (PE) ZrO_2/HfO_2, and PE HfO_2 capacitors, using plasma ALD (300^{o}C) for the PE-HfO_2 and FE-ZrO_2 and ALD (250^{o}C) in thermal mode for the PE-ZrO_2 [9]. The FE inductance and negative capacitance (NC) originated from polarization switching *via* both small- and large-signal operations of the as-deposited FE ZrO_2 layer. The nano FE-ZrO_2 yielded a positive imaginary impedance and the

capacitance enhancement as connected in series with a PE capacitor and demonstrates the FE inductance and NC under small-signal modulation. The FE inductance is useful in wide applications such as wireless communications, radar, and RF-integrated circuits. TEM observation revealed FE domains, which are responsible for the small-signal operation of the FE inductance and NC. We also fabricated three metal-insulator-metal (MIM) structures on TiN/Si substrates: (a) Pt/ZrO_2/Pt, (b) Pt/TiN/ ZrO_2/Pt with a ~10-nm TiN capping layer on the ZrO_2 layer, and (c) Pt/ZrO_2/Pt from which the TiN capping layer was etched away [10]. The ZrO_2 layers were deposited at 200^{o}C or 250^{o}C and the TiN layers were deposited at 300^{o}C, by plasma-enhanced ALD. Electrical measurement, X-ray diffraction, and TEM revealed that the MIM (a) is PE due to amorphous (*a*) ZrO_2, the MIM (b) is anti-FE due to the crystallization of *a*-ZrO_2 to tetragonal (*t*) phase, and the MIM (c) is FE due to transformation of *t*-ZrO_2 to orthorhombic phase by stress relaxation from the capping. The PE/AFE/FE modulation of ZrO_2 thin films was achieved without any high-temperature post-annealing, which is advantageous to the process integration in wearable devices and advanced nanoscale transistor/ memory devices.

1. Chikawa J., Imamura S., Tanaka K., Shiojiri M. Crystal Structures and Electrical Properties of Alkali Antimonides. *J. Phys. Soc. Jpn.* 1961. **16**, 1175-1180.
2. Yamazaki T., Watanabe K., Kikuchi Y., Kawasaki M., Hashimoto I., Shiojiri M. Two-Dimensional Distribution of As Atoms Doped in a Si Crystal by Atomic-Resolution High-Angle Annular Dark Field STEM. *Phys. Rev.* 2000, B **61**, 13833-13839.
3. Watanabe K., Yang J.R., Huang S.Y., Inoke K., Hsu J.T., Tu R.C., Yamazaki T., Nakanishi N., Shiojiri M. Formation and Structure of Inverted Hexagonal Pyramid Defects in Multiple Quantum Wells InGaN/Gan: *Appl. Phys. Lett.* 2003. **82**, 718-720.
4. Tsai H.L., Wang T.Y., Yang J.R., Chuo C.C., Hsu J.T., Feng Z.C., Shiojiri M. Observation of V Defects in Multiple InGaN/GaN Quantum Well Layers. *Materials Transactions* 2007, **48**, 894-898.
5. Watanabe K., Yang J.R., Nakanishi N., Inoke K., Shiojiri M. Direct Determination of Atomic Structure in MQW-InGaN/GaN. *Appl. Phys. Lett.* 2002. **80**, 761-762.
6. Shiojiri M., Chuo C.C., Hsu J.T., Yang J.R., Saijo H. Structure and Formation Mechanism of V-defects in Multiple InGaN/GaN Quantum Wells Layer. *J. Appl. Phys.* 2006. **99**, 073505 (6 pages).
7. Shih H.Y., Shiojiri M., Chen C.H., Yu S.F., Ko C.T., Yang J.R., Lin R.M., Chen M.J. Ultralow Threading Dislocation Density in GaN Epilayer on Near-Strain-Free GaN Compliant Buffer Layer and Its Applications in Hetero-Epitaxial LEDs. *Sci. Rep.* 2015, **5**, Article number 13671.
8. Shih H.Y., Lee W.H., Kao W.C., Chuang Y.C., Lin R.M., Lin HC., Shiojiri M., Chen M.J. Low-Temperature Atomic Layer Epitaxy of AlN Ultrathin Films by Layer-by-Layer *in-situ* Atomic Layer Annealing. *Sci. Rep*. 2017. **7**, Article number 39717.
9. Cheng P.H., Yin, Y.T., Tsai I.N., Lu C.H., Li L.J., Pan S.C., Shieh J., Shiojiri M., Chen M.J. Negative Capacitance from the Inductance of Ferroelectric Switching. *Communications Phys*. 2019. 2:32.
10. Wang C.Y., Wang C.I., Yi S.H., Chan T.J., Chou C.Y., Yin Y.T., Shiojiri M., Chen M.J. Paraelectric/Antiferroelectric/Ferroelectric Phase Transformation in As-Deposited ZrO_2 Thin Films by TiN Capping Engineering. *Materials and Design* 2020. **195**, 109020.

Ultraviolet photodetectors based on polymer/zinc oxide nanoparticles hybrid materials

Stolyarchuk A.I., Dan'kiv O.O., Bachynsky O.I., Stolyarchuk I.D.

Drohobych Ivan Franko State Pedagogical University, Drohobych, Ukraine,
andrii.stoliarchuk@dspu.edu.ua

Recently, inorganic/organic hybrid materials have attracted much attention due to their unique properties and possible applications in different fields. Among other things, these materials are promising for fabrication of ultraviolet (UV) photodetectors. In particular, among advantages of UV photodetectors based on hybrid nanomaterials low cost and narrow band spectral response can be noted.

In presented work, we report on design and characteristics of UV photodetectors based on polymer/ZnO nanoparticles hybrid nanomaterials. The structure of the UV photodetector includes glass substrate with ITO layer, polymer, ZnO nanoparticles and Al top electrode. As a polymer we have used polyvinylcarbazole (PVK) deposited by spin coating technique. The ZnO nanoparticles with average size of 4 nm were prepared according to previously reported method using zinc acetate dihydrate as main chemical reagent [1]. Colloidal suspension with ZnO nanoparticles was spin coated over the PVK polymer layer. The PVK layer acts as the hole transporting layer of the photodetector, and its absorption onset is placed close to the absorption edge of ZnO nanoparticles. The fabricated hybrid device has demonstrated a narrow band spectral response in the range of (300-370) nm, which can be tuned by change of average size of inorganic nanoparticles or replacing of the transparent electrode.

1. Salavati-Niasari M., Davar F., Fereshteh Z. Synthesis and characterization of ZnO nanocrystals from thermolysis of new precursor. *Chemical Engineering Journal*. 2009. V. 146, No. 3. P. 498-502.

Technological aspects of deposition cadmium sulphide thin films as buffer layer

Katanova L.O.[1], *Nykyruy L.I.*[1], *Yavorskyi R.S.*[1], *Kashuba A.I.*[2], *Semkiv I.V.*[2]

[1]*Vasyl Stefanyk Precarpathian National University, Shevchenko Str., 57, 76018 Ivano-Frankivsk, Ukraine,*
[2]*Lviv Polytechnic National University, Bandera Str. 12, 79013 Lviv, Ukraine,*
lilia.katanova@pnu.edu.ua

Considering the properties of cadmium sulfide and cadmium telluride thin films, there are some aspects that are considered critical for the formation of the CdTe/CdS solar cells. First, the uniformity of the film and the thickness of the CdS layer affect the efficiency of the solar cell [1]. The CdS layer can limit current generation due to light absorption, and this problem can be mitigated by using thinner films. Thinner films transmit most of the light, but the thickness of the layer has a lower limit below which this layer becomes ineffective. When reducing the thickness of the layer, the other aspects must be considered, such as suboptimal distribution of the electric field and possible increase in non-uniformity of structure. The aim is to minimize the reduction of V_{OC} and FF values due to the presence of point defects, leakage along grain boundaries and to maximize light transmission through the layer. According to the literature, CdS layers have an optimal thickness of about 100 nm. Decreasing the thickness further (below) than 50 nm leads to severe losses in V_{OC} and FF due to non-uniformity (loss of integrity) of CdS [2].

Another important problem for CdS and CdTe film deposition is the formation of point defects. Thus, substrate cleaning and post-deposition processing also have a significant impact on material properties and performance. Various attempts have been made to overcome these problems, since the deposition of a thin layer of CdS with a second layer of fine grains to fill the point defects (~80 nm), creating a double-layer structure can improve the short-circuit current of the cell. Furthermore, during post-deposition processing, mutual diffusion between S (from CdS) and Te (from CdTe) usually occurs, resulting in CdS consumption. Therefore, this method can be useful to protect the junction properties and preserve the integrity of the CdS layer. By using a bilayer structure, the formation of point holes is reduced while maintaining a relatively thin layer of CdS.

1. Nykyruy L. I. et al. Evaluation of CdS/CdTe thin film solar cells: SCAPS thickness simulation and analysis of optical properties. Optical Materials. 2019. V. 92. P. 319-329.
2. Jaegermann W., Klein A., Fritsche J., Kraft D., Späth B. Interfaces in CdTe solar cells: from idealized concepts to technology. MRS Online Proceedings Library. 2004. V. 865. P. 611-623.

The effect of growth conditions of PbTe layers on their IR properties

Vuichyk M.V., Svezhentsova K.V., Tsybrii Z.F.

V. Lashkaryov Institute of Semiconductor Physics, National Academy of Sciences of Ukraine, Kyiv, Ukraine, vuychik@isp.kiev.ua

Systematic study of the thin films formation processes and research of films properties in relation to growth conditions ensures optimization of technological processes of photoelectronic devices creation.

This work presents the results of PbTe thin films research using atomic force microscopy, Fourier spectroscopy, and photosensitivity studies in the infrared range of the spectrum with the aim of studying the temperature effect during growth on the optical and photoelectric characteristics of thin films. Such studies are relevant because the possibility of using PbTe thin films as thermoelectric, photoreceiving and emitting structures for the IR range, as well as, due to the phase-changing phenomena it can be exploited for active terahertz photonic applications[1, 2].

The layers of PbTe were grown by the hot-wall epitaxy method on freshly cleavaged BaF_2 (111) substrates. By changing the temperature of the substrate (420-520 K), the source (650-750 K) and the sputtering time, the optimal regimes for growing thin (~ 50 – 500 nm) layers of PbTe with a high degree of morphological and structural perfection, were chosen. To create electrical contacts, a thin layer of gold was deposited using a thermal evaporation method, and for soldering the contacts, a multipurpose thermoultrasonic welding device "Hybond 626" was used.

A Femtoscan scanning probe microscope to study the surface morphology of the samples was used. Optical studies in the 1.3 - 25 μm spectrum range were carried out on an IR-Fourier spectrometer "Perkin Elmer" Spectrum BXII.

At the thickness of PbTe up to 200 nm, the transmission spectrum of the film repeats the transmission spectrum of the substrate BaF_2.However, with a film thickness of 200-250 nm, a sharp transmission peak is observed in the transmission spectrum in the main band-band energy transition region, and with a further increase in the film thickness, the transmission coefficient decreases again. The PbTe(250 nm)/BaF_2 structure demonstrated good room-temperature photoresponse in mid-IR range.

1. Nicolas M. Kawahalaet al., Thickness-Dependent Terahertz Permittivity of Epitaxially Grown PbTe Thin Films, Coatings, 2023, 13, 1855.
2. Alessandro Bellucci et al., Nanostructured Thermoelectric PbTe Thin Films with Ag Addition Deposited by Femtosecond Pulsed Laser Ablation, Energies, 2023, 16, 3216.

Thermal conductivity of GeBiTe solid solutions

Matkivskyi O.M., Balan V.R., Dadiak I.B., Horichok I.V.

Vasyl Stefanyk Precarpathian National University, Ivano-Frankivsk, Ukraine,
volodymyr.balan.22@pnu.edu.ua

Solid solutions based on germanium telluride are currently the best medium-temperature thermoelectric materials of p-type conductivity [1-2]. The highest values of thermoelectric factor were achieved for GePbBiTe solid solutions. Their values are ≈2.3 at T = 700 K. This value can be further improved, in particular by optimizing the doping process. However, the energy spectrum of carriers in solutions and its changes upon the introduction of impurities require a more detailed study.

As for other semiconductors of the A^4B^6 group, GeTe is characterized by a complex structure of the valence band. The set of experimental data is usually explained by taking into account two subzones, the distance between which depends on the temperature. However, the information on the numerical values of the characteristics of the band spectrum is incomplete. And the data of different authors do not always agree with each.

The paper calculates the electronic and lattice components of thermal conductivity coefficients for GeBiTe solid solutions. The calculation was carried out using two different models of the band structure of GeTe, which differ in the relative location of the zones of heavy and light holes. The first of the models is generally accepted for A^4B^6 compounds and assumes the location of the zone of light holes above the zone of heavy ones in the energy spectrum. Another model, obtained on the basis of DFT calculation, predicts the location of the zone of light holes below the zone of heavy ones. A significant difference was established in the numerical values of the electronic and lattice components of the thermal conductivity coefficients, depending on the adopted model. The influence of other calculation parameters on the investigated values was analyzed.

1. Dashevsky Z., Horichok I., Maksymuk M., Muchtar A. R., Srinivasan B., Mori T.. Feasibility of high performance in p-type $Ge_{1-x}Bi_xTe$ materials for thermoelectric modules. J. Am. Ceram. Soc. 2022. P. 1-12. https://doi.org/10.1111/jace.18371
2. Matkivskyi O.M., Balan V.R., Halushchak M.O., Dadiak I.B., Mateik G.D., Horichok I.V.. Thermal conductivity of GeBiTe solid solutions. Physics And Chemistry Of Solid State. 2024. V. 25, No. 1. P. 189-190.

Effect of structure defects on the microhardness of CdTe-ZnTe single crystals grown by sublimation

Brytan V.B., Tymkiv A.V., Kovalko M.C., Pavlovsky Y.V., Kovalchuk Yu.V., Uhryn Yu.O.

Drohobych Ivan Franko State Pedagogical University, Drohobych, Ukraine,
vbrytan2@gmail.com

CdTe-ZnTe single crystals are known for their high photosensitivity and ability to detect *X*-rays and gamma rays [1]. However, the presence of electrically active centers can reduce the efficiency of detectors.

The characteristics of semiconductor devices depend to a large extent on the structural perfection of the working elements. That is why the study of the effect of structural defects and mechanical stresses in the crystal matrix on the physical properties of the CdTe-ZnTe material is relevant from a scientific and practical point of view.

In this work, the microhardness of CdZnTe single crystals doped with different types of impurities (*V, Cl, Al* – impurity concentration 10^{19} cm^{-3}) grown by the freeze-drying method was studied [1].

Microhardness is a sensitive characteristic of the structural state of the sample surface. It is a complex integral characteristic when a diamond pyramid (indenter) is pressed in, and the material undergoes elastic-plastic microdeformation processes, resulting in the formation of an imprint. A dislocation structure is formed directly under the indenter, which develops in interaction with the intrinsic defects of the solder overlying layers of the material. By removing the dependence of microhardness on the indenter penetration depth, it is possible to trace the influence of processing and structure of various sub layers and the surface layer on mechanical properties.

Studies have shown that alloying samples with chlorine and vanadium leads to a decrease in microhardness, but their crack resistance increases significantly. Vanadium-alloyed samples have higher microhardness than chlorine-alloyed samples, and their crack resistance threshold is the highest. Aluminum alloying leads to strengthening of the near-surface layers of CdTe-ZnTe single crystals. The single crystals grown in a hydrogen atmosphere have a high threshold of crack resistance, which is a positive result in terms of the mechanical stability of structural and functional elements made on their basis.

1. Szeles C. CdZnTe and CdTe materials for *X*-ray and gamma ray radiation detector applications. *Physica Status Solidi (B)*. 2004. V. 241, No 3. P. 783-790.
2. Brytan V.B., Pigur O.M., Popovich V.D., Tsyutsyura D.I. Preparation and electrical properties of $Cd_{1-x}Zn_xTe$ crystals. *Inorganic materials*. 2005. V. 41, No 7. P. 782-784.

SECTION D:

Synthesis, processing and characterization of multifunctional oxide materials

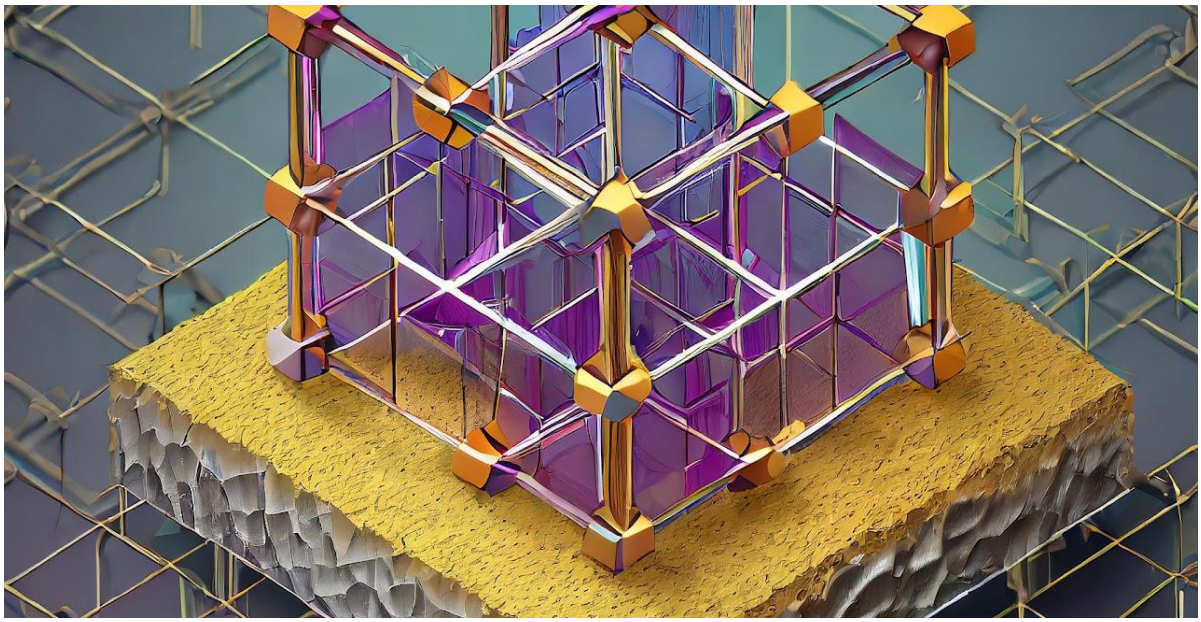

Refractive parameters of rubidium sulfate crystals at low temperatures

Pryshko I.A.[1], *Stadnyk V.Yo.*[1], *Shtuka O.V.*[1], *Novosad I.S.*[1,2]

[1]*Physics Faculty, Ivan Franko National University of Lviv, Lviv 79005, Ukraine*
[2]*Lviv Politechnic National University, Lviv 79013, Ukraine*
pryshko_ivan@ukr.net

Crystals of the $ABSO_4$ group (A, B = K, Li, Rb, NH_4) have an optical isotropic point (OIP), which consists in increasing the symmetry of the optical indicatrix in the case the spectral range or temperature changes. The transition through OIP is accompanied by a change in the sign of birefringence of the crystal, that is, its inversion takes place [1].

Crystals with OIP are interesting due to the possibility of their use as crystal-optical sensors for measuring temperature and pressure, as well as acousto-optical modulators. They create better opportunities for temperature measurement in harsh conditions (high electric and magnetic fields, moving parts) and can provide sensitivity up to 10^{-3} K.

The temperature-spectral dependences of the refractive indices of the studied crystals were carried out by the well-known photographic Obreimov method [2].

The temperature changes of the refractive indices of the Rb_2SO_4 crystal in the region of low temperatures were studied. It was established that with a decrease in temperature the refractive indices n_i for all crystal physical directions increase at different rates ($dn_z/dT > dn_x/dT$), which leads to the intersection of the curves $n_z(T)$ and $n_x(T)$, so that at a temperature of T = 85 K the equality $n_z = n_x = 1.51936$ is observed. This indicates the existence of an optical isotropic point in this crystal, which is confirmed by independent temperature measurements of the angle between the optical axes. It is shown that rubidium sulfate crystals are optically biaxial; at room temperature the angle between the optical axes is $2V = 41.5°$, and with decreasing temperature it decreases almost linearly, so that at T = 85 K the crystal changes from optically biaxial to optically uniaxial ($2V = 0°$).

The temperature changes of the values of electronic polarizability α_i were calculated, and it was shown that they slightly increase as the temperature decrease, so that in the region, where the optical isotropic point exists, the values α_x and α_z are equal to each other. This behavior of $\alpha(T)$ of the rubidium sulfate crystal is similar to the behavior of electronic polarizabilities of isomorphic crystals of the $ABSO_4$ group [3].

1. Bhar G.C. Refractive index dispersion of chalcopyrite cristals. Applied Physics, 1980, V. 13, P. 455.
2. Romanyuk M.O. Crystal Optics. Lviv, Ivan Franko LNU, 2017, 456 p.
3. Bovgyra O.V., Stadnyk V.Yo., Chyzh O.Z. Energy band structure and refractive of $LiRbSO_4$ crystals. Phys. of Solid State, 2006, V. 48, № 7, P. 1268.

Optical characteristics of ZnMnO nanoparticles prepared by ball milling technique

Stolyarchuk A.I., Popovych A.V., Hadzaman I.V., Kuzyk O.V.

Drohobych Ivan Franko State Pedagogical University, Drohobych, Ukraine,
andrii.stoliarchuk@dspu.edu.ua

Transition metal doped ZnO belongs to so-called diluted magnetic semiconductors (DMS) which are promising materials for spintronic device applications. This practical aspect is based on revealing of stable ferromagnetic ordering at room temperature for several DMS oxides in various forms (bulk crystals, thin films and nanocrystals). However, the mechanisms of ferromagnetic behavior in these materials are still unclear. The growth and properties of ZnO-based DMS nanostructures have been extensively studied, but there are still a number of unanswered questions concerning the relationship between fabrication conditions and optical properties.

In this work, $Zn_{1-x}Mn_xO$ nanoparticles were synthesized by a mechanical alloying process of the ZnO and Mn_2O_3 components. The content of magnetic impurities in the nanoparticles was determined by the weight ratio of the initial powders. Over time, small amounts of as-milled powders were periodically taken out of the vial inside the glovebox for structural and optical measurement. Scanning electron microscopy (SEM), atomic force microscopy (AFM), optical absorption and magneto-optical Faraday rotation measurements were main characterization methods in our study. The crystallite size reduced as a function of the milling time. As compared with pure ZnO nanocrystals, the optical absorption edge of the $Zn_{1-x}Mn_xO$ nanoparticles demonstrate significant blue shift and dependence of their size.

The Faraday rotation in $Zn_{1-x}Mn_xO$ nanoparticles gives evidence for paramagnetic behaviour at room temperature.

Influence of the structure of $Fe_xSi_yO_z$ films obtained by the ion-plasma sputtering method on their electrophysical properties

Kykot A.M.[1], *Bratus O.L.*[2], *Gudymenko O.Yo.*[2], *Evtukh A.A.*[2]

[1] *Taras Shevchenko National University of Kyiv, Institute of High Technologies, 2, Glushkova avenue, Kyiv, Ukraine, ankykot@gmail.com*

[2] *V. Lashkaryov Institute of Semiconductor Physics, NAS of Ukraine, 41, Nauky avenue, 03028 Kyiv, Ukraine*

Metal oxide $Fe_xSi_yO_z$ materials can be used in various fields, including wireless communication technologies, electronics, medicine and defense. They allow to reduce the impact of electromagnetic radiation on people and devices in various frequency ranges, and also provide effective electromagnetic interference protection. The prtparation technology and their subsequent temperature treatment have the significant impact on the structure and electrophysical properties of $Fe_xSi_yO_z$ coatings. The purpose of this work is to study the effect of temperature treatment of $Fe_xSi_yO_z$ films in the temperature range of T = 400-1000°C obtained by ion-plasma sputtering on their structure, composition and electrical characteristics.

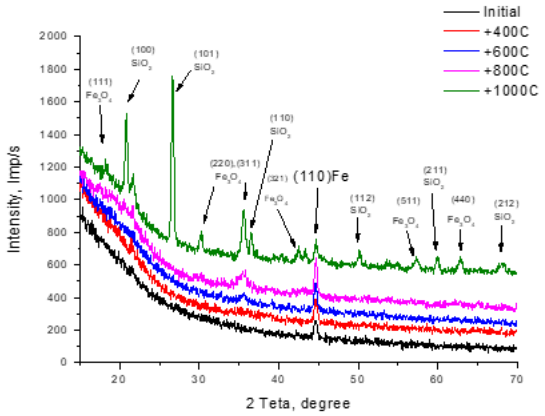

Fig. 1. Diffractograms of the initial and annealed in the temperature range of T = 400-1000°C in the Ar atmosphere for 30 min $Fe_xSi_yO_z$ films

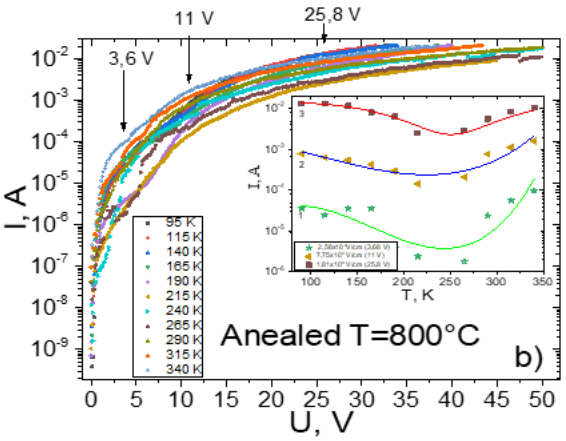

Fig. 2. I-V characteristics in semi-logarithmic coordinates of the sample annealed at T = 800°C. The parameter is the measurement temperature in the range from 95 K to 340 K

Using the method of X-ray diffraction (XRD), the structural transformation of composite $Fe_xSi_yO_z$ films as a result of thermal annealing was established, which leads to the appearance of a dielectric-metal transition and its shift in the current-voltage characteristics of the films.

This research was supported by the project "Development of nanocomposite material technology for highly efficient absorption of electromagnetic radiation" of the National Research Foundation of Ukraine (No. 2022.01/0066).

Transparent conducting In_2O_3:Sn films made by reactive magnetron sputtering from the alloy target oxide

Zayats M.S., Boiko V.G., Pekur D.V., Romanyuk B.M., Gentsar P.O.

V. Lashkaryov Institute of Semiconductor Physics, NAS of Ukraine, Kyiv, Ukraine,
zayats@isp.kiev.ua

In_2O_3:Sn (indium tin oxide – ITO) films were deposited by reactive magnetron sputtering method using a alloy metal target and the low-pressure reactive gas mixture - Ar + O_2. A target for indium oxide deposition were fabricated from the alloy In (95%) + Sn (5%).

Investigations of the sheet resistance ***R*** and transmittance ***T*** from different technological conditions under ITO deposition process were indicated that ***R*** and ***T*** were strongly subjected by value of vacuum in chamber, partial pressure of oxygen, film deposition rate. The dependencies ***R*** and ***T*** versus pressure value in vacuum chamber for two oxygen percentages are shown in Fig. l. The figure clearly demonstrates that increasing the oxygen containing on 2 % in the gas mixture strongly shifts curves to the low-pressure range.

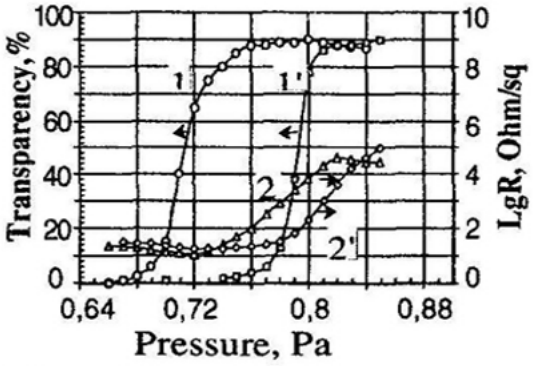

Fig. 1. Dependence sheet resistance ***R*** and transparency ***T*** from pressure of gas in vacuum chamber. Content of oxygen in gas: 1,2 – 20 %; 1',2' – 18 %

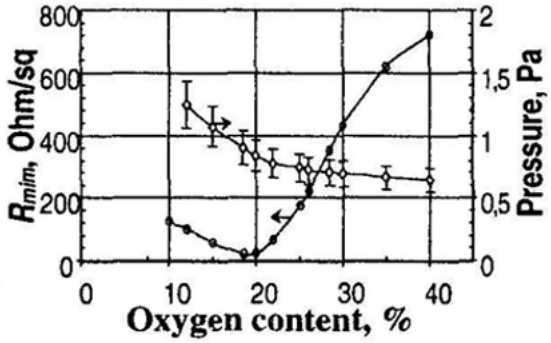

Fig. 2. Dependence of pressure when minimum of sheet resistance occurred and its minimum value R_{min} vs. oxygen partial percentage

The investigation of a sheet resistance minimum at high transparency (non less 85 %) versus oxygen percentages was carried out to determine the optimal gas mixture composition during reactive magnetron ITO deposition. The resistance minima are observed at each oxygen percentages during changing of a total pressure in the operation region. The dependence of pressure value when a sheet resistance minimum occurred and its value R_{min} versus oxygen partial percentage are shown in Fig. 2. The optimal value of oxygen contents (18-20%) could be readily determined from this graphical dependence. The best archived parameters of ITO films were: transparency - not less than 85%; sheet resistance - 10÷20 Ohm/sq. Displays and energy-efficient windows applications put forward other requirements to transparent conductive layers that will be discussed.

Noise properties of n-ZnO/p-Si heterojunctions

Virt I.S., Padalka I.V.

Drohobych Ivan Franko State Pedagogical University, Drohobych, Ukraine,
isvirt@dspu.edu.ua

The article investigated the optoelectronic characteristics of the n-ZnO/p-Si heterojunction photodiode for broadband photodetection. The heterojunction was fabricated by depositing an n-type ZnO thin film on a commercial p-type silicon substrate using pulsed laser deposition (PLD) technology. The structural properties of the PLD-grown n-ZnO material were analyzed. The current – voltage characteristics (CVC) of a photodevice with an n-ZnO/p-Si heterojunction under irradiation with different wavelengths in the range from UV to visible, in particular: 365 *nm*, 485 *nm*, 650 *nm*, respectively, were investigated. The measured barrier heights in the regions of forward and reverse bias are explained by a schematic band model with ZnO/Si interface boundaries.

In the conditions of its own bias, the photodiode shows an excellent sensitivity of 1.5 *A/W* when illuminated by ultraviolet radiation with a wavelength of 365 *nm*. The self-displacement properties of U_{ph} were also investigated under different lighting conditions. In addition, the photoresponse time dependence of the fabricated photodevice was also investigated and discussed in detail. The time dependence of the change in the noise characteristics of the photodevice was also investigated.

In order to evaluate the photosensitive characteristics in the ultraviolet region, noise power spectra (PSD) in heterostructures were investigated. PSD measurements without bias and with detector operating bias (50 *mV*) revealed good frequency stability with low 1/f noise for room temperatures. In particular, at 300 K, thermal noise dominates the noise spectrum at 1 *kHz* and 100 *kHz*, respectively, while 1/f type noise is observed at much lower frequencies. In particular, a noise model is proposed for the interpretation of experimental data in the case of original and artificially degraded silicon-based photovoltaic devices [1]. Such characteristics are explained by the clogging of traps for electron-hole pairs by charge carriers, which reduces the fluctuation possibilities of the transition. In addition, the time dependences of the photoresponse [2] of these photodevices were investigated and discussed.

1. Thongma S., Tantisantisom K., Grisdanurak N., Boonkoom T. UV enhanced white-light response based on p-Si/n-ZnO nanorod heterojunction photosensor. *Sensors and Actuators*, 2019, A 296, pp. 324-330.
2. Elkame I.B., Hamdaoui N., Mezni A., Ajjel R., Beji L. Efects of plasmon resonance on the low frequency noise and optoelectronic properties of Au/Cu codoped ZnO based photodetectors. *Optical and Quantum Electronics*, 2023, V. 55, 148, pp. 1-13.

Obtaining modified $La_{0.7}Sr_{0.3}MnO_3$ for cathodes of fuel cells

Kolkovska H.M.[1], *Kolkovskyi P.I.*[1,2], *Kotsyubynsky V.O.*[1], *Yaremiy I.P.*[1], *Rachiy B.I.*[1], *Ivanichok N.Ya.*[3]

[1]*Vasyl Stefanyk Precarpathian National University, Ivano-Frankivsk, Ukraine, galyna.godovska@gmail.com*

[2]*V.I. Vernadsky Institute of General and Inorganic Chemistry, National Academy of Sciences of Ukraine, Kyiv, Ukraine*

[3]*Joint Educational and Scientific Laboratory of the Physics of Magnetic Films, Vasyl Stefanyk Precarpathian National University, Ivano-Frankivsk, Ukraine*

Recently, the most commercially viable fuel cells are solid oxide fuel cells (SOFCs). $LaMnO_3$ doped by Sr is the most promising material for cathodes SOFC. In addition, perovskites-based material have recently been proposed and investigated for use in polymer exchange membrane fuel cells.

In particular, the optimized perovskite-based cathode material, such as $La_{1-x}Sr_xMnO_{3-\delta}$, is stable at elevated temperatures and has high electron/ion conductivity. In this point of view, perovskite $La_{0.7}Sr_{0.3}MnO_3$ was synthesized by the modified Pechini method, the advantage of which is that various metal ions are chelated with the formation of metal complexes in solution, uniformly distributed at the molecular level.

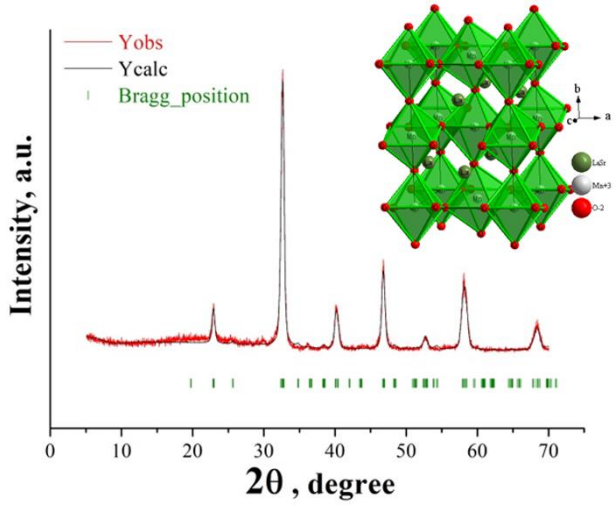

According to experimental X-ray diffraction data (Fig. 1), it was established that $La_{0.7}Sr_{0.3}MnO_3$ with a perovskite structure has an orthorhombic (Pnma) lattice. The model of the $La_{0.7}Sr_{0.3}MnO_3$ crystal structure (view along the C axis) shows that the Mn cation is in an octahedral environment of O_2 anions. The Mn-O bonds formed in the equatorial plane and axial vertices were determined to be about 1.944 Å long, and the O-O bond length across the axial vertices was found to be about 2.7492 Å, according to simulation data. In addition, La ions are located between equally oriented octahedral ones. The lattice constant of the synthesized material is a = 5.4929 Å, the volume V = 235.92 Å^3. According to X-ray data, the density of the material is $\rho = 6.54$ g/cm^3. The average size of coherent scattering regions is 24.

Funding: *This work was funded by the NATO Partnerships and Cooperative Security Committee in the framework of the Science for Peace and Security Programme (G6166).*

Manganese Dioxide (MnO_2) for Supercapacitor Applications

Misiuk O.I.[1], *Kolkovskyi P.I.*[1,2], *Kotsyubynsky V.O.*[1],
Rachiy B.I.[1], *Yaremiy I.P.*[1], *Tymofii T.M.*[1]

[1]*Vasyl Stefanyk Precarpathian National University, Ivano-Frankivsk, Ukraine,*
[2]*V.I. Vernadsky Institute of General and Inorganic Chemistry,*
National Academy of Sciences of Ukraine, Kyiv, Ukraine
santa.misuklord@gmail.com

Supercapacitors, characterized by their high power density and long cycle life, have emerged as a promising energy storage technology. Among various materials MnO_2 has garnered significant attention due to its high theoretical capacitance and natural abundance. The unique layered structure of MnO_2 allows for efficient ion transport, making it an ideal candidate for supercapacitor applications. This study is dedicated to exploring the crystal structure and electrochemical properties, charge-discharge characteristics, and the capacity of the comercial MnO_2 electrode. It is anticipated that these findings could contribute to the understanding of MnO_2 potential in the development of cost-effective and environmentally friendly energy storage solutions.

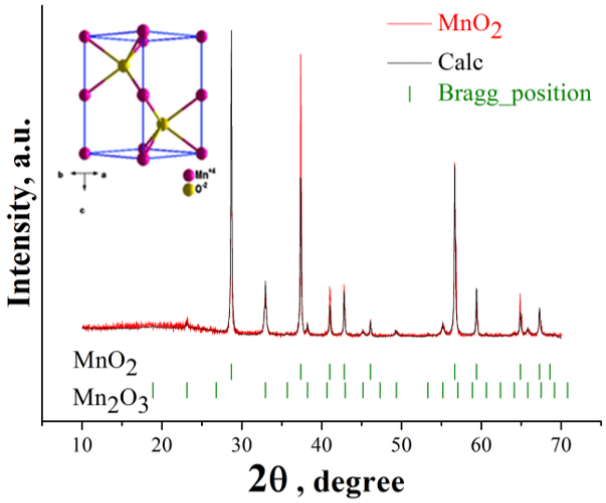

Fig. 1. XRD Pattern and (insert) the model of MnO_2 crystal structure

According to experimental X-ray diffraction data (Fig. 1), it was established that commercial MnO_2 has two phasics in sample including the MnO_2 76.5 % and Mn_2O_3 23.5 %.

Electrochemical properties of this sample manufactured based on three-electrode cells have been performed. Specific capacity calculated based on the cycling voltammetry method (CVA) measured from 1 mV/s to 50 mV/s. It was determined that the value of specific capacity is 45.9 F/g for 1 mV/s and decreased with increasing the scan rate up to 50 mV/s is 21.2 F/g.

Funding: *This work was funded by the NATO Partnerships and Cooperative Security Committee in the framework of the Science for Peace and Security Programme (G6166).*

SECTION E:

Advanced strategies for smart functional and multifunctional bionanomaterials and biointerfaces

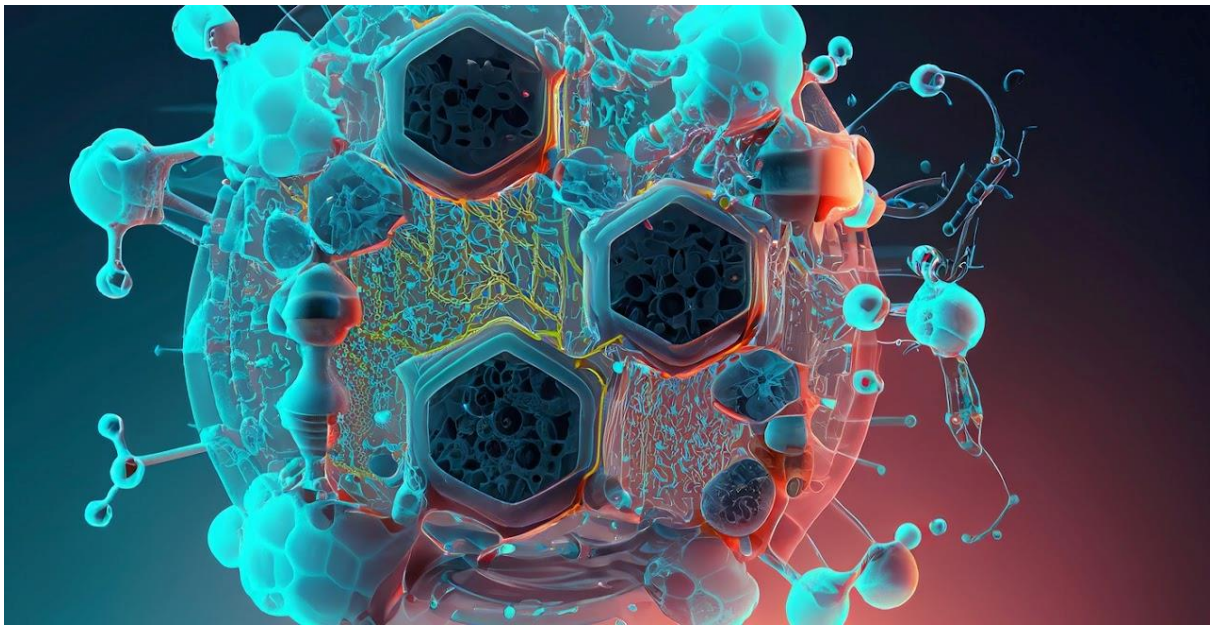

Study of trophic activity of Daphnia magna through analysis of optical density of Chlorella vulgaris

Leshko O.V., Leshko R.Ya., Atamanyuk A.M.

Drohobych Ivan Franko State Pedagogical University, Drohobych, Ukraine,
olha.leshko@dspu.edu.ua

In modern studies of the quality of natural and wastewater, besides traditional chemical analysis, organisms-bioindicators are increasingly used, as they allow for a comprehensive assessment of the impact of a combination of toxicants on living organisms.

The study investigated the toxicity of water from the Stebnik tailings pond using the test organisms Daphnia magna Straus. The culture of cladocerans was cultivated at a temperature of 20-22°C. Acute lethal toxicity of undiluted water and with dilution ratios of 1:2, 1:5, 1:10 was examined. Trophic activity of Daphnia was determined by changes in chlorophyll concentration using a ULAB 101 spectrophotometer based on optical density. For this purpose, Daphnia were kept for 24 hours in the test water samples without feeding. Then, Daphnia were transferred to control water, live Chlorella strain was added with a density of 15-20 million cells/ml, and optical density was measured after 5 hours.

Based on the optical density readings, the concentrations of Chlorella cells in the tested water samples were determined. The change in Chlorella cell concentrations in the control solution and the tested solutions enabled the assessment of the trophic activity of Daphnia magna.

The strongest toxic impact on Daphnia was observed with undiluted water, resulting in only 10% survival of Daphnia by the end of the first day. In the 1:2 dilution variant, over 50% of Daphnia perished within 48 hours (58.6%). Meanwhile, mortality in the control did not exceed 10%, with an average survival rate of 9.67 individuals out of 10 (3.34% mortality). Additionally, a significant decrease in trophic activity was observed in the 1:2 and 1:5 dilution variants due to reduced filtration movements in Daphnia.

Thus, the proposed methodology allows for the assessment of water toxicity based on the indicators of trophic activity of Daphnia magna.

SECTION F:

Laser material processing:

from fundamental interactions to innovative applications

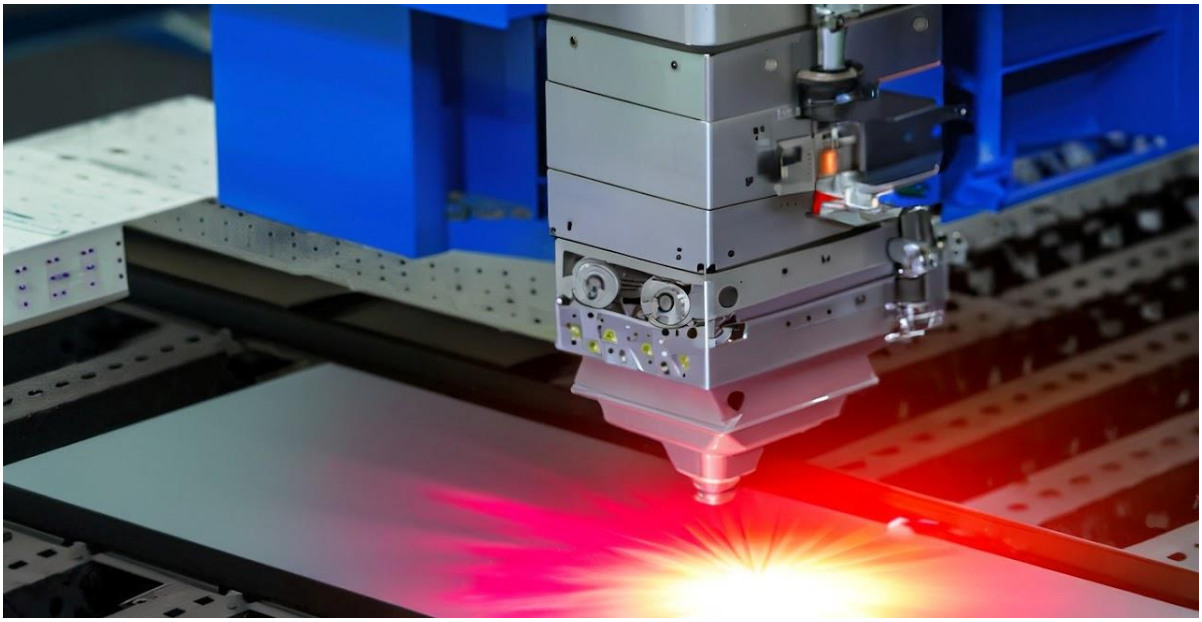

Time-resolved kinetics of laser destruction of materials for optoelectronic applications

Blonskyi I.V., Dmytruk A.M., Dmitruk I.M., Kadan V.M.

Institute of Physics of the National Academy of Sciences of Ukraine, Kiev, Ukraine,
blon@iop.kiev.ua, ukr_patriot@ukr.net

There are two mechanisms of action of laser radiation on matter: non-destructive and destructive. The processes underlying their implementation largely depend on the parameters of the laser radiation, in particular the duration of the pulse and its power. Among new phenomena with non-destructive action, for example, ultrashort laser pulses, considerable attention is paid to the study of processes that belong to non-stationary nonlinear optics, such as: the physics of filamentation of laser beams, generation of conical waves, femtosecond supercontinuum radiation, etc. The results of their research have already been partially presented at a number of conferences.

In this report, the main attention will be paid to those phenomena and processes that are manifested in the studied objects during the destructive action of laser pulses of different power and duration from nano- to femtoseconds. The analyzed results relate to the determination of the melting temperature and solidification of the target surface, the excitation of capillary waves in the melt, the formation of spatially periodic surface structures, the generation of electron-hole plasma and its heating and cooling, the "Coulomb explosion" of photo-excited clusters.

Research objects: optical functional materials - various structural forms of silicon, chalcohalide semiconductor glasses, sapphire, silica, and other objects.

Photon drag effect and diffusion of atoms in multilayer films

Krupa M.M.

Institute of Magnetism of National Academy of Science and Ministry of Education and Science of Ukraine, Vernadsky's bul., 36, 03143 Kiev, Ukraine
krupa@imag.kiev.ua

This report presents the results of experimental studies of photon drag effect in Bi/SiC, FeCo/SiC, $LaSrMn_3$ and NiFe nanofilms. The obtained results show that under the action of nanosecond and picosecond pulses of excimer (λ=248 nm) and neodymium (λ=1,06 μ) lasers, photon drag effect in multilayer nanofilms leads to the injection of electrons from the input nanolayer into the next nanolayer, and also causes the drift of ionized atoms, which leads to laser-stimulated diffusion of atoms in the direction of action of laser radiation. In FeCo/SiC films, where the FeCo magnetic nanolayer has a high degree of spin polarization, as a result of the photon drag effect in the SiC nanolayer, unbalanced magnetization occurs at the time of the laser pulse. Photon drag effect during two-photon absorption of nanosecond and picosecond pulses of a ruby laser (λ=694,3 nm) leads to the appearance of a potential difference between the input and output surfaces of the crystal in high-purity single crystals of CdS and ZnSe, as well as to a decrease in the refractive index in the region of output of laser pulses, which leads to disruption of total internal reflection and scanning of nanosecond and picosecond pulses. With very small impurity absorption of a continuous powerful CO_2 laser (λ=10,6 μ) in CdS and ZnSe crystals, the photon drag effect leads to the appearance of a potential difference between the input and output surfaces of the crystal and to an increase in the concentration of absorbing impurity atoms in the output region of the CO_2 laser beam. Irradiation of finely dispersed NiFe nanofilms and amorphous $LaSrMn_3$ nanofilms with excimer and neodymium laser pulses leads to laser-stimulated recrystallization of the input nanolayer of the film. As a result, under the action of one laser pulse in NiFe films, the value of magnetic susceptibility increases and the value of coercive force decreases. $LaSrMn_3$ films are oxidized in the irradiation zone and change from an amorphous to a polycrystalline state the temperature dependence of their conductivity changes from semiconducting to metallic, and the film becomes magnetic. Under the action of powerful excimer and neodymium laser pulses close to the destruction threshold in strongly absorbing films, the roughness of the film surface decreases, which can be explained by the excitation of surface plasmons in the area of action of the laser pulse. Using focused laser beams and a high-precision system of film movements along two coordinates, we obtained a regular structure of nanoelements in the original nanolayer, whose optical or magnetic characteristics differ from the similar characteristics of the original nanolayer.

Features of the origin and propagation of a shock wave in semiconductors during nanosecond laser irradiation

Cao Z.[1], *Levytskyi S.*[2], *Stronski A.*[2]

[1] *Institute of Physics and Technology, National Technical University of Ukraine "Igor Sikorsky Kyiv Polytechnic Institute", Kyiv, Ukraine*

[2] *V. Lashkaryov Institute of Semiconductor Physics, NASU, Kyiv, Ukraine, levytskyi@ua.fm*

In this work, the process of the occurrence and propagation of a shock wave in CdTe, solid solutions based on it, and the In/CdTe structure during nanosecond laser irradiation with the formation of an inversion layer is considered, and defect formation related to the shock wave is investigated.

During powerful nanosecond laser irradiation of metal(In)/p-CdTe (CdMeTe) structures in the semiconductor, an inversion near-surface layer is formed, that is, a layer of n-type conductivity (relative to p-type conductivity) due to diffusion (mass transfer) processes of indium (In) atoms , who act as donors. With nanosecond irradiation, mass transfer – by definition it is fast diffusion, since this process lasts for tens to hundreds of nanoseconds – occurs due to mechanisms of a different physical nature.

In particular, such a mechanism as the occurrence and propagation of a shock wave leads to the generation, change and redistribution of a system of point and long defects [1]. And also the mechanism of generation and relaxation of sharp spatial gradients and rates of temperature rise and, accordingly, thermal stresses (pressure) (dT/dx, dP/dx, dT/dt, dP/dt), since during laser irradiation with a nanosecond pulse duration, the rate of heat transfer to the near-surface layer (that is, to the depth of the optical skin layer and to the depth $\sqrt{\chi\tau}$) is very significant in relation to the speed of heat propagation in the volume due to heat and temperature conduction.Therefore, it is relevant to calculate the depth of shock wave formation in order to control the diffusion process, as well as to find out the peculiarities of the occurrence and propagation of the shock wave in semiconductors and structures during pulsed laser irradiation.

Using the example of CdTe, it was shown that a shock wave in a solid during its formation and propagation, as well as before its occurrence - due to a gradual increase in the pressure gradient - leads to the formation of dislocations. At the same time, the density of dislocations increases with depth and is maximum at the place of formation of the shock wave.

1. V.P Veleschuk, A.I. Vlasenko, E.I. Gatskevich, V.A. Gnatyuk, G.D. Ivlev, S.N. Levytskyi Toru Aoki. Doping of Cadmium Telluride by Indium at Nanosecond Laser Irradiation of In/CdTe Structure. Journal of Materials Science and Engineering B. – 2 (4), 2012. – P. 230-239.

Calculation of phonon scattering cross sections on impurity atoms (In) in CdTe for thermal diffusion during pulse laser irradiation

Levytskyi S., Stronski A.

V. Lashkaryov Institute of Semiconductor Physics, NASU, Kyiv, Ukraine, levytskyi@ua.fm

This work presents the results of the study of simultaneous physical processes such as thermal and baro-diffusion, concentration diffusion, the process of emergence and propagation of a shock wave during nanosecond laser irradiation of In/CdTe metal film structures.

The complexity of mass transfer mechanisms during nanosecond pulsed laser irradiation is due to non-stationarity, non-equilibrium, physical and geometric nonlinearity, high speed and simultaneity of various physical processes; in particular, this is a change in the aggregate state of a solid body, the generation of elastic and shock waves, significant temperature and stress gradients, defect formation, diffusion, etc. [1].

The purpose of this work was to establish and analyze the dominant mechanisms of indium mass transfer in CdTe during nanosecond laser irradiation of the In/CdTe structure.

The depth of shock wave formation in indium and CdTe was calculated depending on the laser pulse intensity density in a wide range of intensities during the formation of inversion and varizon layers. This calculation of the depth of shock wave formation according to the expression from [1] indicates that such a wave in the optimal range of irradiation - E = 10-500 mJ/cm^2 does not occur in an indium film with a thickness of up to 7 μm, and at a thickness of In 30-400 nm is already formed in the volume of the CdTe crystal at a distance that is much greater than the penetration depth of indium l_{In}, and therefore the process of shock wave formation and propagation is not the dominant mechanism of mass transfer of indium in cadmium telluride, although it leads to the appearance and redistribution of point defects.

The calculations made in the framework of this work can be applied to most structures of a metal-semiconductor film for the analysis of mass transfer (diffusion processes) in different parts of the volume of the structure during pulsed laser irradiation in the process of manufacturing various functional semiconductor structures.

1. V.P Veleschuk, A.I. Vlasenko, E.I. Gatskevich, V.A. Gnatyuk, G.D. Ivlev, S.N. Levytskyi Toru Aoki. Doping of Cadmium Telluride by Indium at Nanosecond Laser Irradiation of In/CdTe Structure. Journal of Materials Science and Engineering B. – 2 (4), 2012. – P. 230-239.

SECTION G:

Modern computational methods and their applications in materials science: synergy of theory and experiment

Machine Learning-Based Characterization of Recombination Active Defects in Photovoltaic Cells

Zavhorodnii O.V., Olikh O.Ya.

Taras Shevchenko National University of Kyiv, Kyiv, Ukraine, nevermor464@gmail.com

The application of artificial intelligence, particularly machine learning (ML), in renewable energy research is gaining traction [1]. Recent studies increasingly employ photoluminescence spectroscopy and ML to investigate defect recombination in solar cells (SC). However, the majority of these studies are not specifically related to point defects. Our study aims to develop a cost-effective ML-based approach for characterizing point defect in silicon SC using I-V measurements.

To showcase our methodology, we focused on assessing the concentration of iron-related defects (Fe_i and Fe_iB_s). Using SCAPS-1D software, we modeled SC characteristics under standard AM1.5 and monochromatic (940 nm) illuminations. The modeled I-V curves provided insight into iron impurity states, allowing us to derive relative changes in short-circuit current (εIsc), open-circuit voltage (εVoc), efficiency (εη), and fill factor (εFF) post Fe_iB_s pairs decay. ML methods, including deep neural networks (DNN), random forest (RF), and gradient boosting (GB), were employed to estimate iron concentration. Prediction accuracy was compared across different lighting conditions and descriptor numbers, encompassing base depth, doping level, temperature, εIsc, εη, εVoc, and εFF. Results are presented in Table 1.

Table 1. Accuracy of iron concentration prediction for test dataset

Algorithm	Number of descriptors	MSE (10^{-3})		MRE (%)		R^2	
		illumination					
		AM 1.5	940 nm	AM 1.5	940 nm	AM 1.5	940 nm
DNN	4	49	10	115	14	0.924	0.972
	5	5	4	13	8	0.991	0.981
	6	2	3	8	9	0.993	0.899
	7	0.6	2	3	9	0.998	0.977
RF	4	41	2	83	8	0.939	0.982
	5	10	3	16	10	0.963	0.977
	6	5	3	10	11	0.971	0.968
	7	5	4	10	12	0.975	0.956
GB	4	41	2	66	7	0.949	0.978
	5	12	2	18	8	0.966	0.969
	6	5	2	9	9	0.970	0.973
	7	4	3	9	11	0.981	0.959

1. Dwivedi P., Weber J. W., Lee Chin R., Trupke T., Hameiri Z. Deep learning method for enhancing luminescence image resolution. *Solar Energy Materials and Solar Cells*, 2023, V. 257, P. 112357.

LIST OF AUTHORS

Atamanyuk A.M. 76
Bachynsky O.I. 62
Balan V.R. 65
Bandura H.Ya. 58
Belyaev A.E. 40
Bilynskyi I.V. 41, 43, 44, 49, 58
Blonskyi I.V. 78
Bobyliev D.Ye. 41
Boiko V.G. 71
Boychuk V.M. 52
Bratus O.L. 70
Brytan V.B. 66
Cao Z. 80
Chen Miin-Jang 60
Dadiak I.B. 65
Dan'kiv O.O. 13, 48, 53, 62
Demchyna L.A. 42, 47, 51, 57
Demkiv O.M. 24
Dluzewski P. 20
Dmitruk I.M. 78
Dmytruk A.M. 45, 78
Dmytruk M. 45
Dremliuzhenko K.S. 36
Dubikovskyi O. 18
Dyachok D.O. 24
Dzhagan V.M. 52
Evtukh A.A. 16, 70
Fedorenko L. 16
Gentsar P.O. 42, 47, 51, 57, 71
Guba S.K. 48, 53
Gudymenko A. 21
Gudymenko O.Yo. 18, 70
Gutsul V.I. 50
Hadzaman I.V. 69
Hnidko I.S. 50
Hoivanovych N.K. 24
Holovata O.B. 34
Holovatsky I.V. 37
Holovatsky V.A. 37, 39
Holska S.V. 54
Holskiy V.B. 54
Horbenko Y.Y. 46
Horichok I.V. 65
Isaieva O.F. 36
Ivakhno-Tsehelnyk O. 52
Ivanichok N.Ya. 73
Kaban I.G. 22
Kadan V.M. 78
Kaliuzhnyi V.V. 40
Karnaukhov A. 52
Karpiy V.R. 54
Kashuba A.I. 63
Katanova L.O. 63
Kavetskyy T.S. 24, 35
Kazuhiko H. 30
Kiv A.E. 24, 35
Kochubei H. 17, 21
Kolkovska H.M. 73
Kolkovskyi P.I. 73, 74
Korbutyak D.V. 16, 33, 36
Korenivski V. 19
Kotsyubynsky V.O. 52, 73, 74
Kovalchuk Yu.V. 66
Kovalenko O.V. 27

Kovalko M.C. 66
Koziarskyi I.P. 50
Kravets A. 19
Krupa M.M. 79
Kuchak A.I. 50
Kuhivchak V.A. 53
Kukhazh Y.Y. 24
Kulbachynskyi O. 18
Kulchytskyi B.N. 36
Kupchak I.M. 33
Kuzma M. 14, 20
Kuzyk O.V. 13, 48, 53, 69
Kyiak J.P. 42, 47, 51, 57
Kykot A.M. 70
Leshko O.V. 44, 76
Leshko R.Ya. 44, 54, 58, 76
Levytskyi S. 80, 81
Lishchynskyy I.M. 22
Lotnyk A. 17
Makhanets O.M. 37, 50
Matkivskyi O.M. 65
Maturin Yu.P. 49
Maziar D. 18
Mazur M.P. 34
Mazur N. 52
Mazur T.M. 34
Medvids A. 30
Melnyk Ya.Yu. 41, 43
Misiuk O.I. 74
Morawiec K. 20
Mykytyuk T.V. 45
Mynaylo M.A. 42, 47, 51, 57
Naidych B.P. 34
Naumov V. 16
Novosad I.S. 68
Nykyruy L.I. 34, 63
Olenych I.B. 46
Olikh O.Ya. 40, 83
Ostapenko N.I. 45
Ostapenko Yu.V. 45
Ostrauskaite J. 24
Padalka I.V. 72
Paiuk O. 21
Parashchuk T.O. 34
Pavlovsky Y.V. 66
Pavlyk M.R. 46
Pekur D.V. 42, 47, 51, 57, 71
Peleshchak R.M. 48, 53
Polynchuk P. 19
Poplavskyy O.P. 22
Popov M.Yu. 41, 43
Popovych A.V. 20, 23, 69
Popovych M. 17
Popovych V.D. 20, 23
Pryshko I.A. 68
Rachiy B.I. 73, 74
Rehei M.A. 23
Romanyuk B.M. 71
Sapon S. 18
Satcyk V.V. 48
Šauša O. 24
Ščajev P. 30
Selyshchev O. 52
Semkiv I.V. 63
Seti Ju.O. 32
Shakleina I.O. 23
Shcherban N.D. 45
Shiojiri Makoto 20, 60
Shportko K. 17
Shtuka O.V. 68
Sizov F.F. 15
Slavnyi V.V. 27
Slusarenko M.A. 43
Soloviev V.N. 35

Stadnyk V.Yo. 68
Stolyarchuk A.I. 13, 69
Stolyarchuk I.D. 13, 20, 48, 53, 62
Strilchyk O.M. 51
Stronski A. 11, 17, 21, 22, 80, 81
Svezhentsova K.V. 64
Terletska H. 29
Tkach M.V. 32
Trischuk L.I. 36, 51
Tsybrii Z.F. 15, 64
Tuzhykov A.V. 35
Tymkiv A.V. 66
Tymochko M.D. 40
Tymofii T.M. 74
Uhryn Yu.O. 25, 66
Venger E. 17
Virt I.S. 72
Vlasenko O.I. 42, 47, 57
Voitkiv H.V. 22
Voitsekhivska O.M. 32
Vorovsky V.Yu. 27
Vuichyk M.V. 42, 47, 51, 57, 64
Yarema V.V. 39
Yaremiy I.P. 73, 74
Yavorskyi R.S. 34, 63
Yavorskyi Y.S. 34
Yukhymchuk V. 16
Zahn D.R.T. 52
Zajkowska W. 20
Zamurujeva O.V. 34
Zavhorodnii O.V. 83
Zayachuk D.M. 38
Zayats M.S. 47, 51, 71
Zdyb R. 28
Zgardzińska B. 24
Żywczak A. 20
Лепіх Я.І. 31

Наукове видання

Topical Problems of Semiconductors Physics

Proceedings of the XI-th International Conference

Редактор
Ірина Невмержицька

Технічний редактор
Ольга Лужецька

Коректор
Ірина Артимко

Відповідальний за випуск
Ігор Столярчук

Усі матеріали подано в авторський редакції.

Підписано до друку 14.05.2024.

Гарнітура “Times New Roman”.

Видавець
Дрогобицький державний педагогічний університет імені Івана Франка
(*Свідоцтво про внесення суб’єкта видавничої справи до державного реєстру видавців, виготівників та розповсюджувачів видавничої продукції ДК № 5140 від 01.07.2016 р.*).
82100, Дрогобич, вул. Івана Франка, 24, к. 31.